National Library of Canada
Acquisitions and Bibliographic Services Branch
395 Wellington Street
Ottawa, Ontario
K1A 0N4

Bibliothèque nationale du Canada
Direction des acquisitions et des services bibliographiques
395, rue Wellington
Ottawa (Ontario)
K1A 0N4

Your file *Votre référence*

Our file *Notre référence*

NOTICE

The quality of this microform is heavily dependent upon the quality of the original thesis submitted for microfilming. Every effort has been made to ensure the highest quality of reproduction possible.

If pages are missing, contact the university which granted the degree.

Some pages may have indistinct print especially if the original pages were typed with a poor typewriter ribbon or if the university sent us an inferior photocopy.

Reproduction in full or in part of this microform is governed by the Canadian Copyright Act, R.S.C. 1970, c. C-30, and subsequent amendments.

AVIS

La qualité de cette microforme dépend grandement de la qualité de la thèse soumise au microfilmage. Nous avons tout fait pour assurer une qualité supérieure de reproduction.

S'il manque des pages, veuillez communiquer avec l'université qui a conféré le grade.

La qualité d'impression de certaines pages peut laisser à désirer, surtout si les pages originales ont été dactylographiées à l'aide d'un ruban usé ou si l'université nous a fait parvenir une photocopie de qualité inférieure.

La reproduction, même partielle, de cette microforme est soumise à la Loi canadienne sur le droit d'auteur, SRC 1970, c. C-30, et ses amendements subséquents.

Canada

Absorption properties of phytoplankton and photosynthetic pigments in seawater

by

Nicolas Hoepffner

Submitted in partial fulfillment of the requirements
for the degree of Doctor of Philosophy

at

Dalhousie University
Halifax, Nova Scotia
July, 1993

© Copyright by Nicolas Hoepffner, 1993

National Library
of Canada

Acquisitions and
Bibliographic Services Branch

395 Wellington Street
Ottawa Ontario
K1A 0N4

Bibliothèque nationale
du Canada

Direction des acquisitions et
des services bibliographiques

395 rue Wellington
Ottawa (Ontario)
K1A 0N4

Your file Votre référence

Our file Notre référence

The author has granted an irrevocable non-exclusive licence allowing the National Library of Canada to reproduce, loan, distribute or sell copies of his/her thesis by any means and in any form or format, making this thesis available to interested persons.

L'auteur a accordé une licence irrévocable et non exclusive permettant à la Bibliothèque nationale du Canada de reproduire, prêter, distribuer ou vendre des copies de sa thèse de quelque manière et sous quelque forme que ce soit pour mettre des exemplaires de cette thèse à la disposition des personnes intéressées.

The author retains ownership of the copyright in his/her thesis. Neither the thesis nor substantial extracts from it may be printed or otherwise reproduced without his/her permission.

L'auteur conserve la propriété du droit d'auteur qui protège sa thèse. Ni la thèse ni des extraits substantiels de celle-ci ne doivent être imprimés ou autrement reproduits sans son autorisation.

ISBN 0-315-93674-6

Canada

Name Nicolas HOEPFFNER

Dissertation Abstracts International is arranged by broad general subject categories Please select the one subject which most nearly describes the content of your dissertation Enter the corresponding four digit code in the spaces provided

OCEANOGRAPHY
SUBJECT TERM

0416
SUBJECT CODE

U·M·I

Subject Categories

THE HUMANITIES AND SOCIAL SCIENCES

COMMUNICATIONS AND THE ARTS
Architecture 0729
Art History 0377
Cinema 0900
Dance 0378
Fine Arts 0357
Information Science 0723
Journalism 0391
Library Science 0399
Mass Communications 0708
Music 0413
Speech Communication 0459
Theater 0465

EDUCATION
General 0515
Administration 0514
Adult and Continuing 0516
Agricultural 0517
Art 0273
Bilingual and Multicultural 0282
Business 0688
Community College 0275
Curriculum and Instruction 0727
Early Childhood 0518
Elementary 0524
Finance 0277
Guidance and Counseling 0519
Health 0680
Higher 0745
History of 0520
Home Economics 0278
Industrial 0521
Language and Literature 0279
Mathematics 0280
Music 0522
Philosophy of 0998
Physical 0523
Psychology 0525
Reading 0535
Religious 0527
Sciences 0714
Secondary 0533
Social Sciences 0534
Sociology of 0340
Special 0529
Teacher Training 0530
Technology 0710
Tests and Measurements 0288
Vocational 0747

LANGUAGE, LITERATURE AND LINGUISTICS
Language
General 0679
Ancient 0289
Linguistics 0290
Modern 0291
Literature
General 0401
Classical 0294
Comparative 0295
Medieval 0297
Modern 0298
African 0316
American 0591
Asian 0305
Canadian (English) 0352
Canadian (French) 0355
English 0593
Germanic 0311
Latin American 0312
Middle Eastern 0315
Romance 0313
Slavic and East European 0314

PHILOSOPHY, RELIGION AND THEOLOGY
Philosophy 0422
Religion
General 0318
Biblical Studies 0321
Clergy 0319
History of 0320
Philosophy of 0322
Theology 0469

SOCIAL SCIENCES
American Studies 0323
Anthropology
Archaeology 0324
Cultural 0326
Physical 0327
Business Administration
General 0310
Accounting 0272
Banking 0770
Management 0454
Marketing 0338
Canadian Studies 0385
Economics
General 0501
Agricultural 0503
Commerce Business 0505
Finance 0508
History 0509
Labor 0510
Theory 0511
Folklore 0358
Geography 0366
Gerontology 0351
History
General 0578
Ancient 0579
Medieval 0581
Modern 0582
Black 0328
African 0331
Asia Australia and Oceania 0332
Canadian 0334
European 0335
Latin American 0336
Middle Eastern 0333
United States 0337
History of Science 0585
Law 0398
Political Science
General 0615
International Law and Relations 0616
Public Administration 0617
Recreation 0814
Social Work 0452
Sociology
General 0626
Criminology and Penology 0627
Demography 0938
Ethnic and Racial Studies 0631
Individual and Family Studies 0628
Industrial and Labor Relations 0629
Public and Social Welfare 0630
Social Structure and Development 0700
Theory and Methods 0344
Transportation 0709
Urban and Regional Planning 0999
Women's Studies 0453

THE SCIENCES AND ENGINEERING

BIOLOGICAL SCIENCES
Agriculture
General 0473
Agronomy 0285
Animal Culture and Nutrition 0475
Animal Pathology 0476
Food Science and Technology 0359
Forestry and Wildlife 0478
Plant Culture 0479
Plant Pathology 0480
Plant Physiology 0817
Range Management 0777
Wood Technology 0746
Biology
General 0306
Anatomy 0287
Biostatistics 0308
Botany 0309
Cell 0379
Ecology 0329
Entomology 0353
Genetics 0369
Limnology 0793
Microbiology 0410
Molecular 0307
Neuroscience 0317
Oceanography 0416
Physiology 0433
Radiation 0821
Veterinary Science 0778
Zoology 0472
Biophysics
General 0786
Medical 0760

EARTH SCIENCES
Biogeochemistry 0425
Geochemistry 0996
Geodesy 0370
Geology 0372
Geophysics 0373
Hydrology 0388
Mineralogy 0411
Paleobotany 0345
Paleoecology 0426
Paleontology 0418
Paleozoology 0985
Palynology 0427
Physical Geography 0368
Physical Oceanography 0415

HEALTH AND ENVIRONMENTAL SCIENCES
Environmental Sciences 0768
Health Sciences
General 0566
Audiology 0300
Chemotherapy 0992
Dentistry 0567
Education 0350
Hospital Management 0769
Human Development 0758
Immunology 0982
Medicine and Surgery 0564
Mental Health 0347
Nursing 0569
Nutrition 0570
Obstetrics and Gynecology 0380
Occupational Health and Therapy 0354
Ophthalmology 0381
Pathology 0571
Pharmacology 0419
Pharmacy 0572
Physical Therapy 0382
Public Health 0573
Radiology 0574
Recreation 0575
Speech Pathology 0460
Toxicology 0383
Home Economics 0386

PHYSICAL SCIENCES

Pure Sciences
Chemistry
General 0485
Agricultural 0749
Analytical 0486
Biochemistry 0487
Inorganic 0488
Nuclear 0738
Organic 0490
Pharmaceutical 0491
Physical 0494
Polymer 0495
Radiation 0754
Mathematics 0405
Physics
General 0605
Acoustics 0986
Astronomy and Astrophysics 0606
Atmospheric Science 0608
Atomic 0748
Electronics and Electricity 0607
Elementary Particles and High Energy 0798
Fluid and Plasma 0759
Molecular 0609
Nuclear 0610
Optics 0752
Radiation 0756
Solid State 0611
Statistics 0463

Applied Sciences
Applied Mechanics 0346
Computer Science 0984
Engineering
General 0537
Aerospace 0538
Agricultural 0539
Automotive 0540
Biomedical 0541
Chemical 0542
Civil 0543
Electronics and Electrical 0544
Heat and Thermodynamics 0348
Hydraulic 0545
Industrial 0546
Marine 0547
Materials Science 0794
Mechanical 0548
Metallurgy 0743
Mining 0551
Nuclear 0552
Packaging 0549
Petroleum 0765
Sanitary and Municipal 0554
System Science 0790
Geotechnology 0428
Operations Research 0796
Plastics Technology 0795
Textile Technology 0994

PSYCHOLOGY
General 0621
Behavioral 0384
Clinical 0622
Developmental 0620
Experimental 0623
Industrial 0624
Personality 0625
Physiological 0989
Psychobiology 0349
Psychometrics 0632
Social 0451

à Domi

TABLE OF CONTENTS

Table of Contents v

List of Figures viii

List of Tables x

Abstract xi

Acknowledgements xii

General Introduction 1

Chapter 1: Bio-optical characteristics of coastal waters: absorption spectra of phytoplankton and pigment distribution in the western North Atlantic

1.1. Introduction 5

1.2. Materials and Methods 6

1.2.1. Data collection 6

1.2.2. The beam-attenuation coefficient 8

1.2.3. Pigment analysis 8

1.2.4. Absorption spectra 10

1.3. Results 11

1.3.1. Biophysical structure of the water column 11

1.3.2. Pigment distribution 18

1.3.3. In vivo absorption spectra of particulate material 29

1.4. Discussion 35

1.4.1. The role of phytoplankton in determining the optical properties of seawater 35

1.4.2. Importance of intracellular pigment composition in the variability of $a^*_{ph}(440)$ 39

1.4.3. Spatial variability in the absorption spectrum of phytoplankton 41

1.5. Conclusions 43

Chapter 2: Effect of pigment composition on the absorption properties of phytoplankton

2.1. Introduction 46
2.2. Material and methods 48
2.2.1. Bio-optical data 48
2.2.2. Decomposition of absorption spectra 49
2.3. Results 52
2.4. Discussion 60
2.4.1. Biological interpretation of the Gaussian Bands 60
2.4.2. Specific absorption coefficients 64
2.4.3. Reconstruction of *in vivo* absorption spectrum 71
2.5. Conclusions 73

Chapter 3: Determination of the major groups of phytoplankton pigments from the absorption spectra of total particulate matter

3.1. Introduction 77
3.2. Materials and Methods 78
3.2.1. Observed data 78
3.2.2. Theoretical considerations 79
3.2.3. Approach 82
3.3. Results 86
3.3.1. Absorption coefficients from field data 86
3.3.2. Decomposition of the absorption spectra of total particles 90
3.3.3. Comparison of computed and observed spectra 93
3.3.4. Decomposition of phytoplankton absorption spectra 94
3.3.5. Estimation of pigment concentrations 103

3.4. Discussion 105
3.4.1. Specific absorption coefficient of pigments 105
3.4.2. Particle size effect 108
3.4.3. Absorption by detrital particles 111
3.5. Conclusions 113

Summary and Conclusions 115

Appendix I 119

References 128

LIST OF FIGURES

Figure 1.1 Study area and station locations in the western North Atlantic . . 7

Figure 1 2 Profiles of fluorescence, beam attenuation coefficient at 660 nm, and temperature for selected stations in the western North Atlantic . 12

Figure 1.3 Variations of the mean extinction coefficient of light, as measured by Secchi disk, *versus* the concentration of total HPLC pigments at the surface 17

Figure 1.4 Vertical distribution of the pigments at selected stations in the western North Atlantic 22

Figure 1.5 HPLC chromatograms of two acidified pigment extracts of samples collected at 5m and 92m in oceanic waters. For comparison, the acidified chromatogram of a marine prochlorophyte in culture is shown . . 26

Figure 1.6 Variations in the specific *in vivo* absorption coefficient at 440 nm for total particles, detritus, and phytoplankton, as a function of the concentration of chl-*a* in the sample 31

Figure 1.7 Spectra of the specific absorption coefficient of phytoplankton at selected stations in the western North Atlantic 32

Figure 1.8 Variations in the shape of the absorption spectrum of phytoplankton, in open-ocean and coastal waters 34

Figure 1.9 *In situ* fluorescence *versus* beam attenuation coefficient at 660 nm for three stations 37

Figure 1.10 Absorption ratio 550:440 nm of phytoplankton, as a function of the ratio of fucoxanthin to chlorophyll-*a* 42

Figure 2.1 Observed absorption spectra, corrected for particle effect, and the corresponding fitted spectra expressed as the sum of 11 Gaussian components for three marine species 54

Figure 2.2 Gaussian band height at 415 nm, 435 nm, 623 nm, and 675 nm, *versus* chl-*a* concentration 65

Figure 2.3 Gaussian band height at 460 nm, 583 nm, and 643 nm, *versus* chl-*c* concentration 67
Figure 2.4 Gaussian band height at 460 nm, 655 nm, *versus* chl-*b* concentration 69
Figure 2.5 Gaussian band height at 489 nm, and 532 nm, *versus* carotenoids concentration 70
Figure 2.6 Reconstruction of *in vivo* absorption spectrum of phytoplankton sample containing Diatoms, Chlorophyceae, and Prymnesiophyceae . . . 74
Figure 3.1 Spectra of light absorption by total particulate matter, non-algal fraction, and specific absorption spectra of living phytoplankton 84
Figure 3.2 Plots of absorption coefficient of phytoplankton at 440 nm, of detritus at 440 nm, and exponential parameter q, as retrieved from Equation 3.8 *versus* observed values 88
Figure 3.3 Spectral values of absorption by phytoplankton and detritus computed from the non-linear regression on total particle absorption spectra and compared with field observations 91
Figure 3.4 Calculated *in vivo* spectral absorption of phytoplankton *versus* observed values for all samples collected in the western North Atlantic . . . 95
Figure 3.5 Decomposition of absorption spectra of natural phytoplankton communities, using the method described in Chapter Two 96
Figure 3.6 Maximum Gaussian absorption *versus* pigment concentrations . . . 99
Figure 3.7 Compared spectral values of the specific absorption coefficient of chl-*a*, -*b*, -*c*, and carotenoids 102
Figure 3.8 Computed concentrations of photosynthetic pigments *versus* HPLC field data 104
Figure 3.9 Comparison between reconstructed absorption spectra of phytoplankton from Equation 3.6 and observed spectra taken from different locations and depths in the western North Atlantic 109

LIST OF TABLES

Table 1.1 Pigment concentrations (in $mg.m^{-2}$) in the euphotic layer 20

Table 2.1 Input specifications of the Gaussian parameters for decomposition of absorption spectra of 4 phytoplankton groups 51

Table 2.2 Averaged values of wavelength positions (in nm) and halfwidths (in nm) of 11 Gaussian bands used to fit the absorption spectra of 3 groups of marine algae 57

Table 2.3 Root mean squares of wavelength positions and halfwidths of 11 Gaussian bands used in decomposition of the absorption spectra from 3 groups of marine algae 58

Table 2.4 Mean characteristics of the Gaussian bands 72

Table 3.1 Spectral absorption coefficient of phytoplankton, normalized at 440 nm and averaged over all samples from the western North Atlantic . . 87

Table 3.2 Input values and mean characteristics of the Gaussian bands reflecting absorption by chlorophylls, and carotenoids 101

Table 3.3 Results from regression analyses between observed absorption spectra of phytoplankton and spectra reconstructed from the knowledge of the specific absorption coefficients of various pigments and the concentrations of these pigments 107

Table 3.4 Mean characteristics of the Gaussian bands and specific absorption coefficients of chl-*a*, -*b*, -*c*, and carotenoids for Georges Bank waters . . 112

ABSTRACT

The vertical structure in fluorescence and beam attenuation (at 660 nm) is related to local hydrographic features and the composition of photosynthetic pigments for the western North Atlantic in September. Phytoplankton and covarying material appear to be the major factors affecting the beam attenuation coefficient through changes in species composition and pigment concentration, and through photoadaptation. Detailed pigment analysis combined with measurements of *in vivo* phytoplankton absorption spectra showed a major regional difference in the specific-absorption spectra of phytoplankton which is directly linked to the structure of the phytoplankton community present in the water column. The results indicate a strong influence of other pigments co-existing with chlorophyll-*a* in algal cells on the variabilities of the specific-absorption coefficient of phytoplankton.

To account for an effect due to pigment composition, absorption spectra of several phytoplankton species were decomposed, after correction for the "particle-size" effect, and the *in vivo* absorption properties of the major light-harvesting pigments were estimated. A Gaussian shape is suitable , theoretically and empirically, to represent the absorption spectra of individual photosynthetic components. The Gaussian parameters agreed well with the expected pigment compositions of 3 groups of algae, and the peak heights were linearly correlated with the concentrations of the 4 major pigments measured in the samples. The linear relationship did not vary with phytoplankton species. The results give estimates of the *in vivo* specific-absorption coefficients of photosynthetic pigments which, then, are used to reconstruct the *in vivo* absorption spectrum of a multi-species samples.

Another application of the previous results is to compute photosynthetic- pigment concentrations in seawater from the knowledge of the absorption coefficient of phytoplankton. The contributions due to detrital particles and phytoplankton to total light absorption are retrieved by non-linear regression on the absorption spectra of total particles from various oceanic regions. The model used explains more than 96% of the variance in the observed particle absorption spectra. The resulting absorption spectra of phytoplankton are then decomposed into Gaussian bands, following a similar procedure as the one previously described. Such a decomposition, combined with HPLC data of phytoplankton pigment concentrations, allows the computation of specific- absorption coefficients for chlorophylls-*a*, -*b*, -*c*, and carotenoids. It is shown that these coefficients can be used to reconstruct the absorption spectra of phytoplankton at various locations and depths. Discrepancies that do occur at some stations are explained in terms of particle-size effect. Lastly, these coefficients can also be used to determine the concentrations of phytoplankton pigments in the water, knowing just the absorption spectrum of light by total particulate matter.

ACKNOWLEDGEMENTS

I would like to thank my supervisor, Dr. Shubha Sathyendranath, and Dr. Trevor Platt for their continuous advice, guidance and encouragement during the course of this thesis. I would also like to express my thanks to Dr. Marlon Lewis, Dr. Bruce Johnson, Dr. Robert Moore, and Dr. Kendall Carder for serving on my doctoral committee, and for their constructive comments.

It is a real pleasure to thank all the scientific and technical staff at the Biological Oceanographic Division of the Bedford Institute of Oceanography for their endless assistance throughout this investigation. In particular, I would like to thank Brian Irwin for his help in the lab and during cruises, and Cathy Porter for her assistance in the computer work.

Financial support during the course of this work was provided by the World Universitary Service of Canada, the Department of Fisheries and Oceans, and the Natural Sciences and Engineering Research Council through operating grants to Dr. Shubha Santhyendranath.

Finally, I am very grateful to all wonderful friends who contributed to the enjoyment of my student career at Dalhousie. Most of all, I thank Dominique, Camille, Victor, and Baptiste for their love and support.

General Introduction

The modification of the path and intensity of a light beam passing through the ocean are determined by the absorption coefficient and the volume scattering function (Kirk 1983). These properties are classified as Inherent Optical Properties (IOP, Preisendorfer 1976) because they do not depend on the angular structure of the incident radiation field but rely, instead, only on the nature of the in-water constituents, *e.g*, their shape, size, and the material of which they are composed. Direct measurements of IOP are difficult to obtain, although a few instruments were designed to monitor underwater absorption (Højerslev 1978, Spitzer and Wernand 1981, Zaneveld *et al.* 1988), and scattering (Tyler 1963, Petzold 1972). On the contrary, Apparent Optical Properties (AOP) such as the diffuse attenuation coefficient and the reflectance of seawater, are routinely computed from the measurements of downwelling and upwelling irradiances (Morel and Prieur 1977, Smith and Baker 1978), as well as from the water-leaving radiances detected from remote sensors (Gordon and Morel 1983). These properties depend on the angular structure of the radiance distribution in the water, as well as on the IOP. Since IOP are linked to the optically-active components in seawater, investigations on changes of these apparent optical properties in relation to biological variables require information on the contributions to absorption and scattering of light by all material present in the water.

Optically-active constituents in seawater are partitioned into molecular water, phytoplankton, dissolved organic substances (or yellow substances), and detrital matter which may include mineral particles, small heterotrophs, bacteria, as well as algal debris. However, absorption and scattering by phytoplankton and covarying constituents are generally considered to be responsible for most of the variations in

the optical properties of case 1 waters (*sensu* Morel and Prieur 1977), which represent 98% of the world's oceans (Morel 1988). Knowledge of these inherent optical properties of phytoplankton is therefore a necessary requirement for computations of the light penetration in seawater (Sathyendranath and Platt 1988), and of the photosynthetically usable radiation (Morel 1978) which, in turn, is used in the determination of the photosynthetic quantum yield and primary production in the ocean (Smith *et al.* 1989). They are also important variables in models of phytoplankton growth rate (Sakshaug *et al.* 1989), and even mixed-layer dynamics (Lewis *et al.* 1983, Sathyendranath *et al.* 1991). Bio-optical models for remote sensing of phytoplankton biomass and primary productivity in the oceans are also based on the optical properties of phytoplankton (Gordon and Morel 1983, Sathyendranath and Morel 1983, Platt 1986, Sathyendranath and Platt 1989). These biomass models are generally more sensitive to changes in the characteristics of spectral absorption than to changes in their scattering properties (Gordon and Morel 1983, Sathyendranath 1986). However, in spite of its importance, the absorption coefficient of natural phytoplankton populations has not been much studied in the past, no doubt because of the difficulty in recovering it from the *in vivo* absorption spectrum of natural particle assemblages, where phytoplankton compete with other material for the capture of photons. In this thesis, I focus on the variabilities of some optical properties of particulate matter in seawater, with special reference to the absorption of phytoplankton, and the problems that are associated with the determination of the phytoplankton absorption coefficient.

Unlike field work, *in vivo* spectral absorption of phytoplankton has been the subject of numerous laboratory experiments related to various subjects. A typical absorption spectrum of marine algae is characterized by maxima at 440 nm and 675 nm which are primarily associated with chlorophyll-*a*, but additional contributions related to secondary chlorophylls, carotenoids and phycobilins are also present. The intracellular pigment composition varies within each algal group, such

that differences could occur in their absorption spectrum (Prézelin 1981). For oceanographic purposes, a quantity of interest is the specific absorption coefficient of phytoplankton, that is, the wavelength-dependent absorption coefficient normalized to chlorophyll-*a*. Results of these studies show that this coefficient at 440 nm varies by a factor of 3 (Sathyendranath 1986). Using culture experiments, Bricaud *et al.* (1983) and Sathyendranath *et al.* (1987) demonstrated that two factors account for most of the variance in the absorption coefficient of algae: the size and configuration of the cells, and the intracellular pigment composition. The former effect, well known as the particle effect (or package effect, or flattening effect), was originally described by Duysens (1956) and describes flattening of absorption spectra of particles in suspension when compared with an equivalent amount of absorbing material in solution. Morel and Bricaud (1981) have investigated this phenomenon in marine algae to correct phytoplankton absorption spectra for this effect. In contrast, the effect of pigment composition has not been significantly documented (but see Sathyendranath *et al.* 1987), probably because of the difficulty in retrieving the "*in vivo*"characteristics of spectral absorption by individual pigments.

In this thesis, *in situ* bio-optical field data and modelling studies are combined to achieve two main goals:

1. To assess the role of various phytoplankton pigments in controlling the magnitude and shape of the specific spectral absorption of light by phytoplankton.

2. To develop a method to determine the specific absorption coefficient of phytoplankton, which will account for the "*in vivo*" absorbing characteristics of various photosynthetic pigments.

In Chapter One, some bio-optical variables of water samples collected in the western North Atlantic are investigated in relation with local hydrographic features and the composition of photosynthetic pigments. Also, detailed pigment analyses are combined with measurements of *in vivo* phytoplankton absorption spectra to

examine the variability in the specific absorption coefficients of phytoplankton in relation to the pigment composition, and, hence, to changes in the structure of the phytoplankton community with sampling location and depth.

In Chapter Two, absorption spectra of several phytoplankton species were decomposed, after correction for the particle effect, to estimate, the *in vivo* absorption properties of the major light-harvesting pigments in marine algae. A Gaussian approximation is used to resolve the spectral absorption of four different pigments in the entire visible range. The reliability of this method is tested against published data on the optical properties of individual pigments obtained with techniques that reduce as much as possible the effect of separation of the pigment from its *in vivo* molecular environment.

In Chapter Three, the contributions due to detrital particles and phytoplankton to total light absorption are retrieved by non-linear regression on the absorption spectra of total particulate matter from various oceanic regions. The resulting absorption spectra of phytoplankton are then used in combination with the model described in Chapter Two to compute specific absorption coefficients of individual pigments. The application of these coefficients to recover biological variables in the oceans are also investigated.

Finally, a synopsis of this thesis is given in a general conclusion, which briefly expands on further applications of this work in different domains of oceanography, particularly remote sensing of ocean colour.

CHAPTER 1

Bio-optical characteristics of coastal waters: absorption spectra of phytoplankton and pigment distribution in the western North Atlantic

1.1. Introduction

Direct measurements of *in vivo* light absorption by phytoplankton are difficult, considering the low concentration of algal cells in the water (when compared with cultures) and the competition for photons between phytoplankton and other particulate material such as detritus and sediment. Recently, however, methods have been developed for measurement of the absorption spectra of live phytoplankton from natural sea-water samples (Yentsch 1957, 1962, Mitchell and Kiefer 1984, Kishino *et al.* 1985, Iturriaga and Siegel 1989). Applications of these methods to field samples are still sparse, particularly in coastal waters which are often of economic importance (but see Yentsch and Phinney 1989).

The Gulf of Maine provides an excellent environment for investigation of the variability in the optical properties of phytoplankton. Several water masses of different regions coexist in that area during summer (Hopkins and Garfield 1979). Their interactions lead to strong biological gradients and an interesting system of particle dynamics (Spinrad 1986).

In this chapter, the vertical structure in beam-attenuation and *in vivo* chlorophyll fluorescence for the Gulf of Maine region in late summer are presented, and interpreted in terms of vertical stability, phytoplankton community structure and photoadaptation. Then, the variability in shape and amplitude if the *in vivo* specific absorption spectra are examined in relation to differences in pigment composition,

and the implications for remote sensing and bio-optical models of primary production are discussed.

The effect of cell size (i.e., package effect) on the absorption coefficient of algal cells has been fairly well studied (Morel and Bricaud 1981, Sathyendranath *et al.* 1987). Yentsch and Phinney (1989) have concluded that it represents the major factor responsible for the variability in the specific absorption coefficient at 440 nm in the western North Atlantic. Using simultaneous measurements of pigment distribution and *in vivo* absorption spectra, the following question is addressed: how the intracellular pigment composition of algal species affects the variability in the chlorophyll-specific absorption spectra of phytoplankton ?

Bio-optical models of light penetration, ocean colour and primary productivity currently in use make little concession to changes in the optical properties of phytoplankton associated with changes in community structure. The results presented here indicate clearly that such changes can be significant, and that information on pigment composition may contain the key necessary to determine the magnitude of these variations and, hence to improve the performance of bio-optical models.

1.2. Materials and methods

1.2.1. Data collection. Data were collected in September 1989 during a cruise of the R/V Cape Hatteras in the Gulf of Maine and Georges Bank region. Hydrocasts were performed at 20 stations (Fig. 1.1) using a sampling rosette (General Oceanic model 1015) equipped with eleven 5 l Niskin bottles. Hydrographic and optical data were obtained simultaneously with a CTD profiler (Neil Brown Instrument System SMART), an *in situ* fluorometer (Sea Tech, Inc.) and an *in situ* transmissometer (Sea Tech., Inc.), all of which were attached to the water sampling rosette. The fluorometer was calibrated against pure chlorophyll *a* (Sigma Chem. Co.).

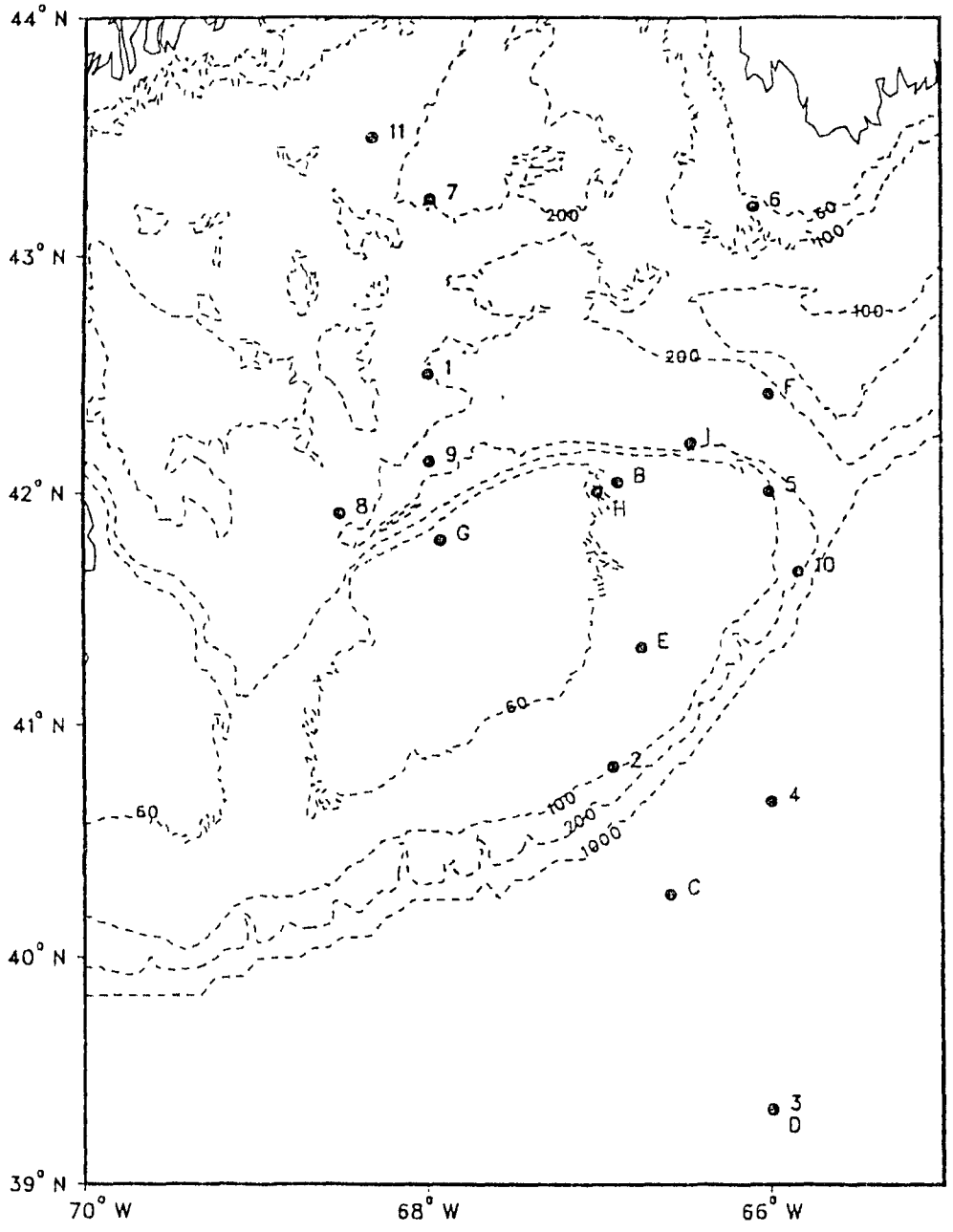

FIGURE 1.1. Study area and station locations in the western North Atlantic. Cruise of the RV "Cape Hatteras" in September 1989.

1.2.2. The beam-attenuation coefficient. The transmissometer was operated with a light-emitting-diode (LED) light source at a wavelength of 660 nm. Light transmittance T measured at this wavelength was used to compute the beam-attenuation coefficient c (m^{-1}) using the following relationship:

$$T(660) = \exp[-0.25\ c(660)]\ , \tag{1.1}$$

where 0.25 is the pathlength of the instrument in meters.

1.2.3. Pigment analysis. Algal pigments were separated and quantified using a reverse-phase, high-performance liquid-chromatography (HPLC) technique with some modifications to the general procedure described by Mantoura and Llewelyn (1983). Samples of 0.3 l to 1.5 l were filtered onto Whatman GF/F filters (2.5 cm in diameter), frozen immediately at liquid N_2 temperature and stored at $-70°C$ prior to analysis. Gieskes and Kraay (1983*a*) have shown that storage of filters in this manner for several months does not significantly affect the pigment composition of the filtered material. The filters were then immersed in 1 ml of 100% acetone and crushed vigorously using a tissue grinder. The pigments were extracted in the dark for several hours at 5°C. Just before HPLC injection, the samples were centrifuged and diluted with deionized water at a ratio of 2:1 (sample:water) to prevent band-spreading in the first eluted peaks (Welschmeyer and Hoepffner, in press).

The instrumentation for HPLC consisted of a Beckman "System Gold" apparatus, including a dual-pump solvent module (Model 126) and a scanning absorbance detector (Model 167). Both the modules and the chromatogram analysis were programmed using an IBM PC loaded with the Beckman "System Gold" software package. Pigments were separated on a short (4.6 mm x 7.0 cm) Ultrasphere XL-ODS column (Beckman), filled with 3 μm (in diameter) packing material. The solvents

were a mixture of methanol and 0.5M ammonium acetate (80:20, v:v) as solvent A, and a mixture of methanol and ethylacetate (70:30, v:v) as solvent B. A linear gradient from 100% solvent A to 100% solvent B was set up from 1 to 16 min of a 23 minute chromatographic run. A pause of few minutes between each sample allowed the baseline to stabilize with 100% solvent A. The pigments were monitored at 440 nm and identified by comparing their retention times and absorption characteristics with quantitative standards. All standards were provided by Dr. R.R. Bidigare as part of an HPLC pigment intercalibration study (SCOR Working Group, 1989).

Pigments quantified by the present method were chl-*a*, -*b*, -($c_1 + c_2$), peridinin, fucoxanthin, 19'- butanoyloxyfucoxanthin, 19'-hexanoyloxyfucoxanthin, alloxanthin, prasinoxanthin, diadinoxanthin, zeaxanthin and β-carotene. The method was not capable of separating either zeaxanthin from lutein, or chl-($c_1 + c_2$) from Mg 2,4- divinylphaeoporphyrin a5 monomethyl ester. Zeaxanthin, however, was assumed to be dominant over lutein, as suggested by other field observations (Gieskes and Kraay 1986, Everitt *et al.* 1990). On the other hand, the distribution of Mg 2,4-D-like pigment in sea water is poorly known (Hooks *et al.* 1988), so that the peak, hereafter referred to as chl-($c_1 + c_2$), should be interpreted with caution. The abundances of chl-c_3, diatoxanthin and α-carotene were determined qualitatively since no standards were available to quantify these pigments. These three peaks were identified by comparison with chromatograms of unialgal species of known pigment composition: *Emiliana huxleyi* for chl-c_3 (see Jeffrey and Wright 1987), *Isochrysis galbana* grown in culture at high light intensity for diatoxanthin (see Welschmeyer and Hoepffner, in press), and marine "prochlorophytes" for α-carotene (see Chisholm *et al.* 1988). For several samples, particularly those collected in oligotrophic waters, the acetone extract was acidified with 1N HCl to note the presence of divinyl phaeophytin-like pigment which characterizes the group Prochlorophyceae, recently discovered in oceanic waters (Chisholm *et al.* 1988).

1.2.4. Absorption spectra. Light absorption by marine particles was determined after concentration of the particles on glass-fiber filters, using the method originally described by Yentsch (1957) and modified later by Kishino *et al.* (1985) to discriminate between absorption by pigmented and non-pigmented particles. Water samples of 0.25 to 1.5 l were filtered onto Whatman GF/F filters (2.5 cm in diameter) with a nominal pore size of 0.7 μm. Optical densities of total particles on filters were measured between 400 and 750 nm, using a UV-visible single-beam spectrophotometer (Philips, model PU-8600) equipped with tungsten-halogen and deuterium arc sources. The instrument displays absorbances up to 3.0 OD unit with an accuracy of $\pm$ 0.002. A special apparatus was designed to hold the filter normal to the light beam and very close to the detector, to allow all transmitted and most of the forward- scattered light to be collected by the detector. Before each scan, the filters were placed on one drop of filtered seawater to ensure complete saturation (Mitchell and Kiefer 1984). A blank filter, wetted with filtered sea water, was used as reference. Optical densities of total particles, $OD_t(\lambda)$, were then converted to absorption coefficient, $a_t(\lambda)$ in m^{-1}, using the following relation:

$$a_t(\lambda) = 2.3\ OD_t(\lambda)\, S/V\ , \tag{1.2}$$

where S is the clearance area of the filter and V the volume of filtered sea water. All samples were taken in duplicate. One set of filters was then extracted with 90% acetone whereas the other set was extracted with a mixture of 90% acetone and DMSO at a ratio of 6:4 (v:v). The solvents were allowed to flow passively through the filter, which required an extracting period of 25 to 30 minutes. The extracted filters were soaked again in filtered sea water and scanned from 400 to 750 nm to measure the absorption coefficient of the particles without their pigments, $a_d(\lambda)$. The absorption of light by just phytoplankton, $a_{ph}(\lambda)$, was obtained by subtracting $a_d(\lambda)$ from $a_t(\lambda)$. A comparative study between both extracting methods showed

that a mixture of 90% acetone and DMSO was more efficient than just 90% acetone for extraction of photosynthetic pigments, as the latter solvent always left a slight absorption at 675 nm due to chl-*a*.

The absorption spectra are corrected for the path-length amplification due to filters (Mitchell and Kiefer 1984). To obtain the correction factors, the absorption coefficient of equivalent amounts of algal cultures was measured in suspension, X^s, (using a scattered transmission accessory similar to that in Sathyendranath *et al.* 1987), and on a filter, X^f. An empirical relationship was established between the two measurements using a series of dilutions made from each culture. The data for all wavelengths were smoothly scattered along the following second order polynomial,

$$X^s = 0.31\ (X^f) + 0.57\ (X^f)^2 \tag{1.3}$$

In order to maintain the same protocol to measure the absorption by cells in culture and natural sea water, all filter samples were frozen ($-70°C$) immediately after collection, and thawed immediately before measurement of absorption. These precautions minimised some of the potential problems associated with this method (Stramski, 1990).

1.3. Results

1.3.1. Biophysical structure of the water column The physical environment affects to a large extent the distribution of particles in the Gulf of Maine (Spinrad 1986). It also controls, over a wide range of time and space scales, the physiology of phytoplankton, by modifying their light and nutrient conditions (Yentsch and Garfield 1981). The vertical profiles of temperature, fluorescence and light transmission are shown in Figure 1.2 for some representative stations.

FIGURE 1.2. Profiles of fluorescence (dotted line), beam-attenuation coefficient at 660 nm (solid line), and temperature (dashed line) for selected stations in the western North Atlantic. The depth of the euphotic zone (1% light level) is indicated by an horizontal dashed line.

Figure 1.2

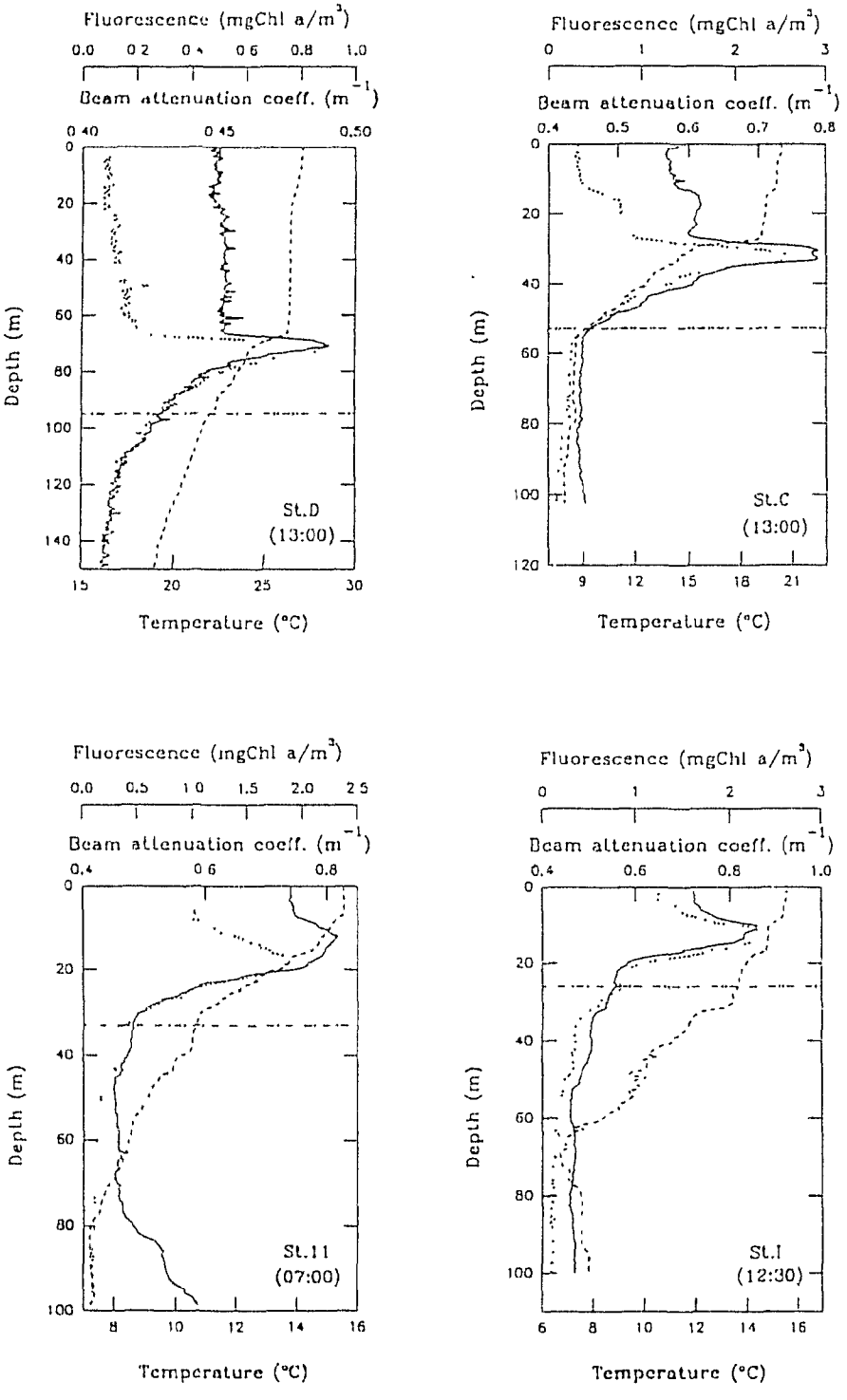
Fluorescence (mgChl a/m³)
Beam attenuation coeff. (m⁻¹)
Depth (m)
Temperature (°C)
St.D
(13:00)
St.C
(13:00)
St.11
(07:00)
St.I
(12:30)

Figure 1.2

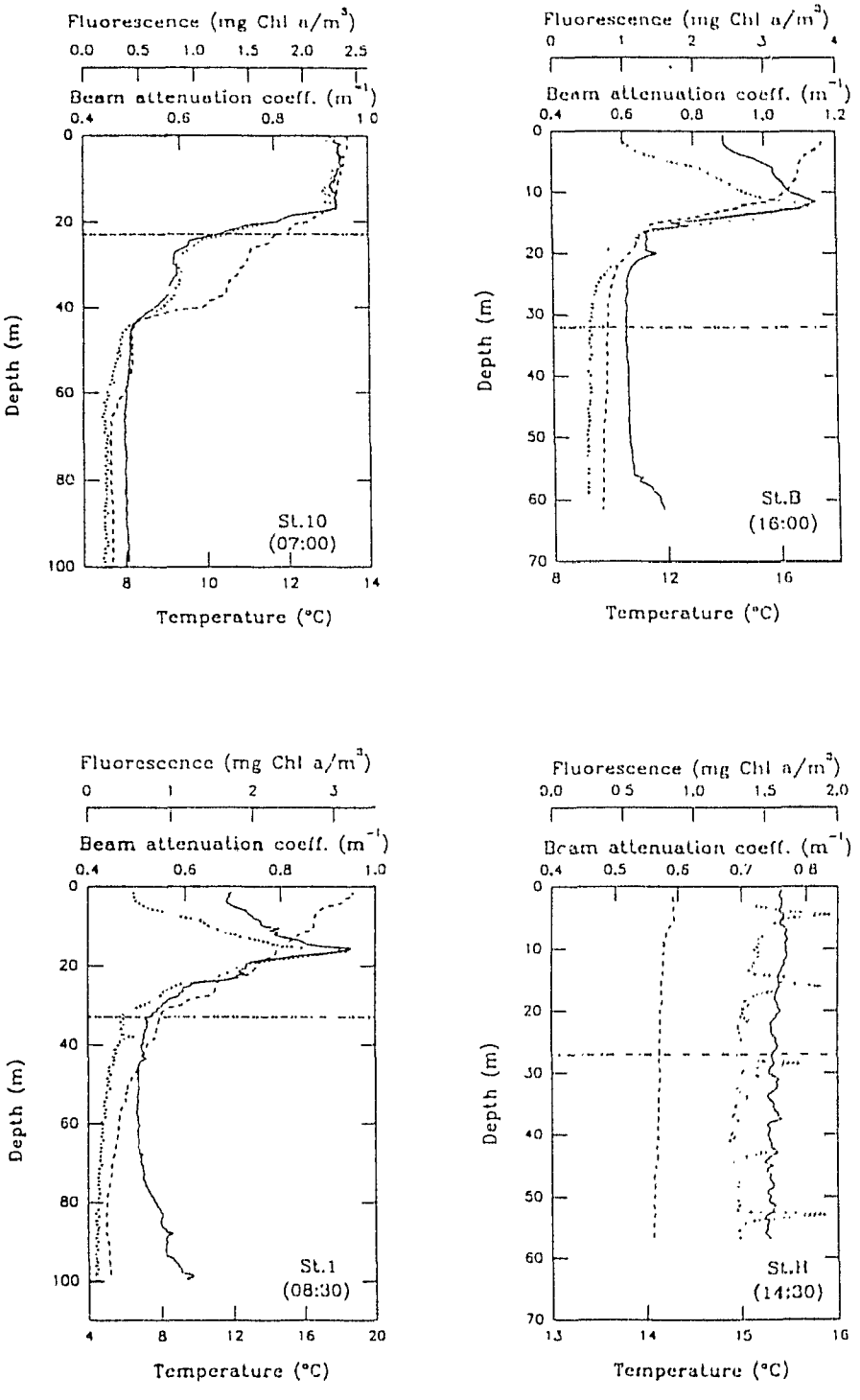
Fluorescence (mg Chl a/m³)
Beam attenuation coeff. (m⁻¹)
Depth (m)
Temperature (°C)
St.10
(07:00)
St.B
(16:00)
St.1
(08:30)
St.H
(14:30)

Vertical temperature structure. A distinct progression from stratified to completely-mixed water column was observed from the stations further offshore (*e.g.* Station D) to the shallowest area over Georges Bank (*e.g.* Station H). The depth of the thermocline, present at most of the stations, varied from 75 m within the clearest deep-ocean waters at Stations 3 and D, to less than 5 m at coastal stations characterized by a water column shallower than 100 m. Station C is an intermediate case with the thermocline at 30 m. However, at several stations, a more complicated structure was recorded in the temperature profile. For example, two distinct thermoclines can be seen at Station 10, the shallower one occurring at 15-20 m and the second one at around 45 m. A similar structure was also observed by Townsend *et al.* (1984) during the same period of the year along the northern edge of Georges Bank. At Station I, the thermocline is less sharply defined. Instead, a staircase-like structure may be observed from 10 m down to about 50 m. At Station 1, the stratification is very shallow, and also has several staircase-like features along the thermocline.

Such variations in the temperature profile are not uncommon, particularly in this region where the vertical structure of the water column is strongly affected by tidal currents and the depth of the water column (Garrett *et al.* 1978, Yentsch and Garfield 1981). Note the change in the vertical structure of the water column between Stations B and H which, in fact, represent the same location sampled on different days. It is well known that a tidal front develops around Georges Bank during the spring- fall period between the well-mixed waters over Georges Bank and the surrounding stratified waters (Garrett *et al.* 1978, Horne *et al.* 1990). The variations in stratification between Stations H and B reflect the dynamic nature of this front whose position varies with the local tidal excursion.

Euphotic depth. At Stations 1 to 11, the euphotic zone, Z_e, defined as the 1% light level, was estimated using the Secchi disk and the following relations (Kirk 1983):

$$Z_e = 4.61/\bar{K} \ , \tag{1.4}$$

with

$$\bar{K} = 1.44/Z_{SD} \ , \tag{1.5}$$

where $\bar{K}$ represents the mean extinction coefficient of light in the water column, and Z_{SD}, the Secchi depth. The relationship between $\bar{K}$ and the pigment concentration (B_0) at the surface, calculated as the sum by weight of all HPLC pigments, is seen in Figure 1.3. The empirical fit to the data set is given by:

$$\bar{K} = 4.6/Z_e = 0.018 + 0.158\,[1 - \exp(-1.19\ B_0)] \ . \tag{1.6}$$

The intercept of the curve at $B_0 = 0$ yields $\bar{K} = 0.018$ m^{-1} which is 2/3 of the mean attenuation coefficient given by Smith and Baker (1978) for clear ocean waters, $\bar{K}_w$ = 0.027 m^{-1}. This relationship (Eq. 1.6) was used to estimate the photic depths for Stations B to I, where no Secchi disk measurements were available. Note that, I do not pretend, using Equation 1.6, to analyse the variability of $\bar{K}$ in oceanic waters. Further, a saturation of $\bar{K}$ at 0.18 m^{-1} for a pigment concentration higher than 3.0 mg.m^{-}3 is probably unrealistic. Sathyendranath and Platt (1988), and Morel (1988), using different methods, have computed higher values of $\bar{K}$ for a pigment concentration of 10.0 mg.m^{-3}: $\bar{K}$ = 0.26 m^{-1} and $\bar{K}$ = 0.32 m^{-1}, respectively. However, within the range of pigment concentrations from 0.0 to 3.0 mg.m^{-3}, both studies give similar $\bar{K}$ values than those obtained from Equation 1.6, supporting then the use of the above formulation to approximate Z_e in Gulf of Maine waters in September. The depth of the euphotic zone for each station is indicated in Figure 1.2.

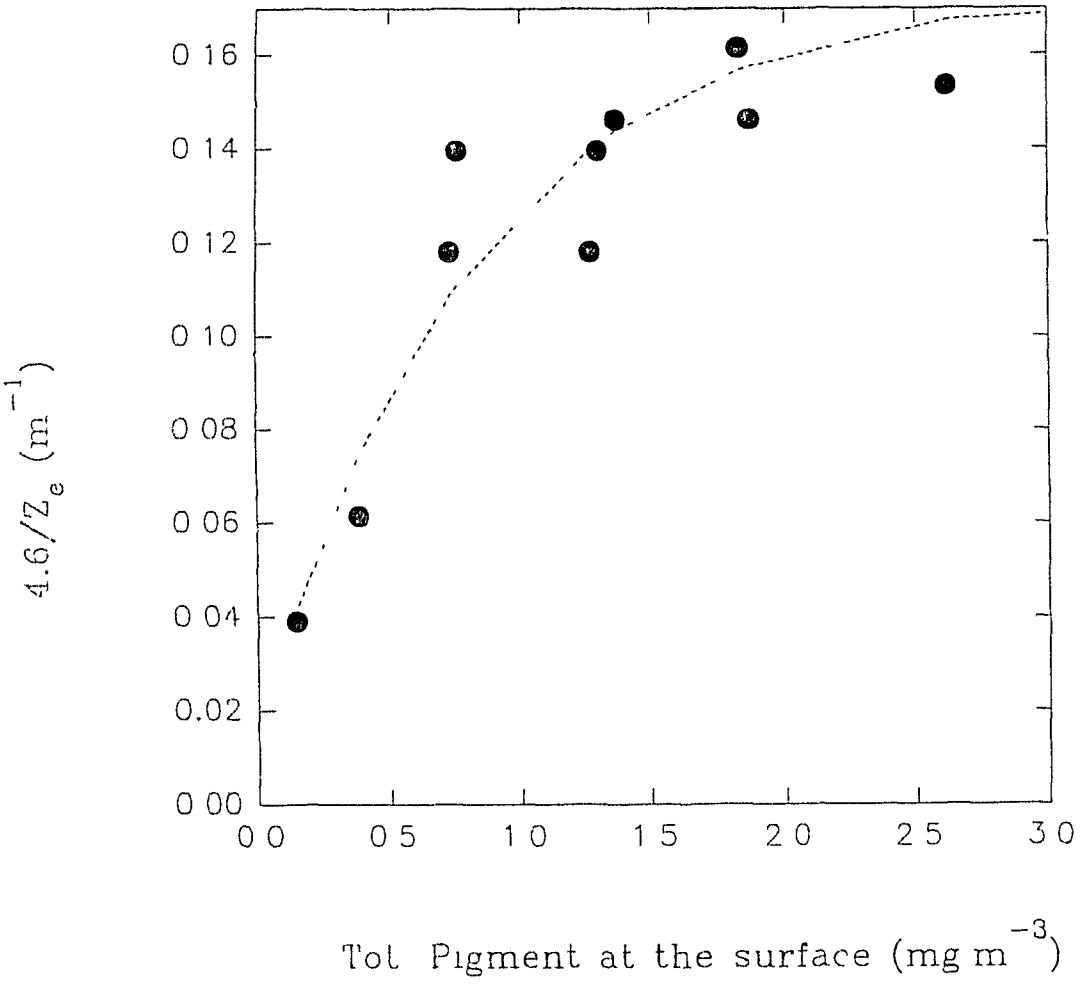

FIGURE 1 3. Variations of the mean extinction coefficient of light, $\bar{K}$, as measured by Secchi disk, *versus* the concentration of total HPLC pigments at the surface. The dashed line represents Equation 1.6.

Subsurface chlorophyll maximum (SCM). At most of the stations, the SCM (as detected by *in situ* fluorescence) was well above the 1% light level, in close association with the thermocline, probably reflecting the vertical distribution of nutrients. At Station 10, however, the fluorescence data show a uniform layer of maximal values in the upper mixed layer. Over Georges Bank, within the 60 m isobath (Station H), the fluorescence was uniformly distributed with depth, as expected according to the strong vertical mixing occurring in that region. A similar fluorescence profile was observed at Station 6, located at the southwest tip of Nova Scotia, known to be a region affected by strong tidal currents (Fournier *et al.* 1984).

Beam-attenuation coefficient. The profiles of the beam-attenuation coefficient, $c(660)$, correspond well with the fluorescence profiles. In a recent study, mainly conducted in open ocean waters, Kitchen and Zaneveld (1990) observed marked differences between the profiles of these variables. In the present data, on the other hand, fluorescence and beam-attenuation coefficient are generally "in phase" at all stations. The upper mixed layer was usually characterized by high values of $c(660)$, ranging from 0.44 m^{-1}, i.e., nearly as low as pure seawater, at Stations 3 and D in open ocean waters, to 0.9 m^{-1} at Station 10. A layer of maximum turbidity was observed in relation with, or slightly above, the chlorophyll maximum. Deeper in the water column, the beam-attenuation coefficient reached minimum values which were often, in coastal waters, over layers of increased turbidity, corresponding, after Spinrad (1986), to the nepheloid layer with resuspension of bottom material.

1.3.2. Pigment distribution.

Chlorophylls. The concentrations of chl-*a*, measured by HPLC, were lower by 24% on average, than the values estimated using conventional fluorometric methods (Yentsch and Menzel 1963). Similar discrepancies (up to 30%) have been reported earlier and shown to be related to the presence of chlorophyll derivatives which have

identical spectral properties but differ in solvent polarity (Mantoura and Llewellyn 1983, Gieskes and Kraay 1983*a*).

The concentrations of pigments per unit area (integrated over the euphotic zone) are indicated in Table 1.1. Chl-*a* concentrations range from 16.5 mg.m^{-2} in oligotrophic waters (Stations 3 and D), to 62.3 mg.m^{-2} at Station 10. Stations G and H on the central part of Georges Bank show high concentrations, with 44.5 and 40.0 mg.m^{-2} respectively. Concentrations of chl-*b* and -*c* are generally low, with values less than 8.0 mg.m^{-2}. Total chl-*c*, however, was underestimated at some stations which had significant amounts of chl-c_3, such as in stratified waters of the Gulf of Maine. Oceanic waters (Stations 3 and D) show the lowest values of chl-$(c_1 + c_2)$. The horizontal distribution of chl-*b* is somewhat inversely related to that of chl-*c*, i.e., the proportion of chlorophyll-*b* increases with distance offshore.

Except over the well-mixed Georges Bank, the vertical distribution of chlorophylls is characterized by a general increase with depth until it reaches a subsurface maximum (Fig. 1.4). Compared with its concentration at the surface, chl-*a* increased by a factor ranging from 2.5 at coastal stations to 6 in open ocean waters. The variations with depth of chlorophylls-*b* and -*c* are similar, except at Station D where chl-*b* increased significantly more than chl-*c* at the chlorophyll maximum. The ratio of chl-*b* to -*a* varied from 0.07 at the surface to 0.2 below the mixed layer, in both coastal and slope waters. In oceanic waters, the ratio ranged from 0.04 at the surface to 0.56 at the base of the euphotic zone. High chl-*b*/*a* ratios at depth have been found in different marine regions (Vernet and Lorenzen 1987). They reflect either a change in the species composition of the phytoplankton community, or a process of photoadaptation under low light energy.

Recently, prochlorophyte-like cells were discovered in great abundance near the base of the euphotic zone in different marine waters (Chisholm *et al.* 1988, Olson *et al.* 1990). HPLC chromatograms of acidified pigment extract (all forms of

Station	*Chl a*	*Chl b*	*Chl* $c_1 + c_2$	*19'hexanoyl.*	*19'butanoyl.*	*Fucoxan.*	*Peridinin*	*Diadino.*	*Zeaxanthin*	*Allozan.*	*Prasino.*	*β-carot.*
1	29.8	2.44	3.57	10.02	1.28	5.63	2.06	3.13	0.94	0.88	-	0.50
2	28.0	4.89	2.64	4.91	1.39	3.39	2.09	2.01	2.99	0.94	0.76	1.04
3	16.6	4.86	1.02	3.20	1.58	0.47	-	0.53	3.35	0.09	-	-
4	26.5	5.96	2.09	6.10	1.56	2.04	1.18	1.58	4.24	0.29	-	0.22
5	23.0	3.17	2.11	5.65	1.03	2.73	1.61	2.01	1.59	0.81	0.35	0.91
6	18.6	2.86	2.04	2.41	0.79	5.17	0.40	1.58	1.06	0.75	1.03	0 56
7	30.3	2.42	3.88	9.98	1.48	3.39	4.87	3.81	1.81	0.62	0.01	1.13
8	-	-	-	-	-	-	-	-	-	-	-	-
9	30.3	·.54	3.82	7.58	1.59	5.09	3.84	3.72	0.98	0.87	0.24	0.79
10	62.3	2.54	3.82	7.58	1.59	5.09	3.84	3.72	0.98	0.87	0.24	0.79
11	34.7	4.33	4.22	8.19	1.52	5.57	4.99	3.78	1.74	1.23	0.43	1.20
B	32.9	3.38	3.43	9.70	0.82	5.66	1.73	2.64	1.05	1.10	-	0.33
C	36.1	6.60	3.93	9.98	2.12	5.14	2.77	2.36	3.00	0.64	0.71	0.38
D	18.2	4.66	1.38	4.27	2.39	0.83	-	0.69	3.52	0.01	-	-
E	33.8	5.18	4.00	8.36	1.19	5.35	3.01	3.58	1.81	1.59	0.40	1.67
F	28.0	4.41	2.44	7.43	0.97	3.29	0.59	1.49	2.12	1.35	0.18	1.18
G	44.6	3.51	4.22	1.29	0.12	16.55	1.40	3.60	0.87	3.55	0.98	1.38
H	40.0	7.31	3.97	5.06	1.00	7.07	1.43	2.90	1.23	3.07	1.24	1.09
I	33.9	5.65	3.54	5.78	1.90	7.06	1.52	2.93	2.40	1.82	1.53	1.22

TABLE 1.1. Pigments concentrations (in $mg.m^{-2}$) integrated over the euphotic layer, defined as from the surface to the 1% light level.

chloropohyll have been transformed into their respective phaeophytin form) from water samples collected at Station 3, which has a similar pigment distribution to Station D, indicate the presence of these "prochlorophytes" (Fig. 1.5). These are characterized by a divinyl phaeophytin *a* (and *b*)-like pigment (Chisholm *et al.* 1988). The ratio of the divinyl form relative to the "normal" phaeophytin *a* was actually higher at the surface, 0.68, than deeper in the water column (0.59 at 92 m). A similar result was obtained at Station D, with ratios of 0.75 at the surface and 0.51 at 92 m. The chromatograms in Figure 1.5 also show that all forms of phaeophytin *b* are practically absent from surface waters. On the other hand, the divinyl phaeophytin *b* reaches 50% of divinyl phaeophytin *a* at 92 m. The chromatograms of acidified pigment extracts from coastal water samples did not reveal any trace of prochlorophytes.

Carotenoids. Quantitative measurements of chlorophylls and the different forms of carotenoids in a water sample provide valuable information for diagnosis of the dominant algal groups in the water column (Liaaen-Jensen 1985, Hooks *et al.* 1988).

Prymnesiophyceae are usually associated with the carotenoid 19'hexanoyloxy-fucoxanthin (Hooks *et al.* 1988). More specifically, Berger *et al.* (1977) have related this pigment to members of the Gephyrocapsaceae (Prymnesiophyceae coccolithophorid) which includes the widely distributed species *Emiliana huxleyi.* All stations contained 19'-hexanoyloxyfucoxanthin in significant concentration (see Table 1.1). Its proportion relative to chl-*a* is higher than the other carotenoids at 13 of the 18 stations analysed. Large amounts of this pigment are seen in surface waters at Station 1 (Fig. 1.4), within the Northeast Channel, and in Jordan Basin (Station 7). Another significant contribution of this group of algae was observed in the deep chlorophyll maximum at Stations 3 and D, in agreement with other studies in oligotrophic waters based on pigment analysis (Gieskes and Kraay 1986) or microscopic observations (Hoepffner and Haas 1990). *Emiliana huxleyi*, in culture, exhibits ratios of chl-*a* to 19'-hexanoyloxyfucoxanthin ranging from 0.7 to 1.3, depending on

FIGURE 1.4. Vertical distribution of the pigments at selected stations in the western North Atlantic. For each station, the left panel represents the distribution of chlorophylls, whereas the other two panels illustrate the distribution of carotenoids.

Figure 1.4

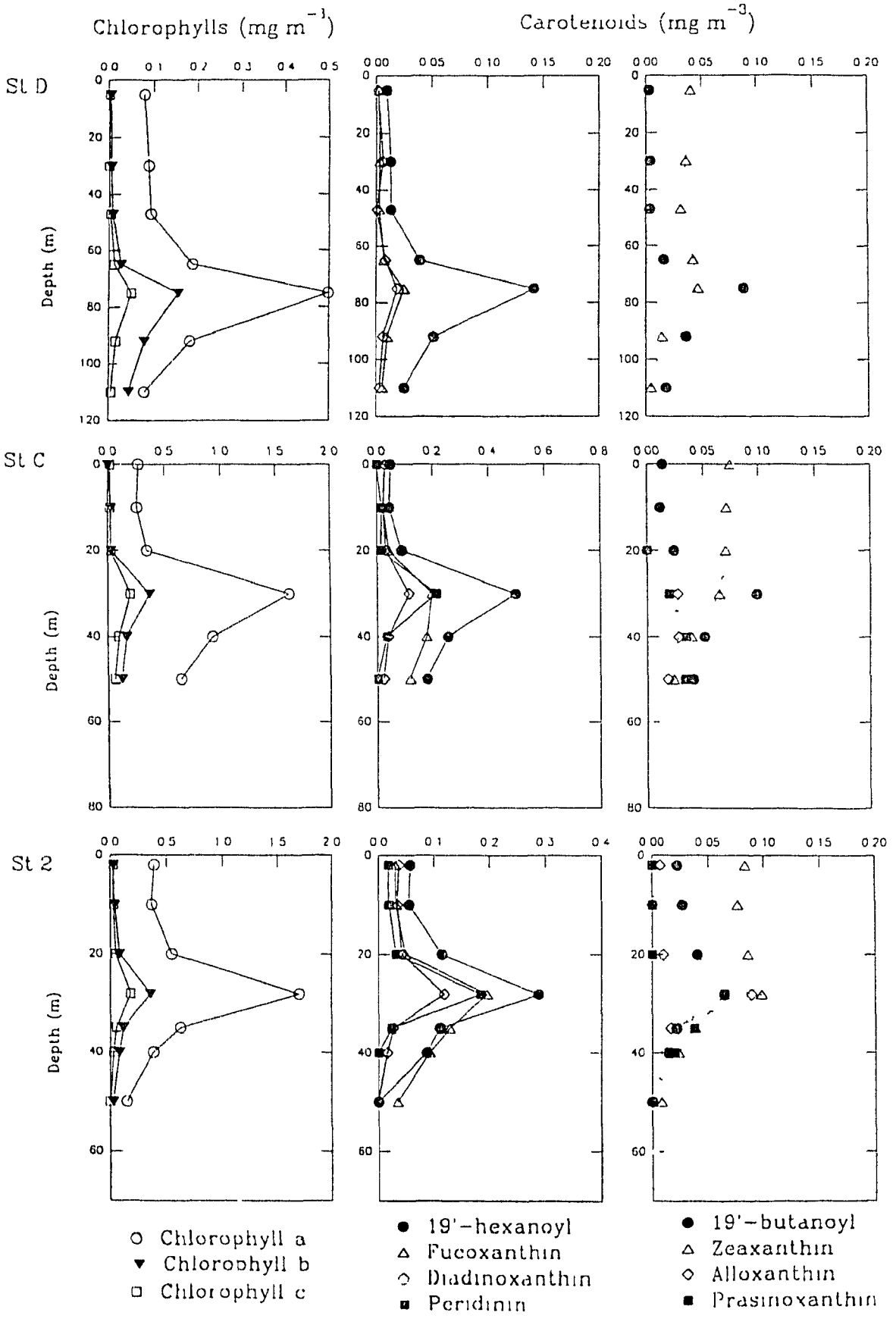
Chlorophylls (mg m^{-3})
Carotenoids (mg m^{-3})
St D
St C
St 2
Depth (m)
Chlorophyll a
Chlorophyll b
Chlorophyll c
19'-hexanoyl
Fucoxanthin
Diadinoxanthin
Peridinin
19'-butanoyl
Zeaxanthin
Alloxanthin
Prasinoxanthin

Figure 1.4

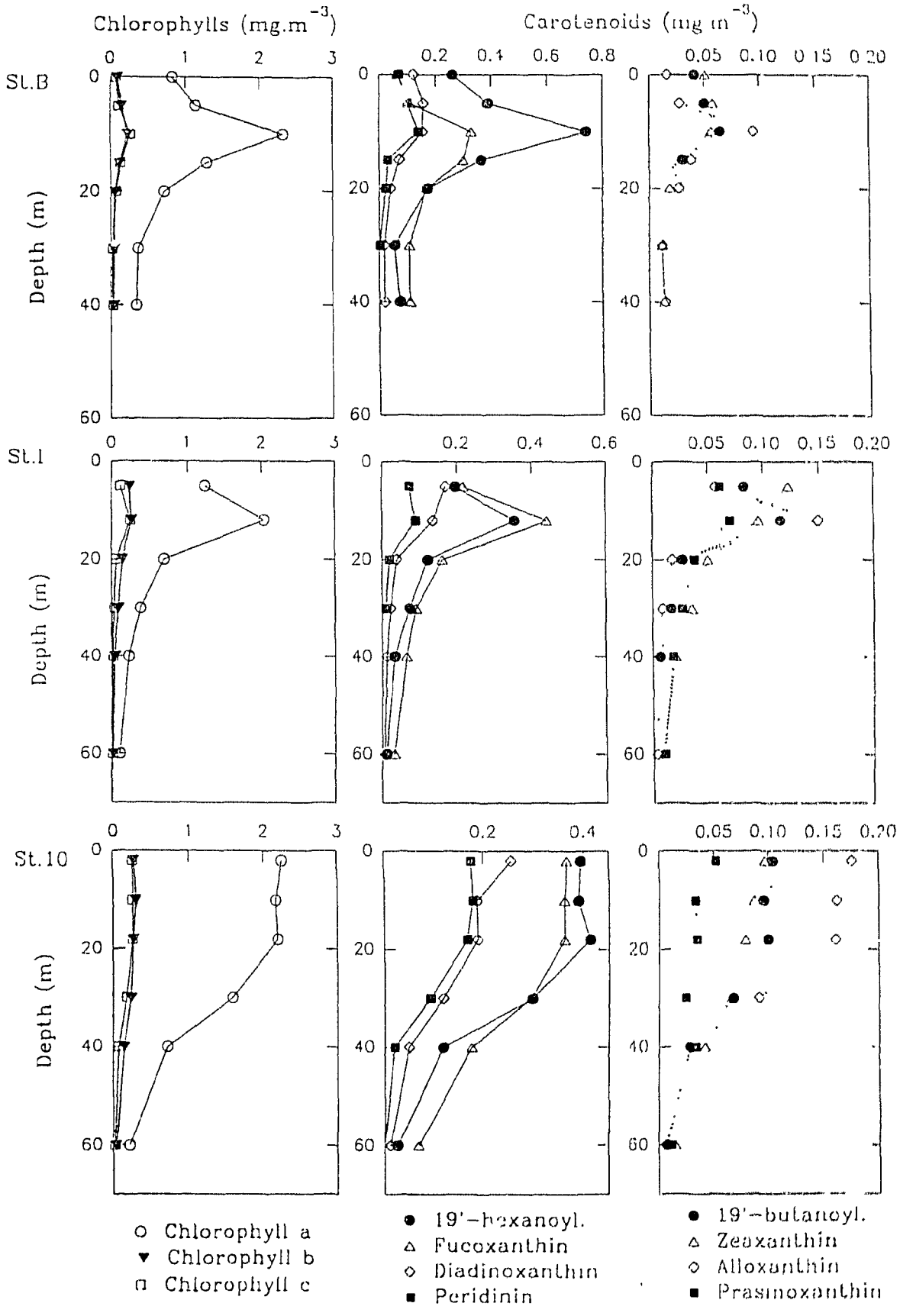
Chlorophylls (mg.m^{-3})
Carotenoids (mg m^{-3})
St.B
St.I
St.10
Depth (m)
Chlorophyll a
Chlorophyll b
Chlorophyll c
19'-hexanoyl.
Fucoxanthin
Diadinoxanthin
Peridinin
19'-butanoyl.
Zeaxanthin
Alloxanthin
Prasinoxanthin

Figure 1.4

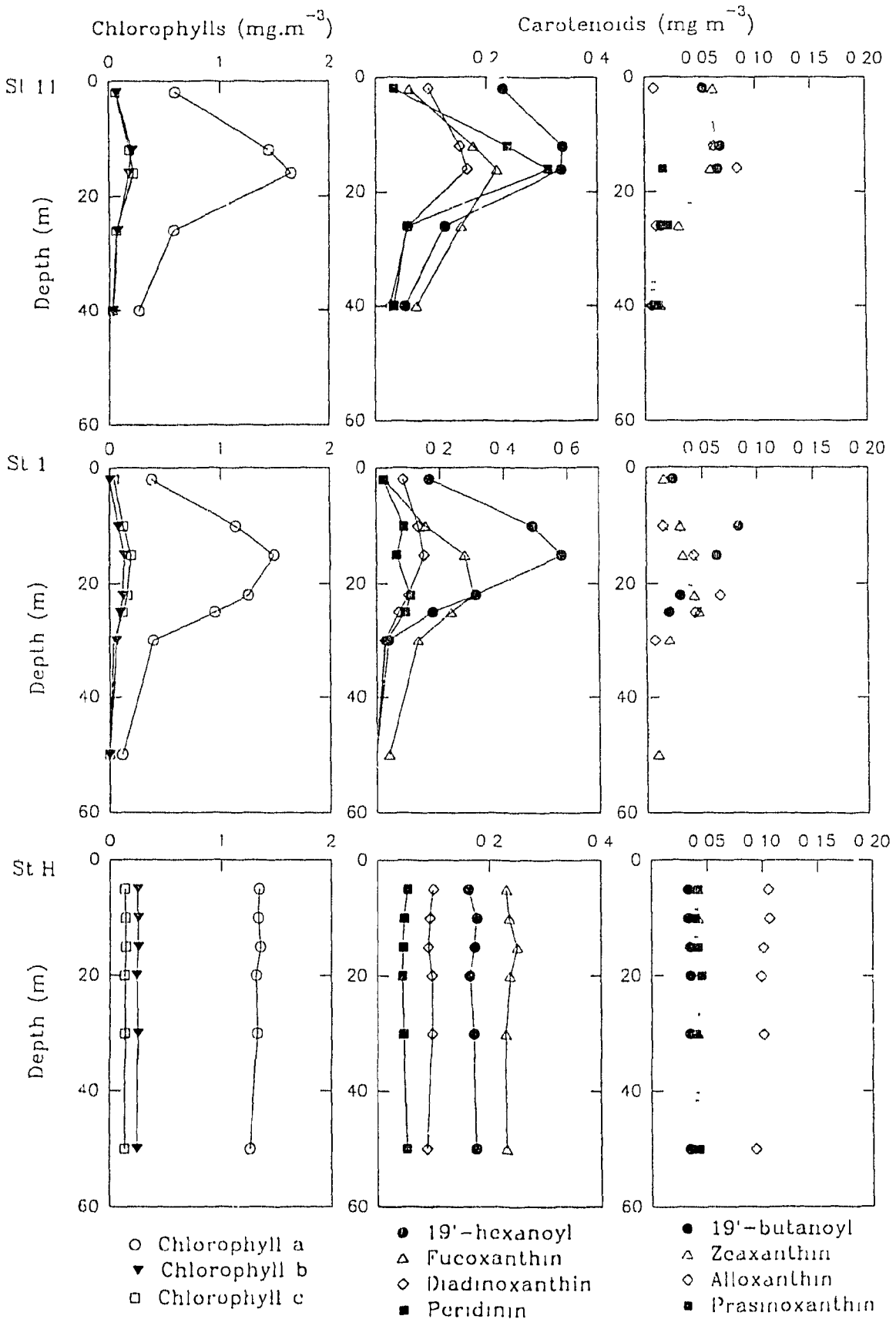
Chlorophylls (mg.m^{-3})
Carotenoids (mg m^{-3})
St 11
St 1
St H
Depth (m)
0
20
40
60
0 1 2
0 2 0 4
0 2 0 4 0 6
0 05 0 10 0 15 0 20
Chlorophyll a
Chlorophyll b
Chlorophyll c
19'-hexanoyl
Fucoxanthin
Diadinoxanthin
Peridinin
19'-butanoyl
Zeaxanthin
Alloxanthin
Prasinoxanthin

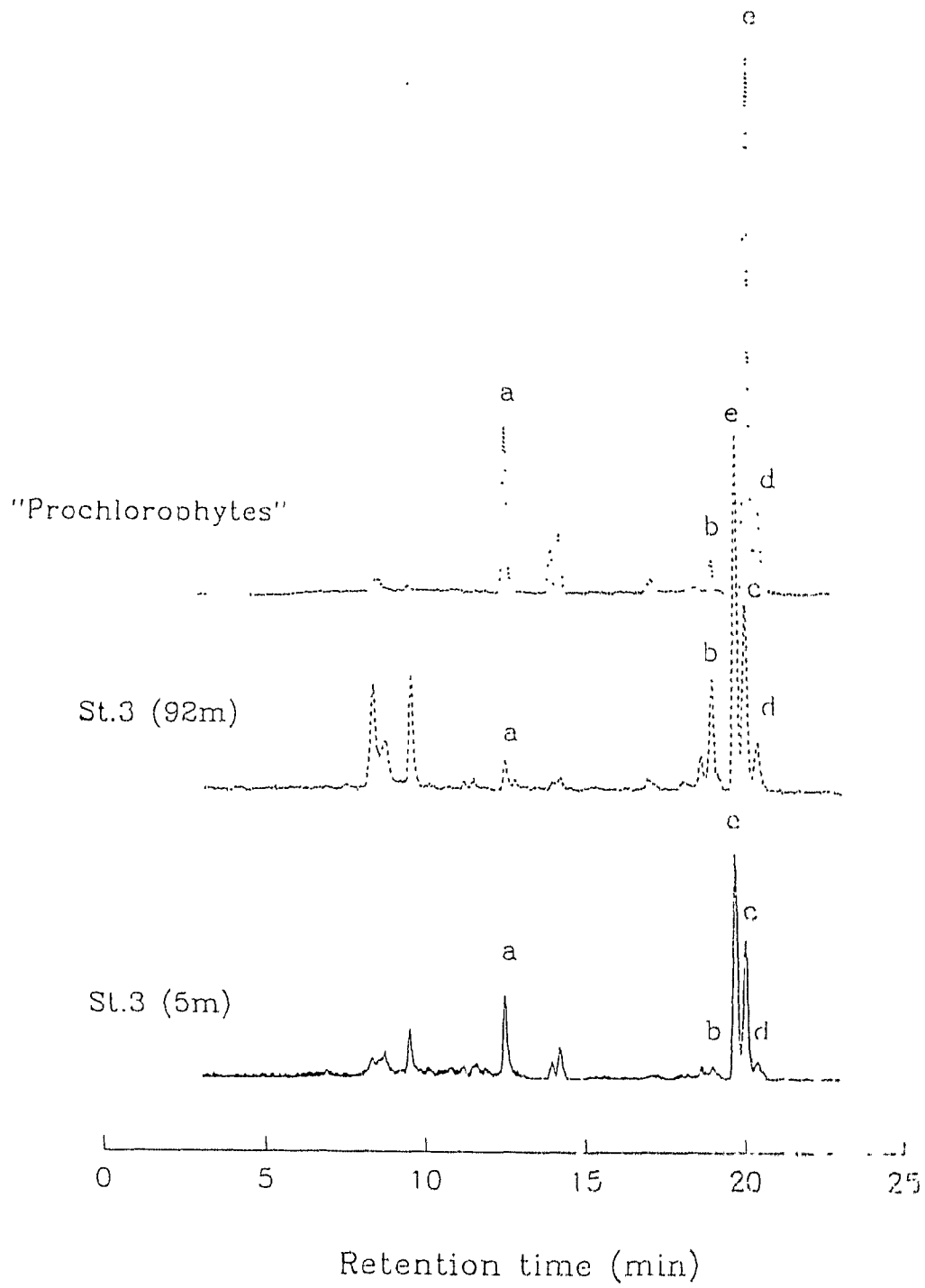

FIGURE 1.5. HPLC chromatograms of two acidified pigment extracts of samples collected at 5m and 92m in oceanic waters (Station 3). For comparison, the acidified chromatogram of a marine prochlorophyte in culture is shown. The peaks are identified as zeaxanthin (a), divinyl-phaeophytin-*b* (b), divinyl-phaeophytin-*a* (c), α-carotene (d), and phaeophytin-*a* (e).

light intensity (unpublished data). Accordingly, the coccolithophorids would be responsible for 30 to 50% of the chl-*a* in surface water at Station 7, and 15 to 25% of the chl-*a* within the SCM at Station 3. In both cases, the occurrence of large amounts of 19' -hexanoyloxyfucoxanthin coincided, on the HPLC chromatograms, with a significant peak in chl-c_3-like pigment which has been identified in several prymnesiophytes (Jeffrey and Wright 1987).

Fucoxanthin was the second most important carotenoid. At Stations 3 and D, however, its concentration per unit area was less than 1.0 mg.m^{-2} (Table 1.1). Fucoxanthin and diadinoxanthin are commonly used as pigment markers for diatoms (Bidigare *et al.* 1989), although these pigments are also present in prymnesiophytes and chrysophytes. It is then difficult to estimate the proportion of each of these algal groups on the basis of fucoxanthin concentration, particularly at stations showing significant amounts of 19'- hexanoyloxyfucoxanthin and 19'-butanoyloxyfucoxanthin which characterize some prymnesiophytes and chrysophytes (Hooks *et al.* 1988, Everitt *et al.* 1990). Over the central part of Georges Bank (Stations G and H) and at Station 6 off the coast of Nova Scotia, fucoxanthin represented the major carotenoid in the water column (see Table 1.1, Fig. 1.4). The ratio of chl-*a* to fucoxanthin for several diatoms in culture averaged 1.6 (unpublished data). Using this factor, diatoms would represent ca. 60% of the phytoplankton population at Station G. An even higher proportion (70-75%) would result if one uses the ratio of 2.0 estimated for two diatoms from a study by Stauber and Jeffrey (1988). Chl-c_3-like pigment was negligible at these stations, supporting further the idea of a population dominated by diatoms, rather than prymnesiophytes or chrysophytes.

Peridinin is a carotenoid typically found in dinoflagellates (Johansen *et al.* 1974). Its concentration per unit area varied from 0 to 4.99 mg.m^{-2}, (not detected at Stations 3 and D, see Table 1.1 and Fig. 1.4). Its importance relative to chl-*a* was usually low, except at three stations in the Gulf of Maine (Stations 7, 9 and 11) where it was 15% or so of the chl-*a* concentration. At these stations,

peridinin concentrations were low at the surface but increased rapidly at depth to become, with 19'-hexanoyloxyfucoxanthin, the major carotenoid within the subsurface chlorophyll maximum (Fig. 1.4). With a peridinin to chl-*a* ratio of 0.42 for the dinoflagellates (Jeffrey *et al.* 1975), these organisms would represent 45 to 55% of the phytoplankton community at this depth.

The cryptophytes are characterized by the carotenoid alloxanthin (Liaaen-Jensen 1985). The relative importance of alloxanthin was highest on Georges Bank where it represented just 8% of the chl-*a* concentration. Gieskes and Kraay (1983*b*) have shown that these organisms can be temporarily abundant in coastal waters. Here, there is no evidence of it (Table 1.1).

The importance of green algae was indicated by the occurrence of chl-*b* and carotenoids such as zeaxanthin, present in chlorophytes, prasinophytes and the marine prokaryote "prochlorophytes" (Liaaen-Jensen 1985, Chisholm *et al.* 1988) and prasinoxanthin, typically found in prasinophytes (Foss *et al.* 1984). Zeaxanthin is also the major carotenoid present in marine cyanobacteria which, on the other hand, do not contain chl-*b* (Guillard *et al.* 1985). In the present data, zeaxanthin-like pigment was present at all stations but its proportion in coastal waters was small when compared to 19'-hexanoyloxyfucoxanthin or fucoxanthin (Table 1.1). On average, it represented less than 10% of the chl-*a* concentration. On the contrary, zeaxanthin-like pigment was important in slope waters and in the open ocean, becoming even the major carotenoid in the upper mixed layer at Stations C and D (Fig. 1.4). The lack of significant amounts of chl-*b* in these waters suggests that a high proportion of zeaxanthin-like pigment is due to cyanobacteria, in agreement with previous studies (Hooks *et al.* 1988, Bidigare *et al.* 1989). However, the chromatograms of acidified solvent extracts (Fig. 1.5) indicate that a large number of prochlorophytes was also present in this area. Furthermore, the chromatograms of non-acidified samples from Station 3 and D (not shown) present a high peak of α-carotene instead of β- carotene, which also supports the idea that prochlorophytes

rather than cyanobacteria are responsible for the zeaxanthin-like pigment observed in these waters. Over the continental slope, at Stations 4 and C, β-carotene was identified in the chromatograms only as a shoulder on the α-carotene peak. On the other hand, in coastal waters, β-carotene was the dominant carotenoid. This, in combination with the lack of divinyl phaeophytin *a*-like pigment in the acidified chromatograms points to the absence of prochlorophytes in these waters.

The importance of prasinophytes can be estimated by the concentration of prasinoxanthin. The identification of this pigment on the chromatograms was, however, uncertain since its elution time, using the HPLC technique described here, may be very close to that of neoxanthin, characteristic of chlorophytes. In any case, the proportion of this pigment in the euphotic layer never exceeded 3% of the chl-*a*. This pigment was usually present at depth in coastal stations (Fig. 1.4).

At Station 2, the vertical distribution of pigments resembled that of deep water stations, in the sense that zeaxanthin-like pigment was the dominant carotenoid in the upper mixed layer (Fig. 1.4), although it is a coastal station (depth less than 100 m) on the southern edge of Georges Bank. This reflects the influence of open-ocean waters intruding episodically onto Georges Bank area (Butman and Beardsley 1987). At the time of the cruise, AVHRR images for this area indicated clearly the presence of a Gulf Stream eddy butting up against the shelf (L.P. Shapiro, pers. comm.).

1.3.3. In vivo absorption spectra of particulate material. When normalized to the biomass (i.e. chl-*a* concentration), the absorption coefficient of total particles, a_t^*, at 440 nm varies from 0.04 to 0.12 $m^2(mgChl\text{-}a)^{-1}$, and shows slightly higher values at low chlorophyll concentrations (Fig. 1.6a). A similar trend is also seen in $a_d^*(440)$, the absorption coefficient of particles after extraction, though this parameter is highly variable at chl-*a* concentrations less than 0.5 $mg.m^{-3}$ (Fig. 1.6b). The high values of $a_d^*(440)$ correspond to samples from the base of the euphotic zone for

several coastal stations, and the entire water column at Station 6. In open-ocean waters with low chlorophyll concentrations, $a_d^*(440)$ was low, with values similar to those recorded for high chlorophyll concentrations in coastal stations.

The absorption coefficient of phytoplankton was obtained as the difference between the absorption coefficient for particles before and after extraction of pigments. Values of specific absorption coefficient of phytoplankton, ($a_{ph}^* = a_t^* - a_d^*$), also showed some variability at 440 nm, ranging from 0.03 to 0.1 $m^2(mgChl\text{-}a)^{-1}$ (Fig. 1.6c), but showed no dependence on the chlorophyll concentrations. A similar range in $a_{ph}^*(440)$ values has been reported for different oceanic regimes using different methods of measurement (Prieur and Sathyendranath 1981, Bricaud and Stramski 1990). The mean value of $a_{ph}^*(440)$ in the euphotic zone decreased from offshore stations to the shallowest area on Georges Bank. In open ocean, $a_{ph}^*(440)$ values averaged 0.064 $m^2(mgChl\text{-}a)^{-1}$ (including Station 2 in the calculation). In the Gulf of Maine, the mean $a_{ph}^*(440)$ was 0.050 $m^2(mgChl\text{-}a)^{-1}$, whereas on the central part of Georges Bank, this value was 0.037 $m^2(mgChl\text{-}a)^{-1}$. The estimation of an averaged $a_{ph}^*(440)$ value in the Gulf of Maine did not include Station 1. The high specific absorption coefficient observed at this station in the blue part of the spectrum (Fig. 1.7) was probably due to a large amount of phaeopigment in the water column, as suggested by a significant shift of the absorption maximum toward shorter wavelength (c.a. 430 nm and less).

A general trend in the variations of $a_{ph}^*(440)$ with depth was difficult to discern. At a few stations (*e.g.* Stations 10 and 11, Fig. 1.7), a slight decrease in $a_{ph}^*(440)$ with depth was observed, probably as a consequence of photoadaptation, e.g. an increase in the pigment content of the cells. On the other hand, a change of species was probably at the origin of the low value of $a_{ph}^*(440)$ observed in the deepest sample at Station C (Fig. 1.7). The fucoxanthin profile for this station (Fig. 1.4) suggests an accumulation of diatoms at the base of the euphotic zone. No explanation has been found for the low values of $a_{ph}^*(\lambda)$ observed at 20 m at Station

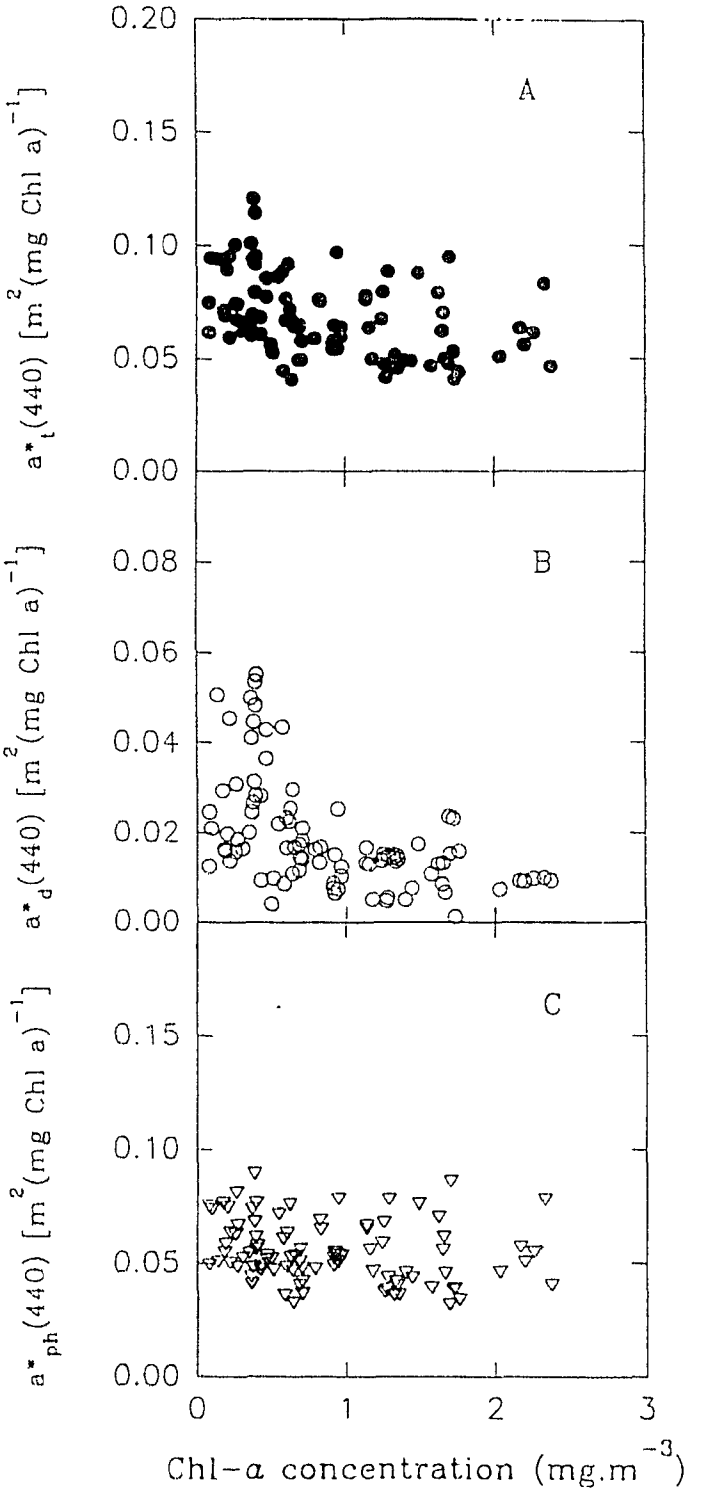

FIGURE 1.6. Variations in the specific *in vivo* absorption coefficient at 440 nm for total particles (A), detritus (B), and phytoplankton (C), as a function of the concentration of chl-*a* in the sample.

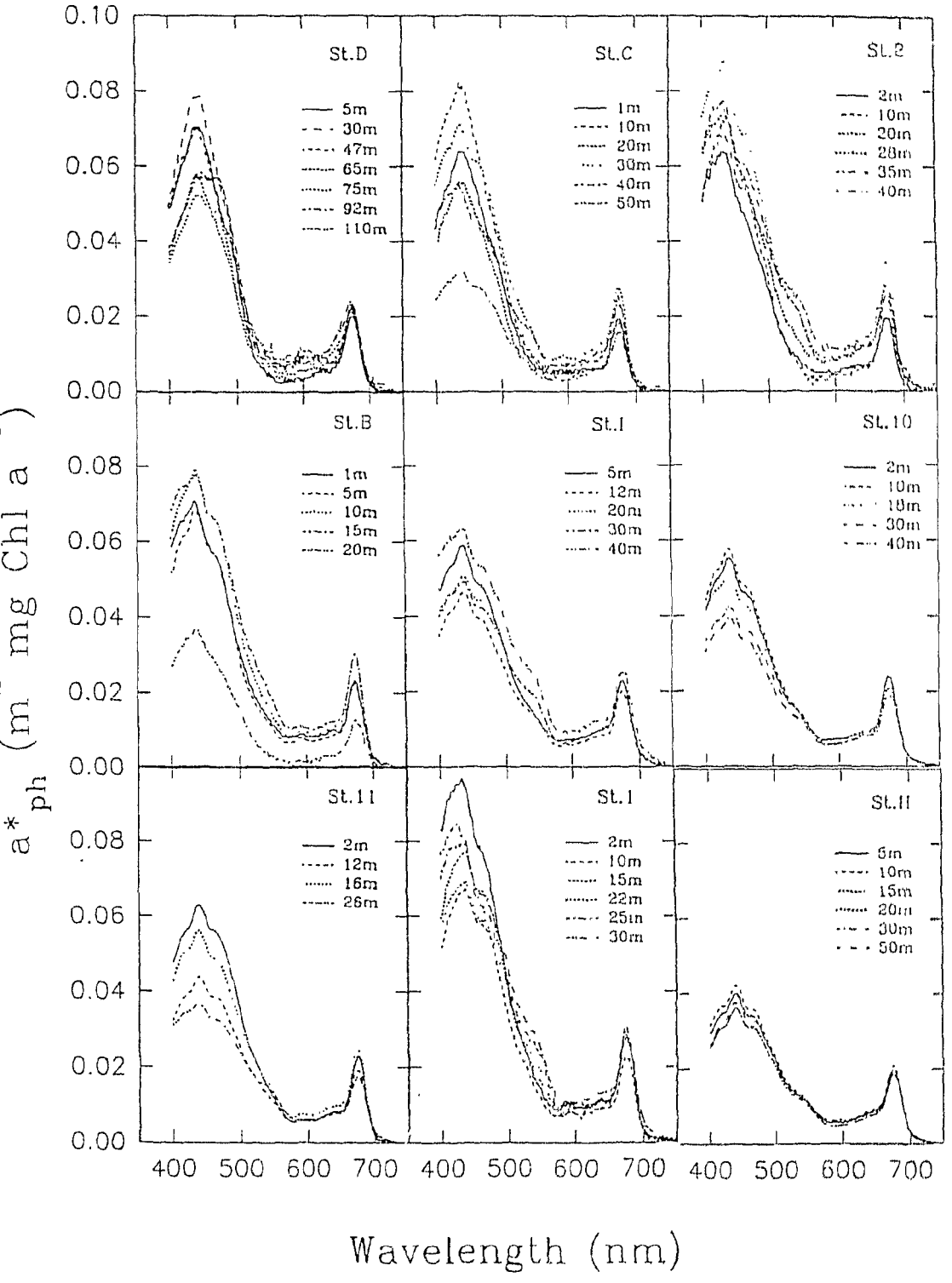

FIGURE 1.7. Spectra of the specific absorption coefficient of phytoplankton at selected stations in the western North Atlantic. Spectra at different depths are presented for each station.

B (Fig. 1.7), and could merely be an error (overestimation) in the chlorophyll concentration or a technical difficulty during the filtration of that sample.

The variability of a^*_{ph} at 674 nm was less than that of 440 nm (Fig. 1.7). The mean value of $a^*_{ph}(674)$ for all stations was 0.025 $m^2(mgChl\text{-}a)^{-1}$, ranging from 0.013 $m^2(mgChl\text{-}a)^{-1}$ at Station B (20 m depth) to 0.034 $m^2(mgChl\text{-}a)^{-1}$. The highest values coincided with absorption spectra that showed evidence of a significant amount of phaeopigment in the sample, for example at Station 1 and, to a lesser extent, at Station 2, where the maximum absorption in the blue region of the spectrum was shifted toward shorter wavelengths. The value of 0.025 $m^2(mgChl\text{-}a)^{-1}$ is slightly higher than other *in situ* values reported in the literature (Maske and Haardt 1987, Bricaud and Stramski 1990), probably because of the differences noted between chl-*a* concentration as measured by HPLC and by other methods.

Variations in the shape of the specific absorption spectrum of phytoplankton were analysed after normalization of $a^*_{ph}(\lambda)$ to its value at 440 nm (Fig. 1.8). Almost all stations with a stratified water column presented a notable change with depth in the shape of the absorption spectra. A distinction, however, should be made between open ocean and Gulf of Maine waters. In open ocean waters, $a^*_{ph}(\lambda)$ to $a^*_{ph}(440)$ ratio increased drastically in the 460-470 nm range, from the bottom of the mixed layer to the base of the euphotic zone (Fig. 1.8a). This feature is related to an increase in chl-*b* relative to chl-*a*, also observed in the pigment profiles at the same station (Fig. 1.4). Moreover, an enhancement of absorption was also observed at depth at around 650 nm, which corresponds to the absorption maximum for chlorophyll-*b* in the red part of the spectrum. Within the mixed layer, the normalized absorption spectra present a sharp peak at 446-448 nm. The peak position is shifted slightly toward higher wavelengths compared with what is observed at the other stations (maximum between 435-440 nm). Such a shift has been reported for absorption by prochlorophytes (Chisholm *et al.* 1988), and in a deep sample from the Sargasso Sea by Bricaud and Stramski (1990).

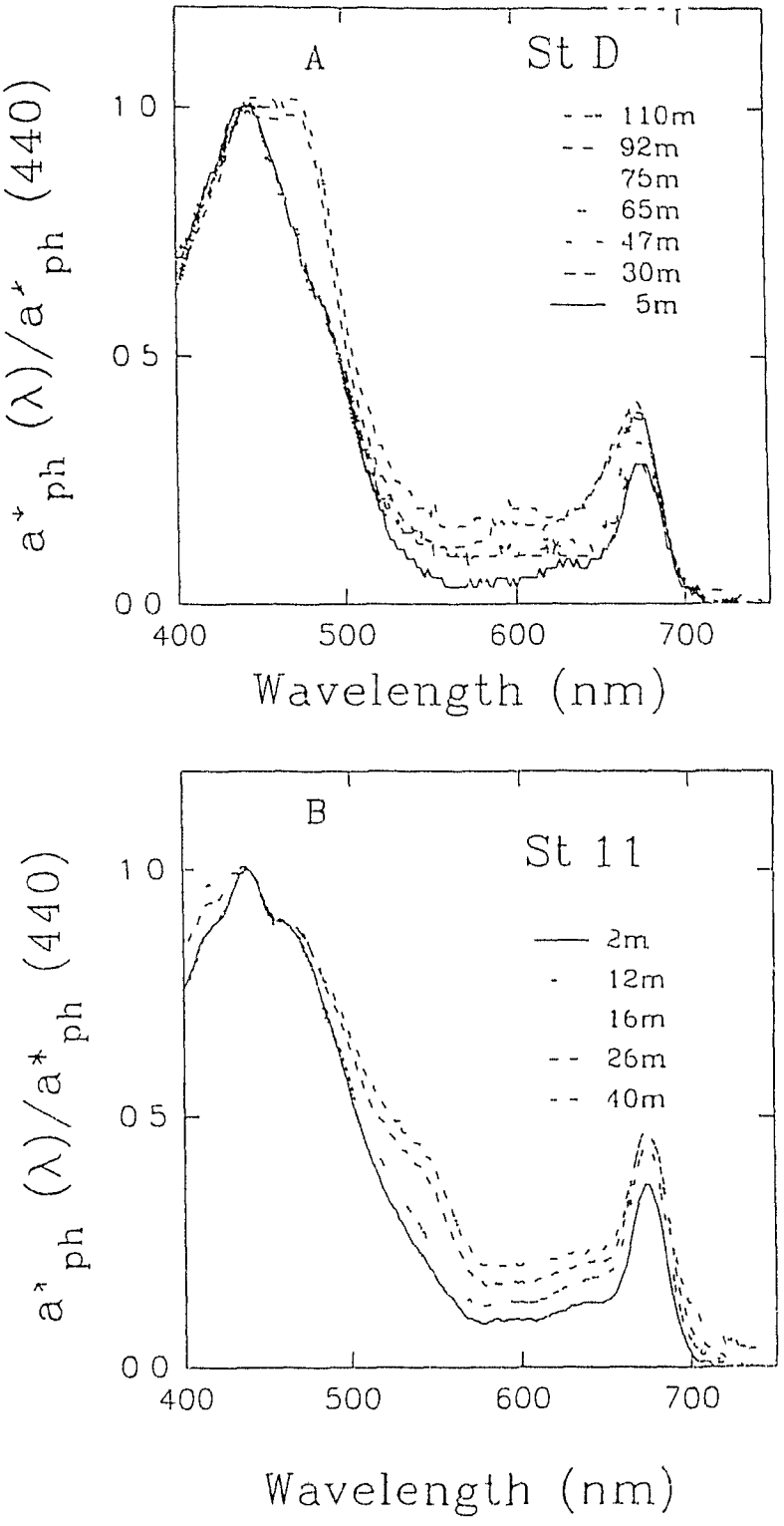

FIGURE 1.8. Variations in the shape of the absorption spectrum of phytoplankton, after normalization at 440 nm, in open-ocean waters (Station D) and in coastal waters (Station 11).

In coastal regions, the most significant change in the specific absorption spectra with depth occurred in the wavelengths between 510 to 570 nm (Fig. 1.8b). The increase in the relative specific absorption coefficient within this range, observed at depths below the chlorophyll maximum, was related to an increase in the carotenoid concentration relative to chl-*a*. A similar feature appeared in samples from Station G and H (Fig. 1.7). A positive correlation (r = 0.86, n = 56) was found between the relative absorption at 550 nm and ratio of fucoxanthin to chl-*a*. This is in agreement with the observations of Goedheer (1970), who noted high absorption at this wavelength in the *in vivo* absorption spectrum of the brown algae *Laminaria digitata*, and attributed it to fucoxanthin.

1.4. Discussion

1.4.1. The role of phytoplankton in determining the optical properties of sea water. The beam-attenuation coefficient is an inherent optical property of the water sample and can be expressed as:

$$c(\lambda) = c_w(\lambda) + c_p(\lambda) + a_y(\lambda) \ , \tag{1.7}$$

where $c_w(\lambda)$ is the attenuation coefficient of pure sea water, $c_p(\lambda)$ is the attenuation coefficient of the particulate material (including phytoplankton) and $a_y(\lambda)$ represents the absorption coefficient of dissolved organic substances. At 660 nm, a_y can be neglected since the dissolved organic substances mostly absorb in the UV and blue parts of the spectrum. Then, with a beam-attenuation coefficient at 660 nm of 0.4 m^{-1} for clear marine waters (Smith and Baker 1981), Equation 1.7 can be rewritten as:

$$c(660) = 0.4 + (B)\, c^*_{ph}(660) + c_d(660) \ , \tag{1.8}$$

where c^*_{ph} is the specific attenuation coefficient of phytoplankton at 660 nm, and B is the phytoplankton biomass as measured by the concentration of chl-a in the water; c_d is the attenuation coefficient of non-chlorophyllous particles. Using Equation 1.8, the contribution to the attenuation coefficient of phytoplankton and associated matter, relative to other particulate material, can be assessed by relating the *in situ* fluorescence to the beam-attenuation coefficient (Fig. 1.9). The plots were made for three representative stations, each of them having slight differences in their turbidity profile (Fig. 1.2). At two of the three stations, the plots are $\wedge$-shaped, comparable with the data obtained by Denman and Gargett (1988) and Kitchen and Zaneveld (1990). From the surface to the chlorophyll maximum, the relationship between $c(660)$ and fluorescence varied from one station to another, depending on the strength of vertical mixing in the upper layer, as well as biological processes. At Station 10, no significant changes in the values of $c(660)$ and fluorescence were observed in that portion of the plot, as expected from the profile shown in Figure 1.2. At Station 11 and D, the fluorescence signal increased without significant variation of the beam-attenuation coefficient. This result suggests that photoadaptation, rather than an accumulation of cells, is responsible for the subsurface chlorophyll maximum at these stations. Here, the pigment data suggest that the photoadaptative mechanism might be a change in the chlorophyll content per cell. Denman and Gargett (1988) have also suggested that photoadaptation was responsible for such phenomena, but they related this photoadaptative process to a photoinhibition of fluorescence at the surface. Neori *et al.* (1984) have also concluded that photoadaptation was the principal mechanism responsible for changes in absorption and fluorescence properties of phytoplankton with depth.

In the section between the subsurface chlorophyll maximum (SCM) and the deep turbidity minimum (DTM), $c(660)$ values decreased in a linear fashion with fluorescence (Fig. 1.9). For all stations, the linear fit to the data for this portion of the curve intercepted the x-axis at $c(660)$ values ranging from 0.37 to 0.71 m^{-1}.

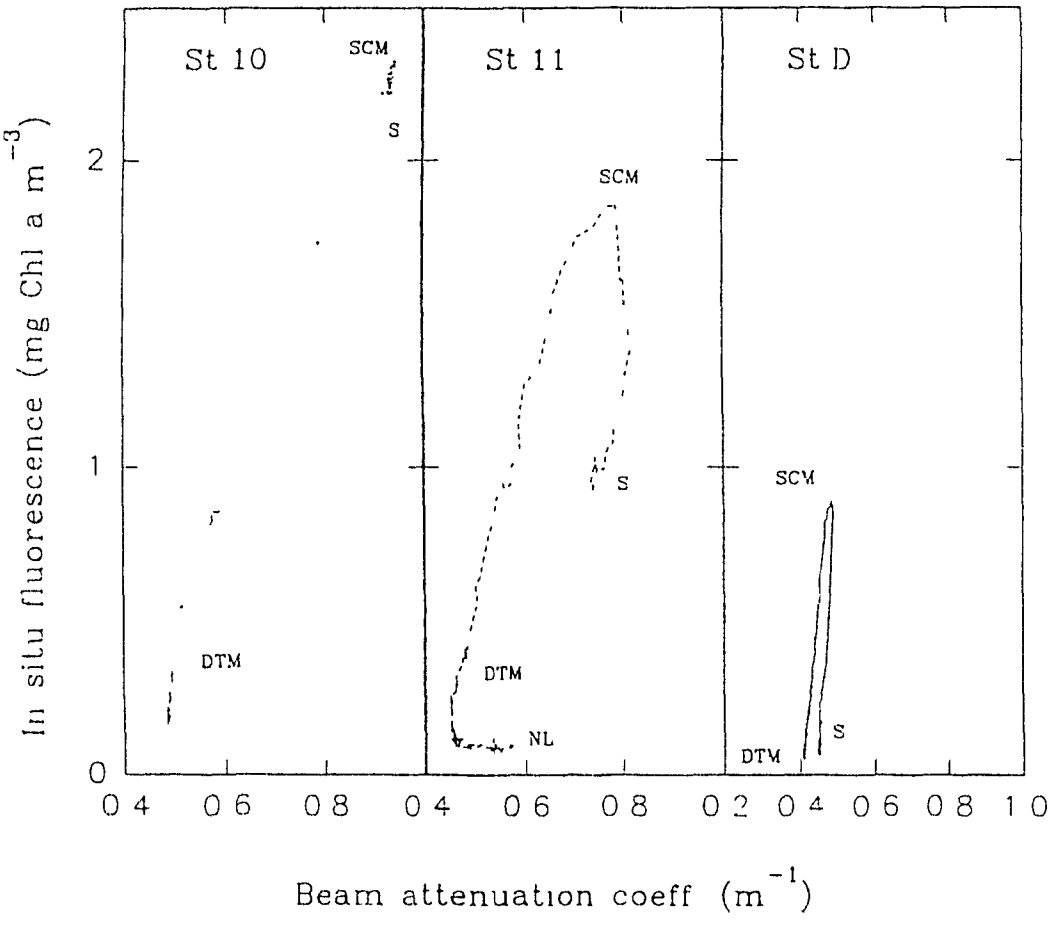

FIGURE 1.9. *In situ* fluorescence *versus* beam-attenuation coefficient at 660 nm for three stations. The surface (S), the subsurface chlorophyll maximum (SCM), the deep turbidity minimum (DTM), and the bottom nepheloid layer (NL) are indicated along each plot.

The highest intercepts were observed at stations with shallow and entirely mixed water columns, in the central part of the Georges Bank, as well as off the southwest coast of Nova Scotia, indicative of a resuspension of sediments within the water column. On average over all stations, the intercept was 0.45 m^{-1}, which is very close to the attenuation coefficient at 660 nm of the clearest water, 0.40 m^{-1} (Smith and Baker 1981). Spinrad (1986) has characterized particle-free water within the Gulf of Maine by a value of $c(660)$ less than 0.46 m^{-1}.

Therefore, at most of the stations, phytoplankton and covarying particulate material can be considered the major component affecting the attenuation coefficients in that section of the water column which lies between the chlorophyll maximum and the deep turbidity minimum. Further evidence of this result is observed from the correlation between the beam-attenuation coefficient at 660 nm and the absorption coefficient of phytoplankton at the same wavelength. Over the entire euphotic zone, the linear fit to the data explains 65% (n = 108, $P < 0.05$) of the variance. The regression line intercepts the y-axis at a value of $c(660) = 0.47$ m^{-1}, again very close to the value proposed for the clearest water. The absorption coefficients of the particles after extraction of pigments (Fig. 1.6b) show that, in the open ocean and slope waters, absorbing material other than algal pigments accounted, at the most, for 30% of total absorption by particles in the blue. This contribution increased in the Gulf of Maine and on the central part of Georges Bank to 38% and 47% respectively due to physical forcing and shallower water depth, allowing for a resuspension of non-algal particulate matter in the euphotic zone.

The slope of the linear regression between (SCM) and (DTM) in Figure 1.9 should provide a measure of the specific beam attenuation coefficient of phytoplankton at 660 nm, $c^*_{ph}(660)$. These values ranged from 0.09 $m^2(mgChl\text{-}a)^{-1}$ at oceanic stations (Stations 3 and D) to 0.57 $m^2(mgChl\text{-}a)^{-1}$ at Station E on Georges Bank. Bricaud *et al.* (1988) have estimated specific attenuation coefficient for different species in culture. Their values at 660 nm range from 0.05 to 0.5 $m^2(mgChl\text{-}a)^{-1}$

approximately, with an average of about 0.2 $m^2(mgChl\text{-}a)^{-1}$, very similar to the present *in situ* observations. It is interesting to note that the low values of $c^*_{ph}(660)$ in Bricaud *et al.* (1988) are associated with Chlorophyceae, whereas the high values seem to be associated with diatoms. A similar distinction can be made with the present *in situ* data in terms of beam-attenuation coefficients, pigment distribution and phytoplankton groups. Low values of $c^*_{ph}(660)$ are strictly observed in oceanic waters characterized by cells containing chl-*b*, whose HPLC signature suggest affiliation to the Prochlorophyceae. On the other hand, high values of $c^*_{ph}(660)$ are recorded over the Georges Bank where diatoms seem to dominate the phytoplankton community. In a recent study (Balch *et al.* 1991), the highest values of the beam-attenuation coefficient within the Gulf of Maine were observed in waters with a dominant population of Coccolithophoridae (Prymnesiophyceae). This case, however, corresponded to a bloom period of the species *Emiliana huxleyi*, which represented almost the entire phytoplankton community. The body scales (i.e., coccoliths) of this organism increase significantly the scattering properties of each cell (Bricaud and Morel 1986) and, consequently, the beam-attenuation coefficient of seawater. Here, although large amount of Prymnesiophyceae are reported from pigment analyses, there is no evidence of such blooms which tend to occur earlier in the summer (ca. June-July, Balch *et al* 1991). Also, the effect of coccoliths on the beam-attenuation coefficient is more pronounced in the blue and blue-green part of the spectrum (Balch *et al.* 1991), than at 660 nm as measured here.

Thus, it is clear that the variability in the optical properties of sea water in the western North Atlantic results mostly from a diversification in the phytoplankton community. A similar observation has been reported by Yentsch and Phinney (1989) from a study in the same area at different periods.

1.4.2. Importance of intracellular pigment composition in the variability of $a^*_{ph}(440)$. Changes in the value of $a^*_{ph}(440)$ can result from either one or both of the two following factors (Morel and Bricaud 1981, Sathyendranath *et al.*

1987): 1) the "package effect", known to flatten the absorption spectra of particles with increasing size and intracellular pigment concentration; and 2) a change in the pigment composition, mainly occurring with variations in the species composition within the phytoplankton community. Yentsch and Phinney (1989) give primary importance to size effect to explain the differences in the averaged value of $a^*(440)$ between open ocean waters and the Gulf of Maine (including Georges Bank). However, flow-cytometric data taken during the cruise, at Stations 1 to 10 (i.e. excluding Georges Bank, see Fig. 1.1), did not show any difference in the size distribution of chlorophyllous particles (in the 3-30 μm size range) between open ocean and Gulf of Maine waters (T.L. Cucci and L.P. Shapiro, unpublished). The particle frequency increased with decreasing particle diameter, similar to the distribution noticed by Kepkay *et al.* (1990) in the Northeast Channel. On the other hand, Kepkay *et al.* (1990) have observed, over Georges Bank, a size distribution of particles that reaches a distinct maximum at 10 μm, which favors the idea that size effect does contribute to the variability of $a^*_{ph}(440)$ between the Georges Bank proper and its surrounding waters.

On the other hand, open-ocean waters were characterized by cells containing chl-*b*, and the Gulf of Maine by chl-*c* containing cells. From the absorbing characteristics of both pigments (Prézelin 1981), it is likely that the overlap between chl-*a* and -*b* absorbing bands is greater than between bands of chl-*a* and -*c*. As a result, Chlorophyceae shows a higher specific absorption at 440 nm than diatoms or other species containing chl-*c*. Therefore, a higher proportion of chl-*b* in offshore water samples would contribute to an enhancement of $a^*_{ph}(440)$, compared to water samples from the Gulf of Maine which contain mostly chl-*c*.

Variations of $a^*_{ph}(440)$ with depth can also be explained in terms of package effect and changes of pigment composition. As suggested by the fluorescence and beam attenuation profiles, the intracellular pigment content increases with increasing depth at some stations, resulting in a reduction of $a^*_{ph}(440)$ due to a stronger

package effect (*e.g.* Stations 10 and 11, Fig. 1.7). When the samples contain chl-*b*, however, an increase of its relative cellular concentration with depth should somewhat counteract the package effect. This may be true of Station D (Fig. 1.7), where $a^*_{ph}(440)$ slightly decreases in the the mixed layer, and increases below 65 m in relation with an increase in chl-*b* relative to chl-*a*.

1.4.3. Spatial variability in the absorption spectrum of phytoplankton. A clear regional distinction emerges from pigment composition (which parallels changes in shape and amplitude of the specific absorption spectra), when the open-ocean data are compared with data from the Gulf of Maine.

The occurrence of large amounts of 19'- hexanoyloxyfucoxanthin in surface waters of the Gulf of Maine agrees well with recent studies using satellite imagery (Ackleson *et al.* 1988) that show extensive blooms of coccolithophores in this area during summer months. On the other hand, fucoxanthin dominates in the water samples taken from Georges bank. Its identification with diatoms confirms observations by Cura (1987) made at the same location. Gieskes *et al.* (1988) have also established a good correlation between fucoxanthin and the presence of diatoms in water samples from the Banda Sea. Finally, the open-ocean waters are also characterized by the presence of prochlorophytes in surface samples. This is rather surprising at this period of the year, since surface maxima of these prokaryotes in the Sargasso Sea have been observed mostly in winter and spring (Olson *et al.* 1991). Their importance relative to cyanobacteria has been mentioned by Everitt *et al.* (1990) in the western equatorial Pacific.

Following the same zonal distinction, one of the main changes in the shape of the specific absorption spectra of phytoplankton between stations occurred in the region of fucoxanthin absorption. Figure 1.10 shows a considerable increase in the ratio of $a^*_{ph}(550)$ to $a^*_{ph}(440)$ as the proportion of fucoxanthin relative to chl-*a* increases in the surface samples. The lowest ratio (open ocean waters) and

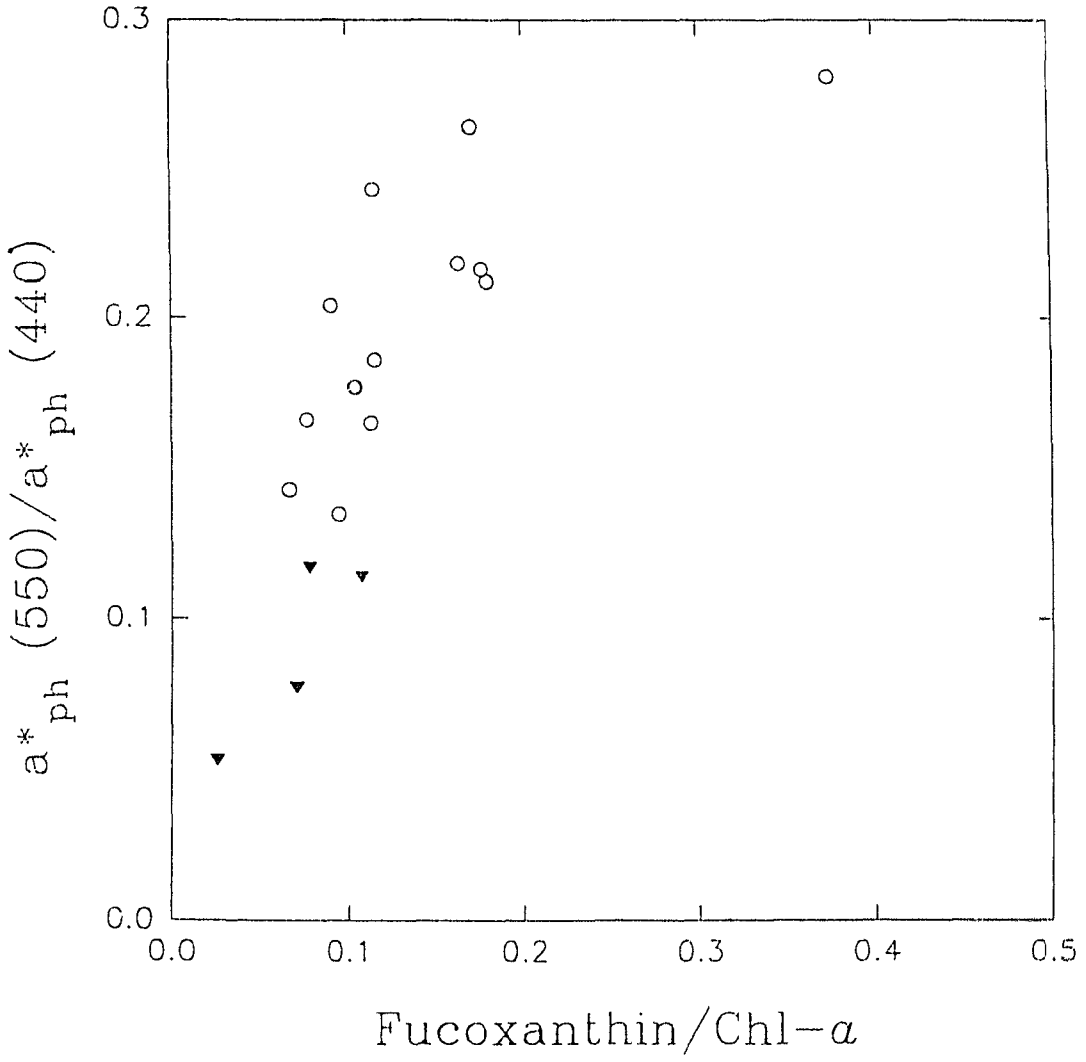

FIGURE 1.10. Ratio of the specific absorption coefficient of phytoplankton at 550 nm to that at 440 nm, as a function of the ratio of fucoxanthin to chl-*a*.

the highest one observed on the central part of Georges Bank differed by a factor of six. Yentsch and Phinney (1982) reported values of green:blue absorption ratio varying from 0.3 to 0.47 for populations dominated by diatoms and dinoflagellates (surface and deep samples), very close to the surface values observed on the central part of Georges Bank. This result can be of direct importance in remote-sensing studies that use the reflectances of sea water at 440 and 550 nm to estimate chl-*a* concentration.

1.5. Conclusions

The data show that variations in both the beam-attenuation coefficient and the absorption coefficient of particulate material in the western North Atlantic are dictated largely by variations in the phytoplankton population. This is true even of Georges Bank, even though the contributions by non -algal particles are relatively more important here than in the open-ocean waters. The study reveals systematic regional differences in the specific optical properties, i.e., in the absorption and the beam-attenuation coefficients normalized to chlorophyll concentrations. Comparison with pigment data from the same stations suggests that these differences are associated with changes in phytoplankton community structure.

A clear regional distinction appears in pigment composition and phytoplankton groups. Offshore stratified waters are typically represented by cells whose HPLC signatures suggest affiliation to the Prochlorophyceae. Within the Gulf of Maine, Prymnesiophyceae appear to dominate in stratified waters, and diatoms in the mixed waters over Georges Bank. This distinction parallels changes in shape and amplitude of the specific absorption spectra of phytoplankton. The absorption coefficient at 440 nm normalised to chl-*a* varies over a factor of two. Yentsch and Phinney (1989) attributed this to the effect of changes in the particle size distribution of phytoplankton. The results, in this chapter, point to an additional factor: changes in the relative importance of chl-*b*, with a large absorption band

that overlaps the blue absorption band of chl-*a*. The changes in the shape of the absorption spectrum are also associated with changes in the contributions of auxiliary pigments. The field results support the conclusions of Sathyendranath *et al.* (1987), based on laboratory measurements, that neglecting either the size effect or the pigment composition leads to an incomplete description of variations in the specific absorption spectrum of phytoplankton.

The chlorophyll-specific, beam-attenuation coefficient at 660 nm from this region is variable, ranging from 0.09 to 0.57 m^2(mg Chl-*a*)$^{-1}$. The changes in this parameter also parallel changes in phytoplankton community, with the low values being associated with Prochlorophyte-dominated, open-ocean waters, and the high values with diatom-dominated Georges Bank waters.

The optical properties also show clear structure in the vertical dimension. This is related to vertical stability of the water column and to photoadaptation. The effects of these physical and biological processes are seen both in the beam-attenuation coefficient and in the absorption spectra. In some stations, the optical properties within the mixed layer show no depth dependence, and probably represent cases where the rate of photoadaptation is low relative to that of turbulence (Lewis *et al.* 1984). Other stations show an increase in chlorophyll fluorescence with depth, which is not accompanied by a change in beam-attenuation, suggesting that the deep chlorophyll maximum at these stations is due to an increase in the amount of chl-*a* per cell, rather than to changes in the number of cells. The pigment data and the absorption spectra indicate that this change may be accompanied by an increase in the relative importance of chl-*b* with respect to chl-*a* as a light-harvesting pigment.

A requirement in oceanography today is the estimation of primary production at large horizontal scale. One approach to this problem is through definition of biogeochemical provinces, within which the parameters of the models may be

considered to be stable. Simultaneous analysis of optical properties and pigment composition provide important information necessary for defining such provinces. The present investigation shows that the western North Atlantic in September can be divided into three provinces, each with its own typical bio- optical characteristics: the open-ocean waters, the stratified waters of the Gulf of Maine, and the mixed waters of Georges Bank. The bio-optical models for these regions can be improved by allowing the optical parameters of phytoplankton to change with the predominant taxonomic group in the province.

A clear change in the spectral shape of phytoplankton absorption is observed in the data, with change in pigment composition. For example, the ratio of the absorption coefficient at 550 nm to the corresponding value at 440 nm is seen to vary by a factor of 6 with changes in the importance of fucoxanthin relative to chl-*a*. Since these wavelengths figure prominently in the algorithms currently in use for estimation of chl-*a* concentrations by remote sensing, these observations point to a possible source of error in these algorithms (see also Yentsch and Phinney 1982). On the other hand, the changes in the shape of the absorption spectrum with changes in phytoplankton community could probably be exploited in the next generation of ocean colour sensors with higher spectral resolution, to differentiate between major phytoplankton pigments and major taxonomic groups of phytoplankton.

CHAPTER 2

Effect of pigment composition on the absorption properties of phytoplankton

2.1. Introduction

To identify the absorption coefficient of phytoplankton at any wavelength λ, it is common practice to express the total absorption coefficient $a_{ph}(\lambda)$ in terms of a "specific absorption coefficient", $a^*_{ph}(\lambda)$, and C, the concentration of chl-*a*, the main pigment in phytoplankton :

$$a_{ph}(\lambda) = C\, a^*_{ph}(\lambda) \tag{2.1}$$

Note that phytoplankton absorption is due to absorption not just by the chlorophyll-*a*, but also by all the auxiliary pigments present. Therefore, $a^*_{ph}(\lambda)$ is not a *true* specific absorption by chl-*a*, but only an *apparent* one. The composition of the auxiliary pigments and the relative importance of their absorption are variable. This variability in pigment composition has been shown to be one of the two important factors responsible for the observed variability in the magnitude and spectral form of $a^*_{ph}(\lambda)$ (Bricaud *et al.* 1983, Sathyendranath *et al*. 1987), the other factor being the particle effect (Duysens 1956, Kirk 1975, Morel and Bricaud 1981). Indeed, the magnitude of a^*_{ph} at 440 nm has been shown to vary over a factor of three (Sathyendranath 1986). The choice of chl-*a* alone for normalization is dictated primarily on practical grounds - chl-*a* is the pigment that is easiest to measure, and it is routinely measured on most biological oceanographic cruises. Its choice is also justifiable in primary production studies because of the central role played by this pigment in photosynthesis. With recent technical developments, however, measurement of auxiliary pigments is becoming more common, and therefore it would be

useful to develop techniques that would account, in a systematic manner, for the consequences of changes in pigment composition on phytoplankton absorption. To do this, Equation 2.1 is rewritten as:

$$a_{ph}(\lambda) = \sum_{i=1}^{n} C_i \, a_i^{\prime}(\lambda) \; , \tag{2.2}$$

where C_i is the concentration of the ith pigment, $a_i^{\prime}(\lambda)$ is the "true" specific absorption coefficient of the ith pigment, and n is the total number of pigments considered (note that chl-*a* is one of the n pigments). To make use of Equation 2.2, the concentrations of the n pigments are required, as well as their specific absorption coefficients.

Very little is known about the *in vivo*, spectral specific absorption coefficients of the major phytoplankton pigments. Bidigare *et al.* (1987) tried to account for the influence of auxiliary pigments, but in the absence of information on the *in vivo* specific absorption coefficients of the pigments, they were obliged to use the values for extracted pigments from a single culture (Mann and Myers 1968). However, absorption by phytoplankton pigments are known to change with extraction(Prézelin and Boczar 1986); besides, estimates from a single culture can hardly be considered to be statistically valid for application to natural populations. Sathyendranath *et al.* (1987) tried to estimate the specific absorption coefficients of major phytoplankton pigments, after correction for the particle effect. But the multiple regression method they used did not yield acceptable values of the specific absorption coefficients because of non-zero covariance among the pigments in the sample set used.

In this chapter, a method for the estimation of *in vivo* specific absorption coefficient of major phytoplankton pigments is outlined. The data of Sathyendranath *et al.* (1987) are reanalysed, but instead of using multiple regression, I have decomposed the spectra into Gaussian absorption bands. This method is statistically more valid, and has the backing of theory as well. The results are based on *in*

vivo spectra that have been corrected for the particle effect, and, therefore, the specific absorption spectra proposed are not influenced by the size of the cells or the intracellular concentration of the pigments. Also, the method is designed for separating absorption by active pigments from any background absorption that may be present. The data consist of *in vivo* absorption spectra of 20 monospecific cultures that were selected to cover three major phytoplankton groups, allowing then a discussion of the results in terms of variability of the absorption characteristics between algal groups. The method separates successfully the absorption due to the different pigments, and, in turn, the specific absorption bands proposed can be used to reconstruct the total absorption coefficient, provided the pigment concentrations are known.

2.2 Material and methods

2.2.1. Bio-optical data *In vivo* absorption spectra, pigment concentrations (chl-*a*, -*b*, -*c* and carotenoids), particle size distribution and cell numbers of twenty different cultures were taken from Sathyendranath *et al.* (1987). Species in culture included three Diatoms (*Chaetoceros protuberans*, *Chaetoceros didymum*, *Skeletonema costatum*), four chlorophyceae (*Dunaliella marina*, *Platymonas suecica*, *Platymonas* sp., *Tetraselmis maculata*) and two Prymnesiophyceae (*Hymenomonas elongata*, *Emiliana huxleyi*), representing major pigment compositions commonly observed in the marine environment (Gieskes and Kraay 1986).

The spectrophotometer was designed with a scattered transmission accessory. It consisted of the sample and reference cells placed very close to the detector, with diffusing plates placed in front of them, to ensure the capture of most of the forward scattered light. The absorption spectra were measured from 340 to 760 nm. The cell size for each culture was estimated from cell volume measurements, and expressed as the diameter of an equivalent sphere. Number of cells per unit

volume was estimated with hemacytometers. To remove the effects of changes in cell size and intracellular pigment concentrations on absorption, all spectra (one spectrum per species) were corrected for the particle effect (Duysens 1956). Morel and Bricaud (1981) and Sathyendranath *et al.* (1987) have shown that this effect can lead to significant modifications in the absorption spectra of phytoplankton. The same algorithms as in Sathyendranath *et al.* (1987)were used, which assume sphericity of the particles and uniform distribution of the absorbing material within the cells. Each absorption spectrum was then corrected for the value at 737 nm, assuming that there is no absorption of light by phytoplankton pigments at this wavelength.

Pigment concentrations were measured spectrophotometrically after extraction in 90% acetone. Chl-*a* was estimated using the equations of Lorenzen (1967); SCOR/UNESCO (1966) equations were used to calculate chl-*b* and -*c*, and the method of Richards and Thomson (1952) was used for carotenoids.

2.2.2. Decomposition of absorption spectra The absorption spectrum from 400 nm to 750 nm of photosynthetic organisms is characterized by a continuous envelope, reflecting a strong coupling in the transfer of the excitation energy between antenna pigment molecules (Förster 1965), until it reaches the photochemical reaction centres in which specialized chlorophyll molecules perform the energy conversion for photosynthesis. The continuous nature of the spectrum renders it difficult to estimate the contribution to the total absorption by each pigment species, unless the spectrum can be suitably decomposed.

One of the simplest theoretical models of absorption is that of Lorentz, which predicts the shape of absorption bands based on the assumption that electrons and ions can be treated as simple harmonic oscillators in an electromagnetic field (Bohren and Huffman 1983). This model has been successfully applied to decompose the spectrum of the imaginary part of the refractive index of the alga *Platymonas*

suecica (Bricaud and Morel 1986). The Lorentz model, however, does not fully account for the effects of overlapping absorption bands and of strong, vibrational interaction between molecules (Knox 1963), as is found in photosynthetic pigments. Toyozawa (1958) proposed a general formalism, which considers the strength of the electron-lattice coupling, for computation of the absorption coefficient. He concluded that, in the presence of a strong interaction between oscillators, an absorption band assumes a Gaussian shape, whereas if the transfer coupling is weak, the absorption tends to a Lorentzian shape.

Empirical evidence on the decomposition of absorption spectra of chl- *a* in solution (Cotton *et al.* 1974, Shipman *et al.* 1976, Katz *et al.* 1977), and of chlorophyll-protein complexes (French *et al.* 1972, Larkum and Barrett 1983), also favours use of Gaussian curves for approximating the individual absorption bands of pigments.

Based on these considerations, absorption spectra in the present study were decomposed using Gaussian curves. A curve-fitting program, initially described by French *et al.* (1967), was slightly modified and adapted to the needs of this study. The input specifications for each absorption spectrum were as follows: 1) only Gaussian curves were used for the curve-fitting analysis; 2) no weighting of the data was done, i.e., all parts of the spectrum were treated as equally important; 3) the program was set up to run a maximum of twenty iterations per spectrum; 4) the wavelength positions (band centre) and the band halfwidths (i.e., 2.35σ) were not allowed to change by more than one nanometer per iteration; 5) the halfwidth is constrained to lie between zero and four times its initial value; 6) the height of each Gaussian band is required to be at least zero.

Since the spectra were corrected for particle effect, the spectral features were emphasized, facilitating the initial estimation of the band parameters according to the presence of peaks and shoulders on the observed spectrum. In the initial runs,

Gaussian parameters	Gaussian band number										
	1	2	3	4	5	6	7	8	9	10	11
Wavelength position (nm)	380	415	440	460	500	545	580	620	645	675	700
Halfwidth (nm)	50	20	40	35	50	30	30	30	30	35	40

TABLE 2.1. Input specifications of the Gaussian parameters for decomposition of absorption spectra of 4 phytoplankton groups. The halfwidth of the right and left side of each band are allowed to vary independently.

eight absorption bands were specified, but it was observed that a better fit was achieved by adding three more bands: one at each extremity of the spectrum, and another at around 550 nm. Therefore, a total of eleven Gaussian curves were used to reflect the absorption spectra. Further increases in the number of bands did not improve the fitting procedure significantly for most of the cultures. Table 2.1 summarizes the input parameters of the Gaussian curves. Wavelength positions and halfwidths (in nm) of the initial guesses were kept the same for all analyses, whereas the initial height of each band (in m^{-1}) was changed according to the biomass in each culture.

2.3. Results

Figure 2.1 shows the observed and estimated absorption spectra for three species from distinct taxonomic groups, together with the results of the decomposition program. In all cases, twenty iterations were sufficient to allow the convergence criterion (percentage difference in standard deviation between successive iterations) of the curve fitting to be less than 0.1%. Maximum deviation of the fitted curve from the observed spectrum was about $\pm$ 0.8 m^{-1}, i.e., less than 1% of the band heights. Maxima of errors are in the 450 to 600 nm region of the spectrum and around 650 nm, which correspond to absorption by accessory pigments.

Table 2.2 indicates the average positions and the halfwidths of the eleven Gaussian curves estimated for the three groups of algae. The peak positions changed little compared to the initial inputs. The halfwidths, however, changed by as much as 19 nm during the computation. Analyses of variances were applied to each of the bands to detect any trends in the variations of the Gaussian parameters (Table 2.3). In almost all cases, the parameters of different algal groups differed more from each other than did the individual values within any one group. In other words, the null hypothesis that the mean squares between and within groups estimate the same variance had to be rejected for all except four of the band centres. In a very

few cases, however, the variances of the data failed to satisfy an homogeneity criterion (Bartlett test, $P < 0.01$). Therefore, a non-parametric method was used in parallel with the analysis of variance (Sokal and Rohlf 1969). No differences were obtained when a Kruskal-Wallis test was used instead of a standard analysis of variances. Both methods showed a substantial "between-group" difference for most of the bands.

For the first band, the statistical analysis (Table 2.3) shows a significant difference between groups in its position ($P < 0.05$) and in its halfwidth ($P < 0.01$). A multiple-range test (Tukey, $P < 0.05$) tends to differentiate the position of this band for the Chlorophyceae from that for the Prymnesiophyceae, whereas the position for Diatoms does not seem to be statistically different from that of the other two groups. On the other hand, the Diatoms have a substantially narrower band than the two other groups (Table 2.2).

Gaussian bands 2 and 3 are centered at 412 and 435 nm, respectively. The analysis of variance on the position of these bands (Table 2.3) did not suggest any difference between the groups of algae. The halfwidths were, however, slightly different ($P < 0.05$) between Diatoms (18.8 and 29.3 nm) and Chlorophyceae (23.3 and 34.7 nm). The Prymnesiophyceae has intermediate halfwidths values of 21.7 and 32.4 nm for band 2 and 3, respectively, which were similar to both the other groups.

The parameters of band 4 are statistically very different between the groups of phytoplankton species. The position of this band is 460.9 nm for Diatoms, which is significantly different from 463.6 nm, the position observed for the Chlorophyceae. The Prymnesiophyceae have an intermediate value of 462.1 nm, not different from that of the two other groups. The halfwidth of band 4 varies very strongly between species, being larger by a factor of 1.7 for Chlorophyceae compared with the two other groups (Table 2.2).

FIGURE 2.1. Observed absorption spectra (solid line) corrected for particle effect, and the corresponding fitted spectra (dashed line) expressed as the sum of 11 Gaussian components for three marine species: (a) Chlorophyceae, (b) Prymnesiophyceae, (c) Diatom. The error curve (difference between observed and fitted curves) of each spectrum is shown in the lower panel. Each error curve is magnified by a factor (indicated in the panel) to avoid changing the ordinate scale. A larger magnification implies a better fit.

Figure 2.1

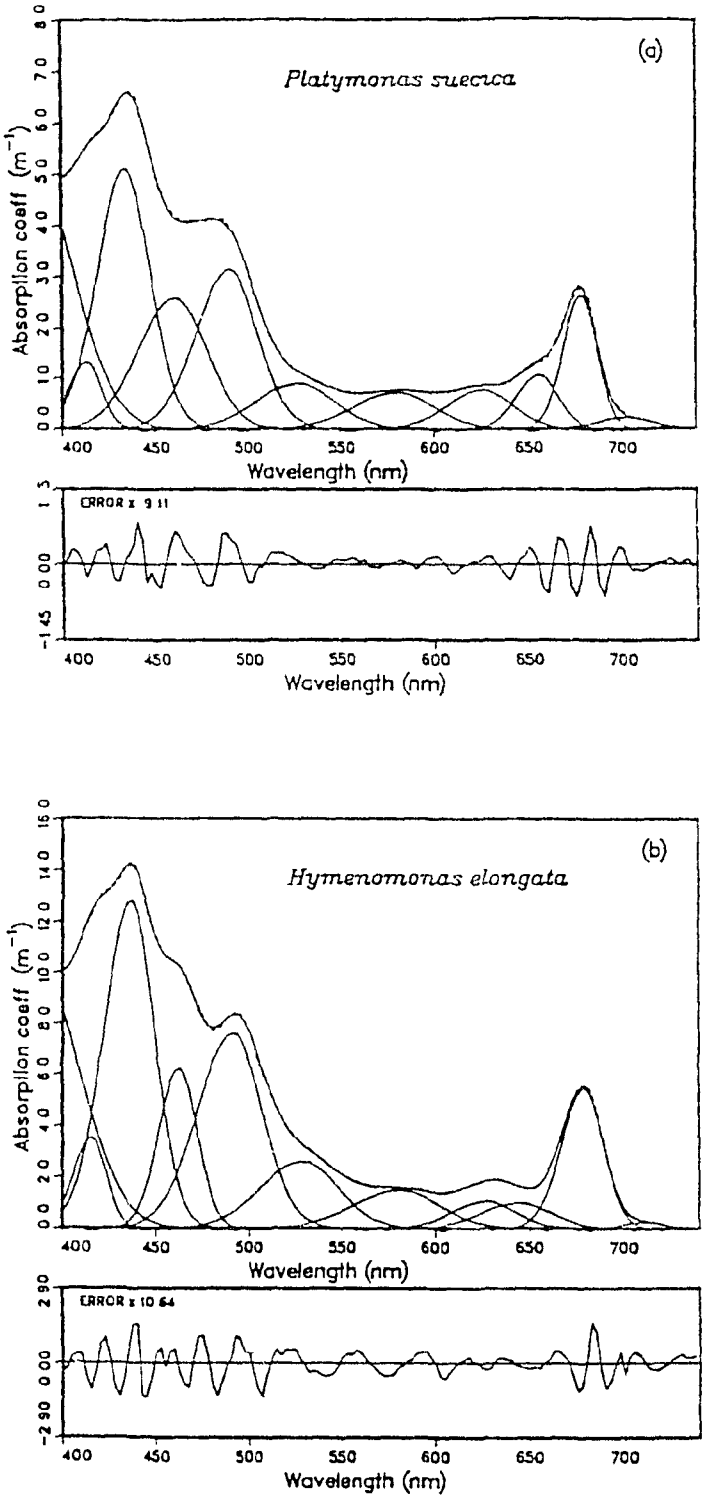
(a)
Platymonas suecica
Absorption coeff (m⁻¹)
Wavelength (nm)
ERROR x 9.11
(b)
Hymenomonas elongata
Absorption coeff (m⁻¹)
Wavelength (nm)
ERROR x 10.64

Figure 2.1

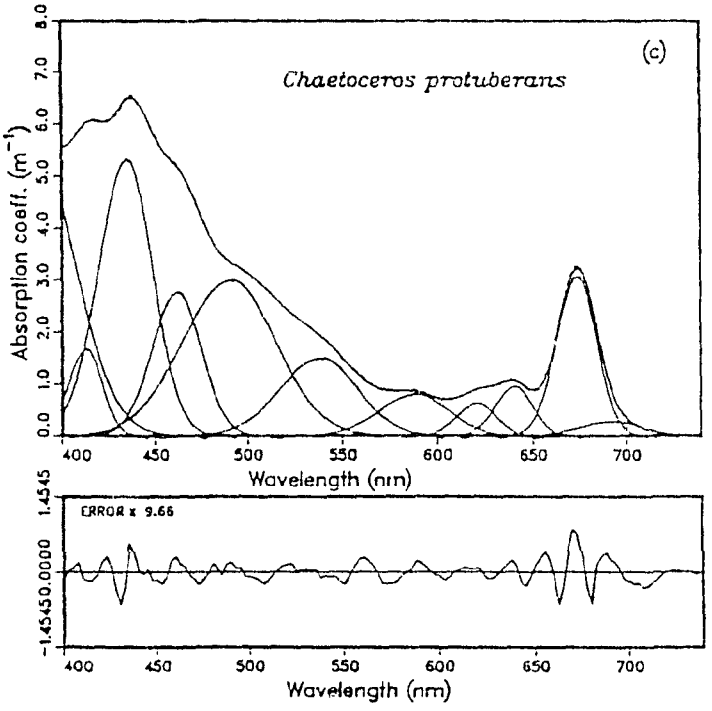
(c)
Chaetoceros protuberans
Absorption coeff. (m⁻¹)
0.0
1.0
2.0
3.0
4.0
5.0
6.0
7.0
8.0
400
450
500
550
600
650
700
Wavelength (nm)
ERROR x 9.66
1.4545
0.0000
-1.4545
400
450
500
550
600
650
700
Wavelength (nm)

Band number	Chlorophyceae		Prymnesiophyceae		Diatoms	
	Center	Halfwidth	Center	Halfwidth	Center	Halfwidth
1	383.06	54.04	384.85	55.18	383.95	52.07
2	411.72	23.34	412.63	21.75	414.03	18.79
3	433.80	34.66	435.40	32.43	435.29	29.28
4	463.68	44.96	462.05	25.65	460.94	28.71
5	488.92	41.28	490.13	41.18	489.95	53.60
6	529.92	47.40	529.53	45.75	536.33	44.46
7	580.66	48.20	579.03	49.20	586.18	43.32
8	623.90	40.42	623.08	38.50	623.41	25.99
9	654.88	24.44	644.33	37.13	642.61	20.73
10	677.80	19.54	678.03	23.43	674.09	21.87
11	700.84	33.62	706.30	27.53	692.03	39.21

TABLE 2.2. Averaged values of wavelength positions (in nm) and halfwidths(in nm) of 11 Gaussian bands used to fit the absorption spectra of 3 groups of marine algae.

Source of Variations	Gaussian band number										
	1	2	3	4	5	6	7	8	9	10	11
Center (in nm)											
Between groups	3 58*	9 89	4 35	13 04**	2 21	107 42**	99 60**	0 79	265 98**	35 97**	345 78**
Within groups	0 81	3 28	1 68	2 05	1 97	5 85	7 37	9 21	1 59	0 21	22 18
Halfwidth (in nm)											
Between groups	16 55**	39 35*	53 14**	559 86**	378 53**	15 04**	71 32**	460 24**	395 18**	17 68**	211 70*
Within groups	1 66	6 69	3 60	13 46	6 21	0 73	3 29	14 81	5 63	1 68	46.18

Tukey test * significant, $p < 0.05$, ** highly significant, $p << 0.01$

TABLE 2 3 Root mean squared deviation of wavelength positions and halfwidths of 11 Gaussian bands used in decomposition of the absorption spectra from 3 groups of marine algae.

Gaussian band 5 is centered at 490 nm and this position does not seem to be influenced by taxonomic group. Its halfwidth, however, varies significantly between the algal groups, with the Diatoms having a slightly larger band (53.6 nm) than the Chlorophyceae and the Prymnesiophyceae (41.3 and 41.2 nm respectively). Gaussian bands 6 and 7 are located in the region of minimum light absorption by phytoplankton cells. They are centered at 529.7 and 579.9 nm respectively for both the Prymnesiophyceae and the Chlorophyceae, whereas the Diatoms tend to absorb at a longer wavelength in both cases (536.3 and 586.2 nm for band 6 and 7 respectively). The statistical analysis on the halfwidths suggest a different behaviour of these bands between groups. Indeed, each of the three algal groups present a significantly different halfwidth for band 6, ranging from 44.5 to 47.4 nm (Table 2.2). On the other hand, the band 7 is significantly narrower for Diatoms (43.3 nm) than for the two other groups (48.7 nm on average).

No difference between groups is observed in the position of the Gaussian band 8, centered at 623.5 nm. This band has a small peak but is proportionately very broad. As with the previous band, its halfwidth is significantly narrower for the Diatoms (26.0 nm) than for the two other groups (38.5 and 40.4 nm for Prymnesiophyceae and Chlorophyceae respectively).

The parameters of the absorbing bands 9 and 10 show significant differences between the groups of algae. Band 9 is centered at 643.5 nm, on the average, for the Diatoms and for the Prymnesiophyceae, which is 10 nm less than the position for the Chlorophyceae (654.9 nm). The halfwidths are significantly different for each of the three groups, varying from 20.8 nm to 37.1 nm (Table 2.2). The difference in the position of band 10 is not so large. Diatoms present a peak absorption at 674.1 nm, which differs from the corresponding peak in the other groups by only 4 nm. The halfwidth is narrower for Chlorophyceae than for the two other groups (Table 2.2).

Finally, the last absorbing component of the spectra is represented by the Gaussian band 11 of low amplitude. Its position ranges from 692 nm to 706 nm with a significant difference between Diatoms (692.0 nm) and the two other groups (700.8 and 706.3 nm). On the other hand, its halfwidth tends to differentiate the Prymnesiophyceae (27.5 nm) from the Diatoms (39.2 nm), while the Chlorophyceae has an intermediate value of 33.6 nm, not significantly different from the two other groups.

2.4. Discussion

Previous studies using a curve decomposition method were concerned mainly with the absorption properties of the chlorophylls in the red part of the spectrum. The results showed the complexity of the pigment system in algae and higher plants in which the absorption maximum of chlorophyll at 670-680 nm could be the result of 6, 10 or even more absorbing components (Katz *et al.* 1977 and references therein). A more simplistic view of the light-harvesting system in algae, such as the one presented here, has the advantage of ease of use in ecological applications such as the estimation of the optical properties of natural communities of phytoplankton and their variation in time and space. Nevertheless, the efficiency of the present model and the associated statistical data must be tested on some physiological basis.

2.4.1. Biological interpretation of the Gaussian bands The first band has a maximum absorption in the U.V range of the spectrum. Physiologically, such a strongly absorbing band is likely to include several components, starting with the absorption by the particulate material itself (i.e., the non-photosynthetic pigments). The absorption spectra of natural communities of phytoplankton, after pigment extraction, often display a monotonous increase from the red to the blue regions of the light spectrum (Kishino *et al.* 1984), similar to the absorption spectra of detritus or yellow substances. Also, some recent studies (Yentsch and Phinney 1989) have demonstrated the presence of mycosporine-like UV absorbing pigments

in significant amounts within several algal species commonly found in the marine environment.

The Gaussian bands 2, 3, 8 and 10 with their maxima at 412, 435, 623 and 675 nm respectively correspond to absorption by chl-*a* *in vivo*. Goedheer (1970) observed that the *in vivo* absorption spectrum of the brown benthic algae *Laminaria digitata* had chl-*a* peaks at 418, 437, 618 and 673 nm. Similarly, the absorption spectrum of P700-Chla-protein complex from *Glenodinium* sp (Prézelin 1980) showed peaks and shoulders at 419, 437, 618 and 675 nm. Owens and Wold (1986) found that the presence of chl-*a* in different pigment- protein complexes was indicated by absorption at 418, 440 and 670-678 nm. The statistical analysis on the data suggests less significant differences between groups for these bands, in agreement with the ubiquitous properties of chl-*a* in autotrophic organisms. Band 10 represents a particular case in the sense that, for the Diatoms, the chl-*a* absorption in the red seems to be shifted significantly to a shorter wavelength (674 nm) than for the two other groups (678 nm). Such a difference can be explained by a variation between groups of algae in the ratio of the photosystem I (PSI) to the photosystem II (PSII). The red absorption band of photosynthetic reaction centre PSII occurs at shorter wavelengths (670-675 nm) when compared with the position of the absorption band associated with the PSI reaction centre (677-680 nm) (Larkum and Barrett 1983). A change in the ratio of PSI to PSII should then induce a slight variation in the wavelength position of the chl-*a* maximum absorption. Falkowski *et al.* (1981) observed a PSI to PSII ratio of approximately one for the Chlorophyceae whereas the ratio was found to attain 0.44 in Diatoms. The red absorption maximum of chl-*a* for Diatoms would then be shifted to shorter wavelengths compared with Chlorophyceae. It is also very likely that this ratio may vary in response to other factors such as the environmental light conditions (Melis and Brown 1980, Owens 1986).

The parameters of the bands 4 and 9 correspond to the absorption characteristics of other groups of chlorophylls, particularly chl-*b* for chlorophyceae and chl-*c*

for Diatoms and Prymnesiophyceae. The two types of algae cannot be differentiated on the basis of the position of the absorption band in the blue. On the other hand, the halfwidth of band 4 differs very significantly ($P << 0.01$) between the groups of algae, with the cells containing chl-*c* having a much narrower band than the Chlorophyceae. A large absorption band for chl-*b* should allow Chlorophyceae and other cells containing chl-*b* to utilize blue light with high efficiency. In this context, it is interesting to note that Chlorophyceae and Prasinophyceae are now generally considered to contribute to a high proportion of ultraphytoplankton in the deep chlorophyll maximum of oligotrophic oceans (Gieskes and Kraay 1986, Hooks *et al.* 1988). In the red part of the spectrum, the wavelength positions of band 9 varies by 10 nm between Chlorophyceae (655 nm) and the two other groups (643 and 644 nm). The results are in complete agreement with absorption spectra of pigment-protein complexes containing chl-*b* (Prézelin and Boczar 1986, Fawley *et al.* 1990) and chl-*c* (Friedman and Alberte 1984, 1986, Owens and Wold 1986, Rhiel *et al.* 1987, Boczar and Prézelin 1989).

Absorption bands 5 and 6 on the decomposed spectra correspond to absorption by carotenoids. The position of band 5 seems to be common to the three groups of algae whereas band 6 is positioned at a longer wavelength for the Diatoms (536 nm) than for the other groups (529 and 530 nms). From this result, it is tempting to identify bands 5 and 6 as representative, respectively, of the carotene and the xanthophyll groups of pigments. Indeed, carotenes, and particularly β- carotene, are present in most algal taxa (Rowan 1989). Also, the presence of β-carotene in the absorption spectra of pigment-protein complexes is indicated by a shoulder at 485-495 nm (Thornber and Alberte 1977, Boczar and Prézelin 1989). On the other hand, the hypothesis that xanthophylls are responsible for band 6 is supported by the work of Owens and Wold (1986) who pointed out that an increase in the background absorption within the 480-550 nm range on the absorption spectra of pigment-protein complexes of Diatoms is attributable to fucoxanthin. They also

noticed a large decrease in absorption at these wavelengths for P700-chl*a*-protein complex and chl*a*-chl*c* light harvesting complex, both containing no or very little fucoxanthin but having some β-carotene as indicated by a shoulder at 490 nm. Fucoxanthin was also detected in the *in vivo* absorption spectrum of *Laminaria digitata* as a feature at 530-545 nm (Goedheer 1970). Such a differentiation between carotenes and xanthophylls, although an attractive idea, may be too simplistic. In fact, up to 500 carotenoids occur naturally (Liaaen-Jensen and Andrewes 1985) and all of them absorb light within the 400-550 nm region. Their absorbing properties are known to change with some differences in their chemical structure, such as the number of double bonds and the degree of cyclisation (Britton 1983). Although xanthophylls differ from carotenes by the presence of oxygenated groups in their molecules, such a factor is not sufficient to distinguish specifically the absorption properties of the two types of pigments. Therefore, both bands 5 and 6 may very well correspond to the absorption of light by a mixture of carotenes and xanthophylls.

The small Gaussian band 7 contributes to the optical properties of phytoplankton in the region of minimum absorption. Its position varies from 579 nm to 586 nm according to species. Such a band may represent a small absorbing component of the chlorophylls. The presence of a small feature at 585 nm due to chl-*c* was observed in the *in vivo* absorption spectrum of *Laminaria digitata* (Goedheer 1970). The same feature was observed in some absorption spectra of chl*a*- chl*c*-protein complexes (Rhiel *et al.* 1987, Boczar and Prézelin 1989). On the other hand, chl-*a* may also contribute to absorption in that region of the spectrum. Prézelin (1980) and Fawley *et al.* (1990) observed a slight absorption at 470-600 nm in the spectra of P700-chl*a*-protein complexes. An *in vivo* spectrum of *Nannochloris salina*, containing neither chl-*b* nor chl-*c*, also showed an absorption at around 580 nm due to chl-*a* (Owens *et al.* 1987).

Band 11 does not have a clear physiological explanation. The decomposition of the chl-*a* peak in the red by French *et al.* (1972) produced a similar unexplained

Gaussian component with a peak position varying from 700 to 706 nm. Later, Katz et al. (1977) postulated that all chlorophyll structures absorbing at 685 nm and higher wavelengths are mainly the results of different interactions between the chl-*a* molecules and other compounds such as water or phaeophytins.

2.4.2. Specific absorption coefficients A non-linearity in the relationship between the absorption coefficient $a_{ph}(\lambda)$ and the concentration of chl-*a* has often been observed in natural environments, particularly at low chlorophyll concentrations (Prieur and Sathyendranath 1981, Kiefer and Soohoo 1982, Yentsch and Phinney 1989). Such a non-linearity has been related either to the particle effect, the pigment composition effect, or to a combination of both. Also, detrital compounds covarying with phytoplankton can be in higher proportions at low concentrations of chlorophyll.

In the present study, the relationship between the height of each Gaussian band and the pigment concentration to which it corresponds is expected to be linear since the particle effect and the differences in pigment composition have been successively removed from the initial absorption spectra. In Figures 2.2, 2.3, 2.4 and 2.5, a linear fit has been applied to the data. In most cases, the fitted curves explained more than 80% of the variances and the correlations were significant at 0.01 probability level. Note that here, the linearity is maintained for a multi-species sample set. Until now, a linear relationship had been observed between the apparent absorption coefficient $a(\lambda)$ and the concentration of chl-*a* on only monospecific algal cultures (Sathyendranath *et al.* 1987).

Due to the high correlation between concentrations of the various pigments (e.g. $r^2 = 0.9$, between concentrations of chl-*a* and carotenoids), it is clear that a good linear fit could also be observed by regressing the height of a Gaussian band with the pigment concentration to which it does not correspond. For example, a coefficient of determination $r^2 = 0.88$ is obtained from a linear regression analysis

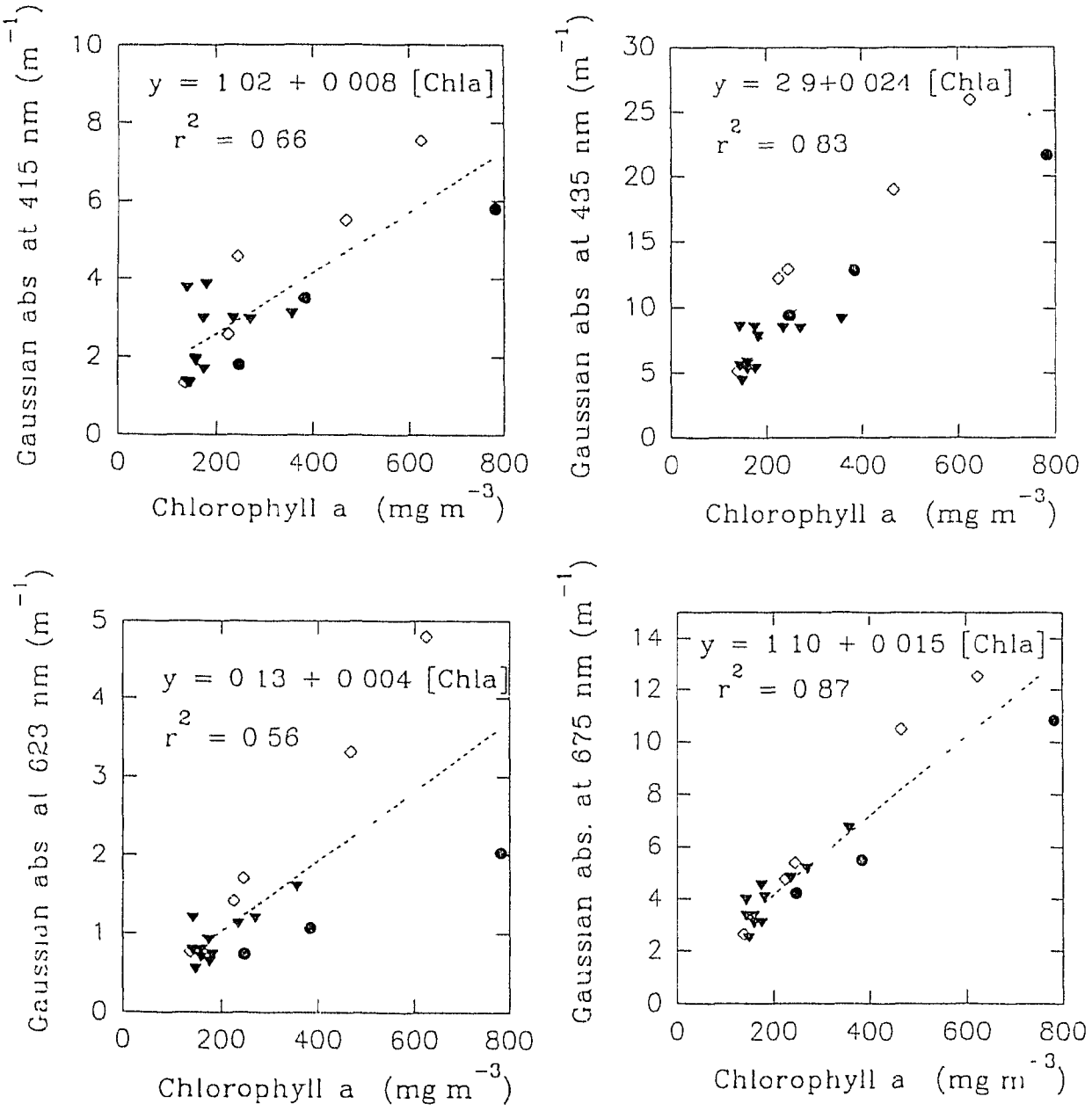

FIGURE 2.2. Gaussian band height at (a) 415 nm, (b) 435 nm, (c) 623 nm, and (d) 675 nm, *versus* chl-*a* concentration. *(filled triangle)* Diatoms, *(open diamond)* Chlorophyceae, *(filled circle)* Prymnesiophyceae.

between Gaussian heights at 532 nm (i.e., wavelength allocated to absorption by carotenoids) and the concentration of chl-*a*. This result, however, is unrealistic considering what it is known about spectral absorption by chl-*a* (e.g. Prézelin 1980), showing minimal absorption in the range ca. 500 - 600 nm.

An increase in the scatter amongst the data points was observed with the low-amplitude Gaussian bands (Figs. 2.2a, 2.2c, 2.3b). In these particular cases, the linear fit still explains more than 50% of the variances but the data were probably affected by covarying absorption by more than one pigment, which failed to be separated by the method. For example, it has already been mentioned that band 7 (Fig. 2.3b) most likely included absorption by chl-*c* as well as a small contribution from chl-*a*. A multiple regression analysis describes the relationship between the height of band 7 (y) and the concentrations of chl-*a* and -*c* as follows:

$$y = 0.26 + 0.003C_{chlc} + 0.002C_{chla},$$

with a regression coefficient r^2 of 0.89. At these low levels of absorption, the data might also be affected by instrumental noise.

A linear relationship between the Gaussian absorption at 460 nm and chl-*c* concentration (Fig. 2.3a) explained only 33% of the variances, but the correlation was still significant at the 0.05 probability level. Note, in this case, that the data points representing the Prymnesiophyceae tend to lie above the regression line and above the data obtained for Diatoms. The same trend is maintained in Figures 2.3b and 2.3c. Most of the Diatoms, particularly the species used in the present study, are known to contain chl-c_1 and -c_2 (Stauber and Jeffrey 1988). In addition to these two pigments, the Prymnesiophyceae have a third form, chl-c_3, which possess slightly different optical properties (Fawley 1989). This difference may explain the higher absorption coefficient of Prymnesiophyceae when compared with that of Diatoms. As a result, the regression in Figure 2.3 are probably biased by the preponderance of Diatoms. I corrected for this effect by using the geometric regression line whose

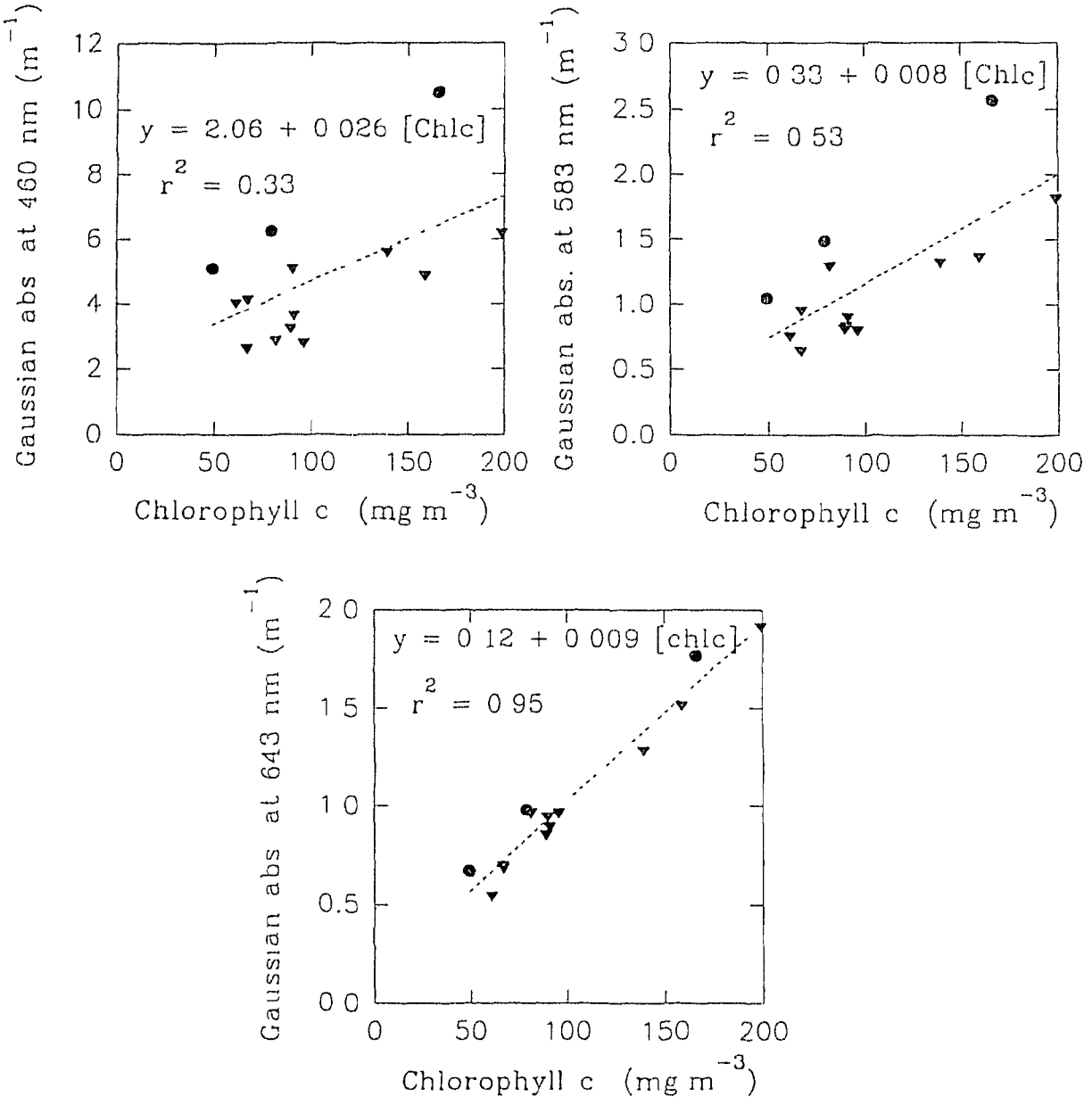

FIGURE 2.3. Gaussian band height at (a) 460 nm, (b) 583 nm, and (c) 643 nm, *versus* chl-*c* concentration. *(filled triangle)* Diatoms, *(open diamond)* Chlorophyceae, *(filled circle)* Prymnesiophyceae.

slope is given by the ratio of the actual slope to the correlation coefficient (Ricker 1984), . This procedure gave a value of (a'_{chlc}) at 460 nm of 0.045 m^2 (mg Chl c)$^{-1}$.

The true specific absorption of chl-*a* at 435 nm is given in Figure 2.2b by the slope of the regression line. Note that the "true", *in vivo* specific absorption coefficient of chl-*a*, after correction for particle effect, has not been reported previously in the literature. For this reason, comparisons with the "apparent" value of a^* reported so far in the literature have to be made with caution. Nevertheless, the specific absorption coefficient obtained from Figure 2.2b fits well within the wide range of values given in the literature for the apparent specific absorption coefficient of chl-*a* in the blue region (Sathyendranath *et al.* 1987, Maske and Haardt 1987, Mitchell and Kiefer 1988). The present decomposition method suggests that the high variability in a^*_{chla} at 435-440 nm depends on the species involved. The decomposition of absorption spectra from Chlorophyceae (Fig. 2.1a) showed that chl-*b* contributes to a high proportion (*ca.* 30-35%) of the total absorption of the cells at 435-440 nm. This explains why a^*_{chla} obtained from Chlorophyceae cultures (e.g. Table 4 in Mitchell and Kiefer 1988) would be systematically higher than the a'_{chla} value proposed here. On the other hand, the contribution to total absorption at 435-440 nm by pigments other than chl-*a* is less in the case of Diatoms and Prymnesiophyceae (Fig. 2.1). Again, it explains why the apparent values of a^*_{chla} for cells containing chl-*c* (e.g. Mitchell and Kiefer 1988) become more similar to a'_{chla}.

In the red part of the spectrum, the particle effect is not as important as at shorter wavelengths where the absorption is higher (Kirk 1983). On the other hand, the contribution to total absorption at 675 nm by pigments other than chl-*a* is minimal (Fig. 2.1). As a result, the range of values for a^*_{chla} at 675 nm, 0.010-0.030 m^2 (mg Chl a)$^{-1}$ (Maske and Haardt 1987, Bricaud *et al.* 1988) is much narrower than for a^*_{Chla} in the blue region and tends on an average to become reconciled with the present value of a'_{chla} of 0.015 m^2 (mg Chl a)$^{-1}$ (Fig. 2.2d).

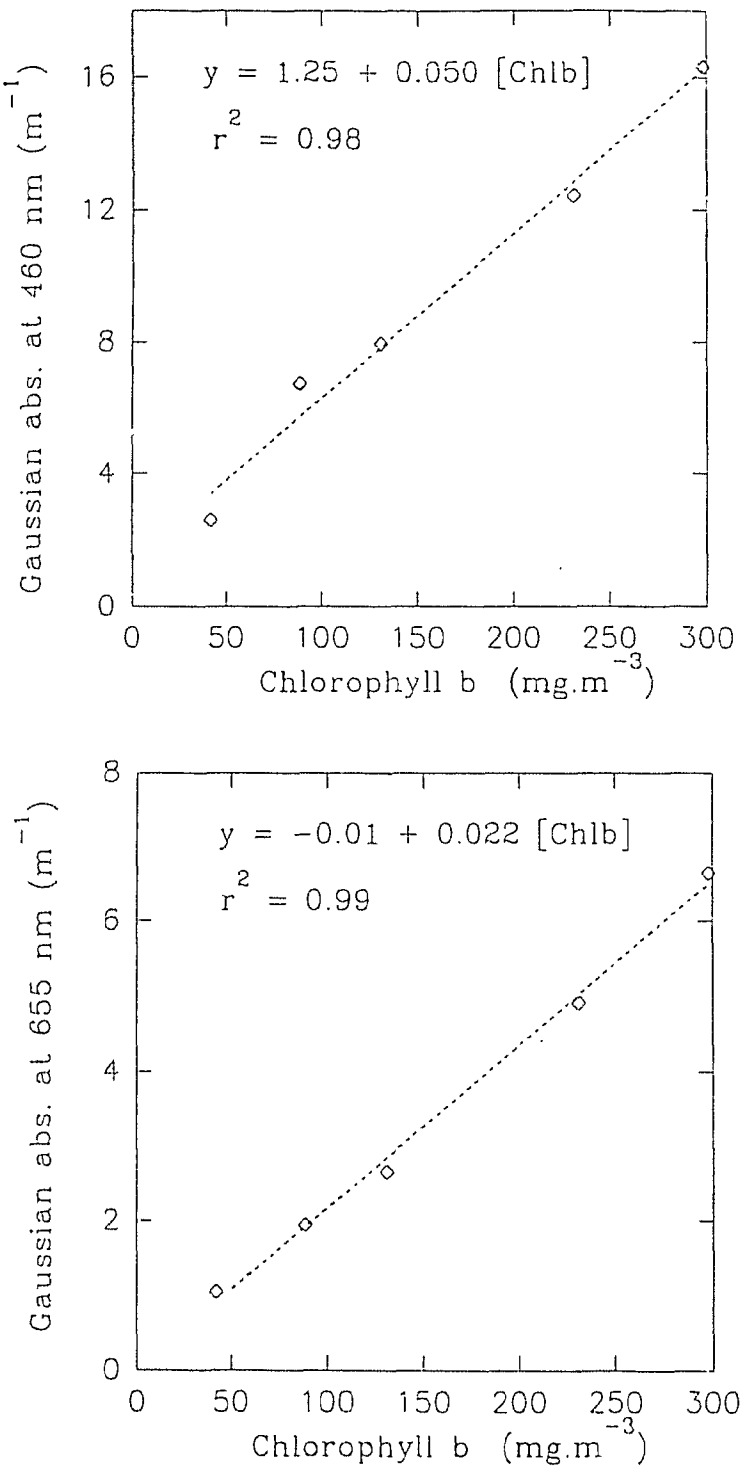

FIGURE 2.4. Gaussian band height at (a) 460 nm, and (b) 655 nm, *versus* chl-*b* concentration. *(filled triangle)* Diatoms, *(open diamond)* Chlorophyceae, *(filled circle)* Prymnesiophyceae.

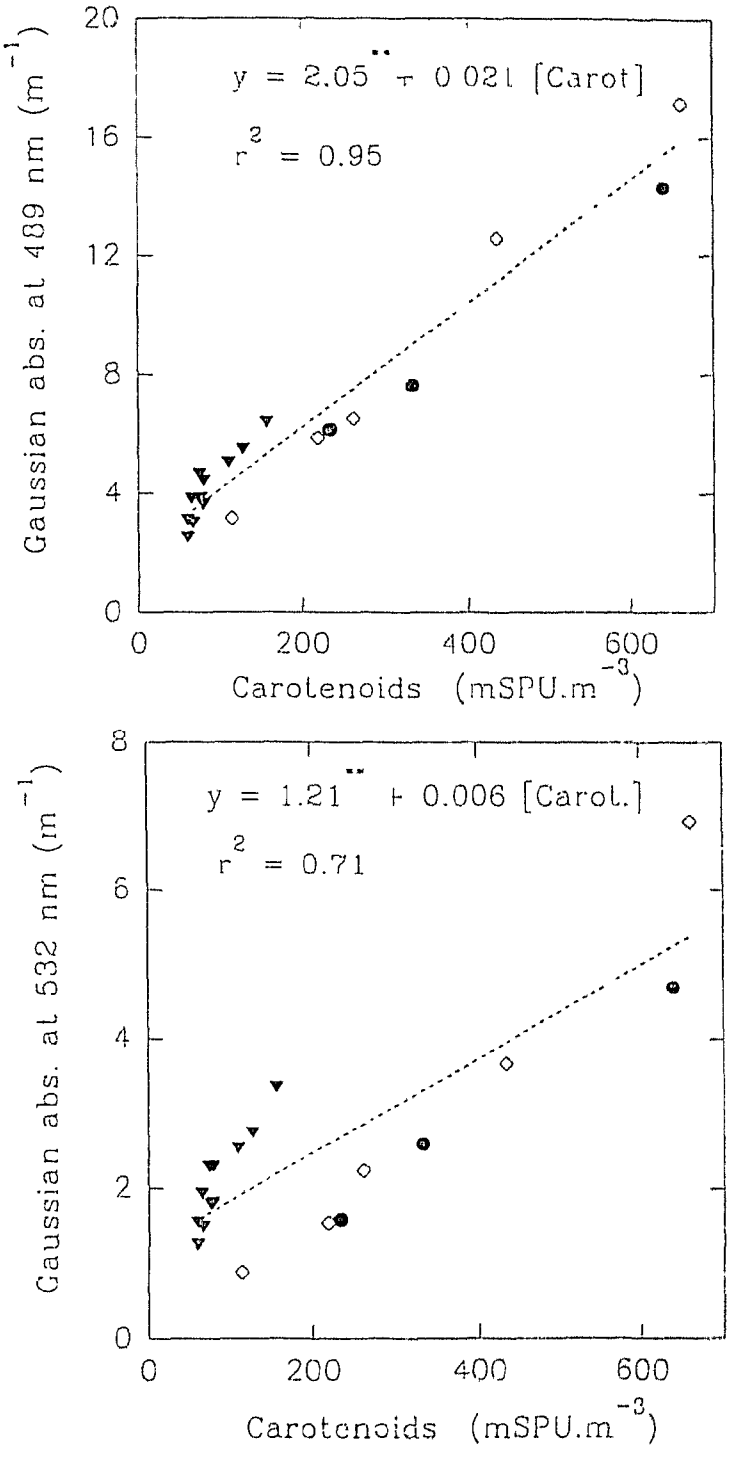

FIGURE 2.5. Gaussian band height at (a) 489 nm, and (b) 532 nm, *versus* carotenoids concentration. (**) indicates an intercept significantly different from 0. *(filled triangle)* Diatoms, *(open diamond)* Chlorophyceae, *(filled circle)* Prymnesiophyceae.

The decomposition of absorption spectra also gives the true specific absorption coefficient of chl-*b* (Fig. 2.4) and carotenoids (Fig. 2.5) at their wavelengths of maximum absorption. The intercepts of the regression lines relating absorption bands 5 and 6 to the carotenoid concentrations (Fig. 2.5) were significantly different from zero. Problems with carotenoids, however, are not unexpected, considering the imprecise method used to measure their concentrations (Parsons *et al.* 1984).

Regression analysis should give the specific absorption coefficient for each band. However, the technique of least-square analysis tends to assign more weight to the data points that are most distant from the origin. To avoid this effect, I used the specific absorption coefficent as computed by the mean of the specific absorption coefficient calculated for each sample. These values are shown in Table 2.4. The absorption of the first and last bands have been normalized to chl-*a* since the heights of both bands showed a good correlation with the concentration of this pigment (r^2 = 0.84 and 0.87).

2.4.3. Reconstruction of in vivo absorption spectrum From the present analysis, it is possible to recover the entire absorption spectrum of any phytoplankton sample. Such reconstruction will be based on the sum of several Gaussian curves:

$$a_{ph}(\lambda) = \sum_{j=1}^{l} a'_j(\lambda_{mj}, \sigma_j \exp\left[-\frac{(\lambda - \lambda_{mj})^2}{2\sigma_j^2}\right] \qquad (2.3)$$

where the height of each Gaussian curve is represented by the product of the specific absorption coefficient of the j-th band-pigment (one pigment can be represented by several absorption bands in the visible range) and the concentration of that pigment C_j, λ_{mj} is the position of the maximum absorption and σ_j represents the halfwidth of the Gaussian curve. Figure 2.6 illustrates the reconstructed absorption spectrum of a population containing Chlorophyceae, Diatoms and Prymnesiophyceae. The

Characteristic	Gaussian band number and associated pigment species												
	1	2	3	4c[a]	4b[a]	5	6	7[b]	8	9c[a]	9b[a]	10	11
	Chl-*a*	Chl-*a*	Chl-*a*	Chl-*c*	Chl-*b*	Carot	Carot	Chl-*c*	Chl-*a*	Chl-*c*	Chl-*b*	Chl-*a*	Chl-*a*
Spec abs. coeff[c]	0 037	0 012	0 039	0 051	0 061	0 038	0 017	0 012	0 005	0 010	0 022	0 020	0 002
Halfwidth (nm)	53 8	21 3	32 1	27 2	45 0	45 1	45 9	46 3	35 0	28 9	24 4	21 6	33 5
Center (nm)	384	413	435	461	464	490	532	583	623	644	655	676	700

[a] The characteristics of these Gaussian bands change depending on whether the cells contain chl-*c* (Bands 4^c and 9^c) or chl-*b* (Bands 4^b and 9^b) In the case of a mixture of cells containing both chl-*c* and -*b*, all 13 bands in the table would have to be used rather than just 11

[b] The specific absorption coefficient is calculated as a fuction of chl-*c* only, even though chl-*a* also appears to have an effect (see text)

[c] Specific absorption coefficient has units of m^{-1} per unit pigment concentration Chlorophyll concentrations are in mg m^{-3}, while concentration of carotenoids is in mSPU m^{-3}

TABLE 2.4. Mean characteristics of the Gaussian bands Chl = chlorophyll carot = carotenoids Spec abs. coeff = specific absorption coefficient.

observed absorption spectrum has been made up by averaging the absorption spectra of the twenty algal cultures used in the present study. In the same way, the concentrations of the major pigments were averaged over the values for the twenty cultures (Sathyendranath *et al.* 1987). The resulting spectrum represents the absorption properties of both cells containing chl- *b* and -*c*. Since each of these two accessory chlorophylls are represented by one absorption band in the blue and one in the red, 13 Gaussian bands were used to fit the data instead of 11 that were used for unialgal culture of cells containing either chl-*b* or -*c*. Each band is characterized by the parameters shown in Table 2.2 (Gaussian absorbance) and Table 2.4 (centre and halfwidth).

The reconstructed absorption spectrum closely matches the observed curve. Slight differences occur in the region of minimum absorption, where the estimated absorption coefficient is systematically lower than the observed values. This discrepancy probably results from an underestimation of the height of band 7 which has been related to the absorption properties of chl-*c* only.

2.5. Conclusions

The present study has shown that the *in vivo* absorption spectra of phytoplankton cells, after correction for the particle effect, can be represented as the sum of a dozen or so Gaussian absorption bands. Linear correlation of the different peak heights with the concentrations of one or the other of the five major pigments in the samples indicates that the method has been successful in separating the absorptions due to each pigment. One exception to this is the small absorption band at 579 - 586 nm region, which appears to be influenced by both chl-*a* and chl-*c*. The role of UV-blue absorbing material appears to be non-negligible in the samples, but I was unable to propose a specific absorption coefficient other than one normalized to chl-*a* for the Gaussian peak associated with this absorption, since no measurements

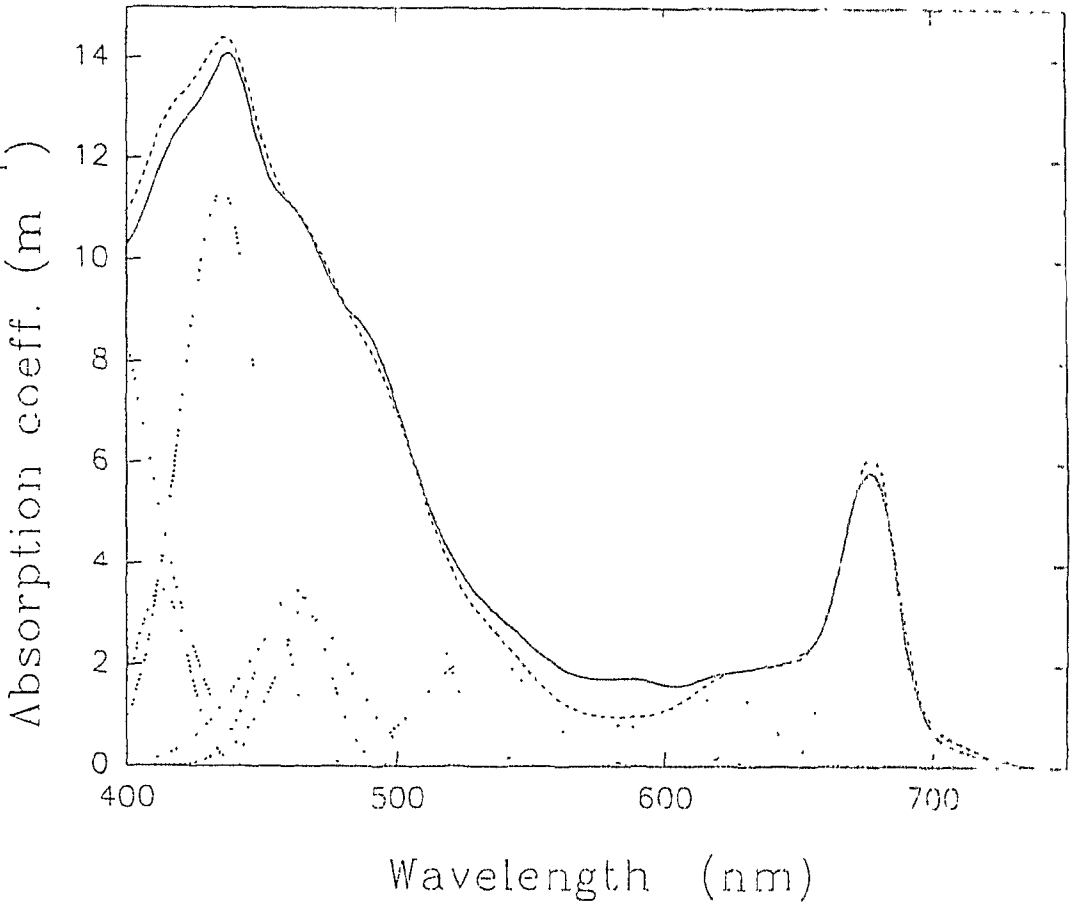

FIGURE 2.6. Reconstruction of *in vivo* absorption spectrum of phytoplankton sample (solid line) containing Diatoms, Prymnesiophyceae, and Chlorophyceae. The fitted spectrum (dashed line) has been estimated by the sum of 13 Gaussian bands which represent the absorption properties of the major pigment groups in the ...

were made of the concentrations of the pigments that may be responsible for this absorption.

The relationship between peak heights and pigment concentrations are hardly affected by the phytoplankton species. This may be considered an indication of the validity of the simple model of particle effect applied to the data set: if this effect had not been corrected for adequately, the consequence would have been a greater dispersion between the results for different species. On the other hand, some inter-species differences in peak characteristics were noted, especially in the peak positions and in the band widths. These differences, however, can be explained in terms of the known variations in the pigment composition from species to species. Note that the possibility exists that these differences could be exploited for the identification of major phytoplankton species present in a natural sample from an analysis of its absorption spectrum. No experiments were made with marine cyanobacteria although they can be abundant in oligotrophic waters. Lewis *et al.* (1986) observed, however, that none of the studies on absorption and action spectra of natural phytoplankton has shown any indication of the presence of phycobiliproteins which are characteristic pigments of cyanobacteria.

I have presented here the first estimates of the "true" *in vivo* specific absorption coefficients of five major pigments, after correction for particle effect. This opens the possibility of estimating the absorption spectrum of a phytoplankton sample from measurements of its pigment concentrations and cell size. With the advent of the modern techniques of flow cytometry and HPLC, the measurements required for the application of these results are becoming increasingly common. The proposed method to measure the absorption spectrum of phytoplankton is indirect, but has the advantage of circumventing the problem of separating absorption by live phytoplankton from background absorption by covarying substances. This method is also free of some of the pitfalls of other methods that have been proposed, such as the

problem of obtaining measurements on a representative sample set for microphotometry (Iturriaga and Siegel 1989), and the problem of quantifying the results from the filter technique of Yentsch (1962) and Mitchell and Kiefer (1984). The analysis presented here is based on estimates of pigment concentrations from the absorption spectra of acetone extracts. I do not yet know how well these results would apply to concentration data estimated by other techniques, for example the HPLC method. But I anticipate that, in the future, as more accurate HPLC measurements become more routine, they would facilitate refinement of the results presented here.

CHAPTER 3

Determination of the major groups of phytoplankton pigments from the absorption spectra of total particulate matter

3.1 Introduction

New techniques to retrieve *in vivo* spectral absorption by phytoplankton, separating it from that of "detrital" matter and dissolved organic substances which coexist with phytoplankton, have been instrumental in recent advances in marine optics (Prieur and Sathyendranath 1981, Kishino *et al.* 1985, Iturriaga and Siegel 1989). Applications of these methods to field samples (Bricaud and Stramski 1990), as I did in Chapter One, have shown, indeed, a significant contribution due to non-chlorophyllous or "detrital" particles to the absorption properties of total particulate matter, even in oceanic regions that may be considered to be case 1 waters (*sensu* Morel and Prieur 1977).

Also, recent developments in techniques for pigment analysis have made it easier to collect information on auxiliary pigment concentrations, in addition to that of chlorophyll-*a*, and to improve our understanding of the role of these pigments in modifying the absorption spectrum of phytoplankton. In Chapter Two, I have decomposed the *in vivo* phytoplankton absorption coefficient into components associated with the major photosynthetic pigments, and computed "true" specific absorption coefficients of chl-*a*, -*b*, and -*c*, and carotenoids. These values, which were corrected for the package effect (Duysens 1956), showed no significant dependence on species. It is also suggested that these coefficients could be used to reconstruct the *in vivo* absorption spectrum of a mixed algal population, knowing the concentrations of the pigments. Inversely, knowing the absorption spectrum

of phytoplankton community in the water, one could also use these "true" specific absorption coefficients to evaluate the concentrations of pigments in the sample.

In this chapter, an inverse method is outlined to determine the spectral characteristics of absorption by phytoplankton cells and the concentrations of the main pigments, solely from knowledge of the absorption coefficient of total particulate matter in seawater. Absorption by detrital matter is taken into account using a parametrization that reflects the shape of observed data from field studies, while the specific absorption coefficients of various pigments are determined following the model described in Chapter Two. The data set used here (see Chapter One), representative of different oceanic conditions, included absorption spectra of total particles and detailed pigment analyses using liquid chromatography.

Earlier works (Roesler *et al.* 1989, Bricaud and Stramski 1990) have used the spectral shape of light absorption by detritus to assess the respective contributions of algal and non-algal components on the absorption spectrum of total particulate matter. The model presented in this work follows a similar approach, but the assumptions in the model have been relaxed, and each major photosynthetic pigment has been treated individually.

3.2 Materials and Methods

3.2.1. Observed data All data were collected during a cruise in the northwest Atlantic Ocean in September 1989. Sampling sites included water masses, ranging from "blue" open-ocean waters (Sargasso Sea) to highly productive areas (Georges Bank), and several intermediate types in the Slope region and in the Gulf of Maine proper. Sampling locations and variables monitored are described in detail in Chapter One, and only a brief summary is given here.

Absorption spectra. About one hundred absorption spectra of total particulate matter were collected at various locations and depths in the sampling area. Spectral

values of the absorption coefficient were monitored every 2 nm from 400 to 750 nm, using the filter technique (Mitchell and Kiefer 1984, 1988). In addition, absorption by non-pigmented material (or detritus) was estimated using a solvent extraction procedure (90% acetone and DMSO) according to Kishino *et al.* (1985). Absorption due to phytoplankton pigments was then computed as the difference between absorption by total particulate matter and detritus. Details regarding the method, and correction of the data for pathlength amplification due to the filter, also called the β- factor (see Mitchell and Kiefer 1984), have been presented in Chapter One.

Pigment data. In parallel with absorption measurements, samples were collected for detailed pigment analysis, using the reverse-phase, high-performance liquid-chromatography (HPLC) technique. The method allowed us to quantify the major groups of chlorophylls and nine species of carotenoids, including important biological markers such as fucoxanthin, peridinin, and 19'-hexanoyloxyfucoxanthin. Instrumentation for pigment analysis was a Beckman "System Gold" apparatus equipped with a scanning absorbance detector. A binary solvent system was used to separate pigments on a short (0.46 x 7.0 cm) Ultrasphere XL-ODS column (Beckman) filled with 3 μm packing material. A linear gradient from 100% solvent A (solution of methanol and 0.5M ammonium acetate) to 100% solvent B (solution of methanol and ethylacetate) was set up from 1 to 16 min of a 23 min chromatographic run. The pigments were monitored at 440 nm and identified by comparing their retention time and absorption properties with quantitative standards. For the purpose of the present work, all carotenoids have been combined into a single group.

3.2.2. Theoretical considerations Inherent optical properties of seawater, as defined by Preisendorfer (1961), are independent of the light field and result from as many additive components as there are optically active constituents in the water column. Thus, the total absorption coefficient of seawater, a_t, at wavelength λ, can be expressed as:

$$a_t(\lambda) = a_w(\lambda) + a_p(\lambda) + a_y(\lambda) \ , \tag{3.1}$$

where the subscripts w, p, and y refer to molecular seawater, particulate material, and yellow substances, respectively. The spectral values of a_w are well known (Morel 1974, Smith and Baker 1981). They are similar to that of pure water, and considered to be invariant (but see Højerslev and Trabjerg 1990). The remaining two terms in the right-hand side of Equation 3.1, namely the absorption coefficient of particulate matter and that of dissolved organic substances, are variables and are capable of modifying the total absorption significantly.

In marine waters, dissolved organic substances that contribute to absorption are mainly composed of a mixture of humic and fulvic acids which present slight differences in their optical properties (Carder *et al.* 1989). Nevertheless, several investigations in various water masses (Bricaud *et al.* 1981, Højerslev 1988 and references therein) reveal a similar spectral behaviour of absorption for these substances, often referred to as yellow substances. It is now well admitted that $a_y(\lambda)$ can be expressed as:

$$a_y(\lambda) = a_y(\lambda_0) \ \exp\left[-0.014\ (\lambda - \lambda_0)\right] \ , \tag{3.2}$$

where λ_0 is a reference wavelength in the blue or UV region (e.g. 300 or 440 nm). To simplify further the contribution due to yellow substances, Prieur and Sathyendranath (1981) suggested that 20% of the total absorption at 440 nm could be attributed to dissolved organic material in open ocean (case 1) waters.

The total absorption coefficient can then be computed for the open-ocean waters, if the absorption by particulate matter, $a_p(\lambda)$, is known. Particulate absorption

can in turn be decomposed into contributions from phytoplankton pigments, $a_{ph}(\lambda)$, and from other particulate material, mainly detritus, $a_d(\lambda)$:

$$a_p(\lambda) = a_{ph}(\lambda) + a_d(\lambda) \ , \tag{3.3}$$

In fact, the term "detritus" should include unpigmented parts of algal cells and mineral particles, as well as breakdown products of photosynthetic pigments such as phaeopigments. Recent field measurements (Roesler *et al.* 1989, Bricaud and Stramski 1990) show that detrital matter absorbs visible light in a similar fashion to yellow substances. In other words, $a_d(\lambda)$ can be expressed as an exponential function, analogous to that of yellow substances:

$$a_d(\lambda) = a_d(\lambda_0) \ \exp\left[-q\ (\lambda - \lambda_0)\right] \ , \tag{3.4}$$

where the exponent, q, takes values of the same order of magnitude as the exponent in Equation 3.2. It varies, however, over a wide range, 0.006 to 0.016 nm^{-1} (Roesler *et al.* 1989, Bricaud and Stramski 1990), and cannot be considered constant. Combining Equation 3.3 and 3.4, the absorption of total particulate matter can be expressed as:

$$a_p(\lambda) = a_{ph}(\lambda) + a_d(440) \ \exp\left[-q\ (\lambda - 440)\right] \tag{3.5}$$

Since the absorption of light by phytoplankton pigments reflects absorption by the major component, chl-*a*, and by secondary (or auxiliary) pigments, including other chlorophylls and carotenoids, $a_{ph}(\lambda)$ can be expressed as:

$$a_{ph}(\lambda) = \sum_{i=1}^{n} a_i^*(\lambda)\ C_i \ , \tag{3.6}$$

where n represents the total number of pigments considered; $a_i^*(\lambda)$ is the specific absorption coefficient of the ith pigment at wavelength λ, and C_i is the concentration of this pigment. According to Chapter Two, the specific absorption coefficients of each pigment can be estimated using a decomposition of $a_{ph}(\lambda)$ into several Gaussian bands simulating the absorbing properties of these pigments. This result allows Equation 3.6 to be rewritten as:

$$a_{ph}(\lambda) = \sum_{j=1}^{l} a_j^*(\lambda_{mj})\, C_j \;\exp\left[-\frac{(\lambda-\lambda_{mj})^2}{2\sigma_j^2}\right] , \tag{3.7}$$

where λ_{mj} is the position of maximum absorption for the jth Gaussian band, σ_j determines the width of the peak, and $a_j^*(\lambda_{mj})$ is the specific absorption coefficient for the jth absorption band at the wavelength of maximum absorption (λ_{mj}), l is the total number of Gaussian bands, and C_j is the concentration of the pigment responsible. Since a given pigment may be responsible for more than one absorption band, $l > n$. In theory, if the package effect (Duysens 1956) is not significant, these specific absorption coefficients are "true", i.e., independent of the algal species, and therefore can be used to determine pigment concentrations at any location from the knowledge, at a few wavelengths, of the local absorption coefficient of phytoplankton.

3.2.3. Approach. The application of the bio-optical model previously described requires several steps to facilitate the computation and to validate the results of the model. The procedure I adopted is as follows:

1. The observed absorption spectra of detrital matter were fitted with an exponential function (Equation 3.4) to retrieve the exponent and the absorption coefficient at the reference wavelength. The fitted exponent obtained from the detrital spectra is designated q_1.

2. To obtain a typical shape for the absorption spectra of phytoplankton, each measured absorption spectrum of phytoplankton was normalised at 440 nm, and the average computed for each wavelength. This average normalised absorption spectrum for phytoplankton is designated $a^{*'}_{ph}(\lambda)$, (see Table 3.1).

3. The first term in the right-hand side of Equation 3.5 can now be rewritten as the product of the normalized average absorption spectrum, $a^{*'}_{ph}(\lambda)$ and the absorption coefficient of phytoplankton at 440 nm:

$$a_p(\lambda) = a_{ph}(440)\ a^{*'}_{ph}(\lambda) + a_d(440)\ \exp\ [-q_2(\lambda - 440)] \tag{3.8}$$

Given $a_p(\lambda)$ from field measurements, Equation 3.8 was solved for three unknows, $a_{ph}(440)$, $a_d(440)$, and q_2, by non-linear regression. Note that the term q_2 should be similar to q_1. However, both values are obtained using different methods (i.e., q_1 by applying Equation 3.4 on the observed $a_d(\lambda)$ data; and q_2 by applying Equation 3.8 on the observed $a_p(\lambda)$ data), such that a different subscript is used to compare both estimates of q. After reconstruction of $a_d(\lambda)$ for each sample, the local spectral absorption by phytoplankton was then estimated as:

$$a_{ph}(\lambda) = a_p(\lambda) - a_d(440)\ \exp\ [-q_2(\lambda - 4400)] \tag{3.9}$$

Note that, in this procedure, a fixed shape for phytoplankton absorption is assumed merely to estimate the detrital absorption. Once the detrital absorption is determined, this constraint is dropped.

4. Half of the computed absorption spectra of phytoplankton, $a_{ph}(\lambda)$, were decomposed into Gaussian components, as described in Equation 3.7. The remaining spectra were used to test the accuracy of pigment retrieval from absorption spectra of particulate material.

FIGURE 3.1. Spectral values of light absorption by (a) total particulate matter, (b) non-algal fraction, and (d) specific absorption spectra of living phytoplankton, obtained by subtracting (b) from (a) and normalized to the concentration of chl-*a*.

Figure 3.1

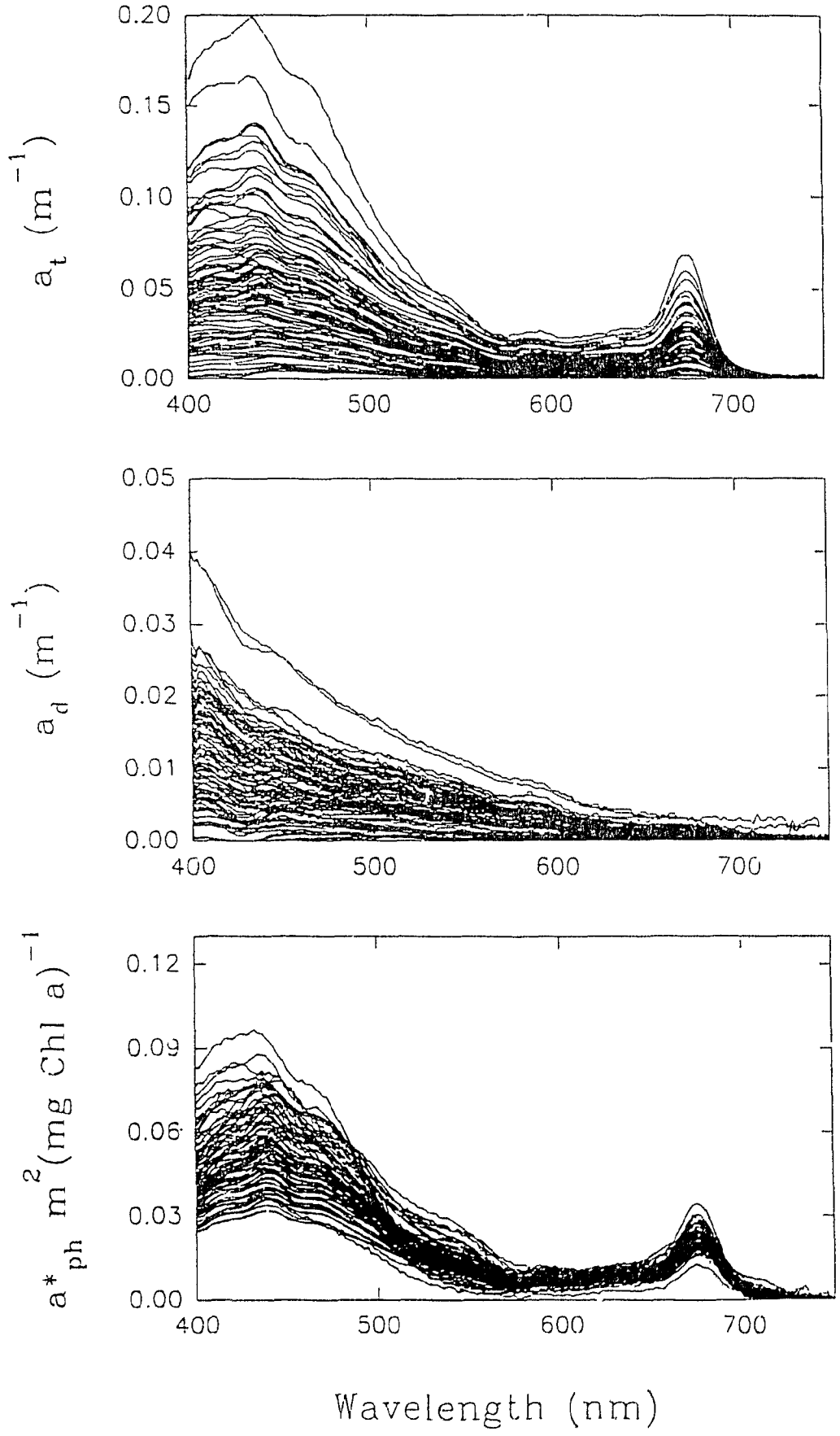
0.20
0.15
0.10
0 05
0.00
a_t (m^{-1})
400
500
600
700
0.05
0.04
0.03
0.02
0.01
0.00
a_d (m^{-1})
400
500
600
700
0.12
0.09
0.06
0.03
0.00
a^*_{ph} m^2(mg Chl a)$^{-1}$
400
500
600
700
Wavelength (nm)

3.3 Results

3.3.1. Absorption coefficients from field data Absorption by total particulate matter, $a_p(\lambda)$, by detritus, $a_d(\lambda)$, and specific absorption by phytoplankton, $a^*_{ph}(\lambda)$, are shown in Figure 3.1 for all samples collected in the western North Atlantic. Contributions from detritus to the total particle absorption in the blue part of the spectrum (ca. 440 nm) varied with water mass (Chapter One), reaching a maximum of 45% over the central part of Georges Bank, a shallow, well-mixed, productive area. When normalized to the biomass (figure not shown), $a^*_p(440)$ ranged from 0.04 to 0.12 m^2(mg Chl-a)$^{-1}$. A similar variability was observed for $a^*_{ph}(440)$, which was not related to the chlorophyll concentration in the sample (Chapter One). In fact, values of $a^*_{ph}(440)$ were closely coupled with the pigment composition of the sample, and reflected regional differences in the dominant phylogenic group of phytoplankton species.

Detrital absorption, $a_d(\lambda)$, increased exponentially toward short wavelengths (Fig. 3.1b). This pattern is consistent with previous studies (Roesler *et al.* 1989, Bricaud and Stramski 1990) and enable us to apply Equation 3.4 as a parametrisation of the spectral variations of the absorption coefficient due to detritus. Indeed, a very good correlation was obtained between observed spectra of a_d and the exponential fit using λ_0 = 440 nm in Equation 3.4. For all samples (n =102), the exponential model explained more than 98% of the variance in the observed data. The exponent, q_1, varied from 0.004 to 0.020 nm^{-1}, extending the range of values given by Bricaud and Stramski (1990), 0.007 to 0.016 nm^{-1}, for samples collected in the Sargasso Sea. Only 10 values of q_1 out of 102 were less than 0.006 nm^{-1}. In these instances, I observed (detailed figure not shown) a significant depression in the $a_d(\lambda)$ spectra in the vicinity of 410 nm, which could be responsible for the low values of q_1 obtained. This feature cannot be explained by an incomplete extraction of photosynthetic pigments on the filter samples since the spectra showed no evidences of a residual peak of absorption at 675 nm due to chl-a.

λ	$a^{*'}_{ph}$	λ	$a^{*'}_{ph}$	λ	$a^{*'}_{ph}$	λ	$a^{*'}_{ph}$	λ	$a^{*'}_{ph}$	λ	$a^{*'}_{ph}$
400	0.794	460	0 866	520	0 382	580	0.132	640	0.180	700	0 077
402	0.804	462	0.862	522	0 371	582	0.132	642	0.182	702	0.067
404	0.823	464	0 858	524	0 360	584	0 132	644	0.184	704	0.061
406	0.839	466	0.853	526	0 348	586	0.134	646	0.186	706	0 053
408	0.858	468	0.845	528	0 339	588	0 135	648	0 188	708	0 049
410	0.874	470	0 835	530	0 330	590	0 136	650	0 191	710	0 043
412	0.887	472	0.822	532	0.323	592	0 135	652	0 196	712	0 039
414	0.900	474	0.808	534	0.314	594	0 136	654	0 204	714	0.035
416	0.907	476	0.791	536	0.308	596	0 136	656	0 214	716	0 031
418	0.916	478	0.772	538	0.300	598	0.136	658	0.231	718	0 028
420	0.920	480	0 753	540	0 293	300	0 135	660	0 251	720	0 024
422	0.925	482	0 734	542	0 285	602	0 135	662	0 278	722	0.022
424	0.929	484	0.715	544	0.277	604	0 135	664	0.307	724	0.018
426	0.940	486	0 698	546	0.269	606	0 137	666	0 341	726	0.016
428	0 951	488	0 680	548	0.258	608	0 138	668	0.373	728	0.015
430	0 965	490	0 662	550	0 248	610	0 141	670	0 401	730	0 013
432	0 979	492	0 643	552	0 237	612	0 143	672	0.419	732	0 010
434	0 993	494	0 622	554	0.225	614	0.146	674	0 429	734	0.009
436	1 000	496	0 601	556	0.213	616	0 149	676	0.426	736	0.008
438	1 002	498	0 579	558	0 200	618	0 152	678	0 415	738	0.004
440	1.000	500	0 556	560	0.188	620	0.154	680	0 392	740	0.003
442	0.989	502	0 534	562	0 178	622	0 156	682	0 362	742	0.002
444	0 974	504	0 509	564	0 168	624	0 158	684	0 324	744	0.001
446	0 957	506	0.488	566	0 160	626	0.162	686	0 284	746	0.001
448	0.937	508	0 468	568	0.152	628	0.165	688	0 241	748	0.000
450	0.917	510	0 450	570	0.145	630	0.168	690	0 201	750	0.001
452	0.901	512	0 434	572	0.140	632	0.171	692	0.164		
454	0 886	514	0 420	574	0 136	634	0.173	694	0 133		
456	0.877	516	0 407	576	0 134	636	0 175	696	0 109		
458	0 871	518	0 393	578	0 132	638	0 177	698	0 091		

TABLE 3.1. Spectral values of absorption coefficient of phytoplankton, normalized at 440 nm and averaged over all samples taken from the western North Atlantic (see Chapter One).

FIGURE 3.2. Plots of (A) absorption coefficient of phytoplankton at 440 nm (in m^{-1}), (B) absorption coefficient of detritus at 440 nm (in m^{-1}), and (C) exponential parameter q (in nm^{-1}), as retrieved from Equation 3.8 *versus* observed values. Note that q_2 derived from the model is compared with q_1 obtained from the exponential fit on the observed spectra of detrital particle. Regression lines were calculated for untransformed data:

$$[a_{ph}(440)]_{calc.} = 0.0016 + 0.96[a_{ph}(440)]_{obs.}, \qquad r^2 = 0.98$$

$$[a_d(440)]_{calc.} = -0.0009 + 1.14[a_d(440)]_{obs.}, \qquad r^2 = 0.80$$

$$q_2 = -0.0014 + 1.16q_1, \qquad r^2 = 0.73$$

Figure 3.2

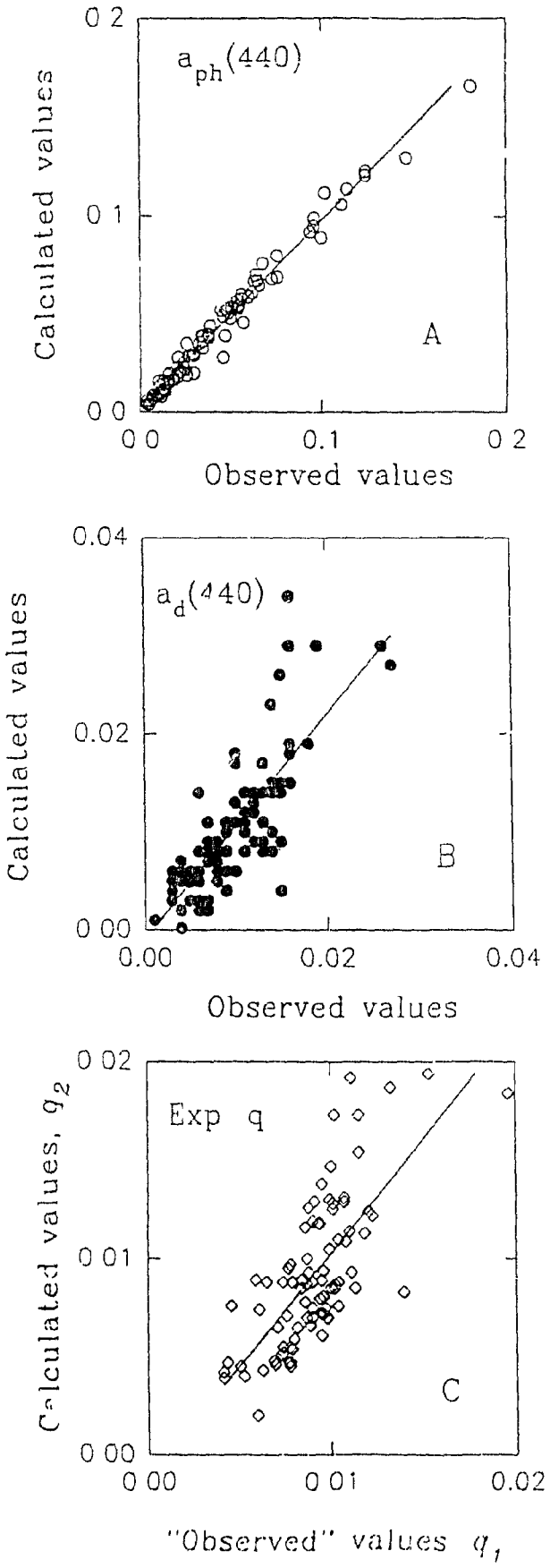
0 2
$a_{ph}(440)$
Calculated values
0 1
A
0 0
0 0
0.1
0 2
Observed values
0.04
$a_d(440)$
Calculated values
0.02
B
0 00
0.00
0.02
0.04
Observed values
0 02
Exp q
Calculated values, q_2
0 01
C
0 00
0 00
0 01
0.02
"Observed" values q_1

3.3.2. Decomposition of the absorption spectra of total particles Each absorption spectrum of phytoplankton, computed as the difference between total particle and detritus absorption spectra (Fig. 3.1c), was normalized to its value at 440 nm. The average value for each wavelength is given in Table 3.1 at 2 nm interval from 400 to 750 nm. Note that the dimensionless values of $a^{*'}_{ph}(\lambda)$ thus obtained are close ($r^2 = 0.97$, $n = 30$) to the comparable curve proposed by Prieur and Sathyendranath (1981), although they applied a different method to data from other regions. This result demonstrates the underlying stability in the spectral shape of absorption by phytoplankton, when a normalized absorption spectrum is obtained from averaging data over various oceanic regimes.

Knowing $a_p(\lambda)$, $a^{*'}_{ph}(\lambda)$, and the spectral shape of $a_d(\lambda)$ as described above, a non-linear regression analysis was applied to Equation 3.8 to retrieve: $a_{ph}(440)$, $a_d(440)$, and q_2. A linearization of Equation 3.8 through logarithmic transformation was not recommended as it would require assumption of normality in the error distribution (Seber and Wild 1988), and it would also have reduced the significance of the parameters. For all samples, the model described in Equation 3.8 predicted spectral variations of total particle absorption successfully. An analysis of variance on the fitting process showed a minimum r^2 value of 0.965, with a mean value of 0.98 ($n = 102$).

In Figure 3.2, the observed and computed values of the parameters are compared. In the case of the exponent, the values obtained from $a_t(\lambda)$, q_2, are compared with those obtained from the exponential fit on the observed spectra, q_1. All plots (Fig. 3.2) showed a one-to-one relationship between observed and calculated values, with an intercept not significantly different from 0. Further, the model can explain 99% and 81% of the variance in the values of $a_{ph}(440)$ and $a_d(440)$, respectively (Fig. 3.2a and b). Greater scatter of the data is observed for the exponent q (Fig. 3.2c). The regression analysis showed, however, a coefficient of determination, $r^2 = 0.73$, still significant at the 0.05 probability level.

FIGURE 3.3. Spectral values of absorption by phytoplankton and detritus computed from the non-linear regression on total particle absorption spectra and compared with field observations. Station names refer to the sampling schedule, described in Figure 1.1.

Figure 3 3

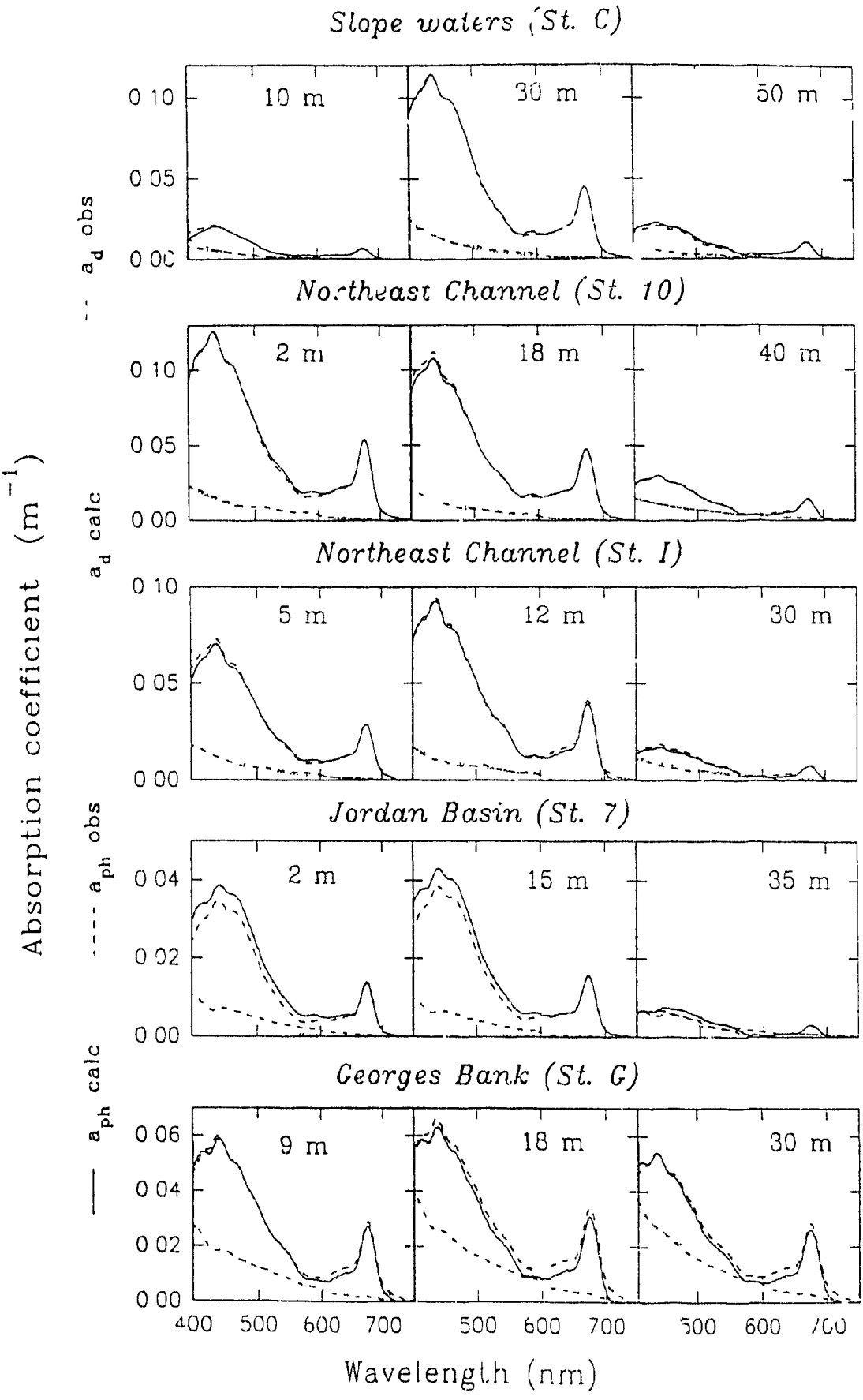
Slope waters (St. C)
10 m
30 m
50 m
Northeast Channel (St. 10)
2 m
18 m
40 m
Northeast Channel (St. I)
5 m
12 m
30 m
Jordan Basin (St. 7)
2 m
15 m
35 m
Georges Bank (St. G)
9 m
18 m
30 m
0 10
0 05
0 00
0 04
0 02
0 06
400
500
600
700
Absorption coefficient (m⁻¹)
Wavelength (nm)
a_d obs
a_d calc
a_ph obs
a_ph calc

3.3.3. Comparison of computed and observed spectra Based on the computed values of q_2 and $a_d(440)$, the spectral variations of $a_d(\lambda)$ were reconstructed for each sample, and the absorption spectra of phytoplankton were then retrieved by subtracting $a_d(\lambda)$ from $a_p(\lambda)$. Reconstructed spectra are shown in Figure 3.3 for some representative water masses, together with the observed data. Results are very satisfactory and show a good agreement between observed and decomposed spectra within various environments such as oligotrophic and coastal waters, surface and deep layers.

In some cases, the observed absorption coefficients of detrital particles were significantly different from the model estimates, particularly in the blue part of the spectrum. This observation can be partly explained by the error distribution in the estimated parameters. Standard relative errors on the first parameter of Equation 3.5, i.e., $a_{ph}(440)$, varied from $\pm$ 0.7% to $\pm$ 5.9%, with a mean value of $\pm$ 1.7%. Higher errors in the determination of $a_{ph}(440)$ were observed at depth, below the euphotic depth. In absolute values, the magnitudes of the error on $a_{ph}(440)$ were similar to those on $a_d(440)$. Thus, in situations were $a_d(440)$ was several times less than $a_{ph}(440)$, an insignificant error in the determination of $a_{ph}(440)$ could become severe for $a_d(440)$. This phenomenon is well illustrated in Figure 3.3, showing a depth variation of detrital and phytoplankton absorption spectra in Jordan Basin (Gulf of Maine). From surface to 15 m, corresponding to the mixed layer, the model underestimates the absorption coefficient of detritus by a factor up to 3 when compared with observed data. The error on $a_d(440)$ decreased from $\pm$ 27% at the chlorophyll maximum (ca. 22 m) to $\pm$ 5.7% and $\pm$ 2% at 35 m and 50 m, respectively, as the contribution from detritus to total particle absorption increased. In most cases, however, the mean standard error on the determination of $a_d(440)$ remained reasonably low, $\pm$ 5.5%, and the model was able to predict accurately the absorption spectrum of phytoplankton in all pelagic environments which characterize the western North Atlantic. Figure 3.4 shows a

one-to-one correspondence ($r^2 = 0.99$, n = 17500 data points) between estimated and observed values of $a_{ph}(\lambda)$ for all stations.

3.3.4. Decomposition of phytoplankton absorption spectra In Chapter Two, I have decomposed the absorption spectra of algal cells into several Gaussian bands, simulating the optical properties of the major groups of pigments. Using this approach, I estimated *in vivo* specific absorption coefficients, $a_i^*(\lambda)$, for chl-*a*, -*b*, and -*c*, and carotenoids. The analyses, however, were based on spectrophotometric determination of pigment concentrations. It is known (Gieskes and Kraay 1983) that liquid chromatography technique can yield estimates of pigment concentrations that differ significantly from spectrophotometric estimates. Therefore, new estimates of $a_i^*(\lambda)$ for the various pigments were necessary in the present work.

The curve fitting program was used as in Chapter Two, with slight modifications in the initial values of the parameters to allow a decomposition of each spectrum into 13 Gaussian bands. Note that only 11 bands were used to represent absorption spectra of unialgal cultures of species containing either chl-*c* or -*b* (Chapter Two). Both types of species are likely to occur in natural phytoplankton assemblages, and consequently, the number of bands corresponding to both chl-*c* and -*b* should be taken into account in the decomposition analysis. The initial values of halfwidths (equal to 2 σ) and centres of maximum Gaussian absorption were taken from Chapter Two (see Table 2.4), as they are the mean values obtained from cultures of three most important phytoplankton groups (Diatoms, Haptophyceae, Chlorophyceae).

Figure 3.5 illustrates the process of decomposition applied on absorption spectra of natural phytoplankton measured at 2 different locations and depths, together with the fitted curve. In all cases, the convergence criterion, less than 0.1% variation in the least-square estimates of the parameters, was reached with less than 10 iterations, and the standard deviation of the fitted spectrum was significantly

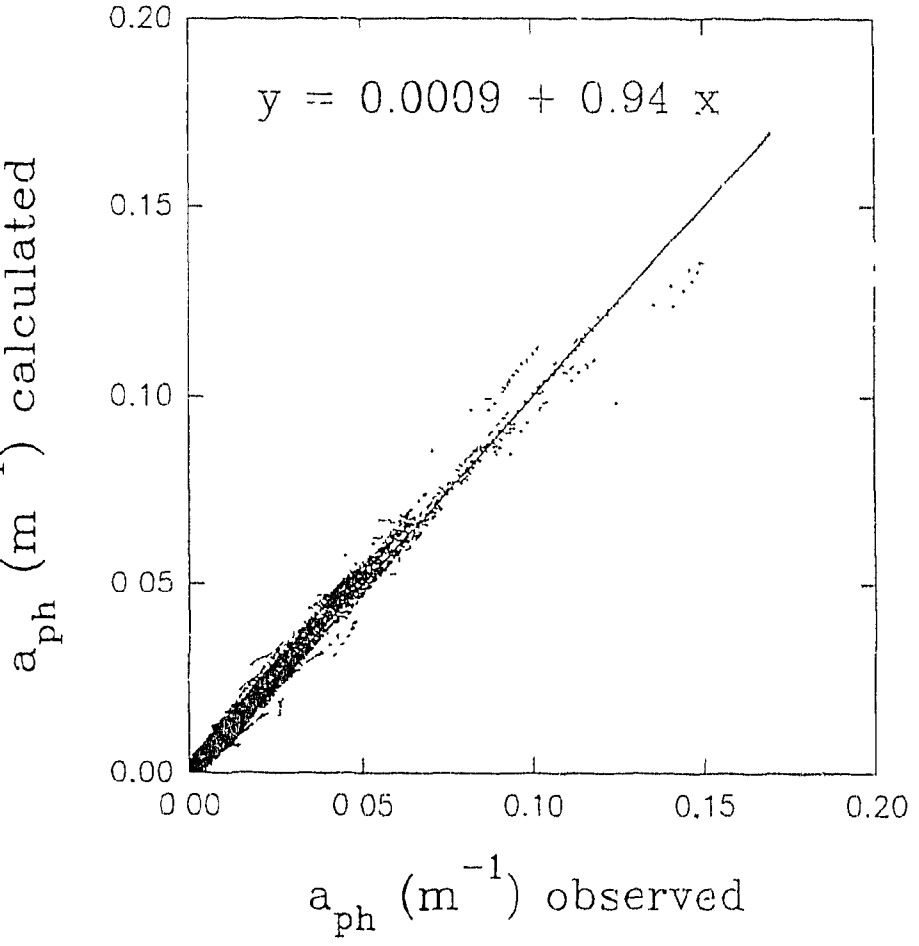

FIGURE 3.4.. Calculated *in vivo* spectral absorption coefficient of phytoplankton *versus* observed values for all samples collected in the western North Atlantic (Chapter One). The coefficient of determination is r^2 = 0.99, n= 17500 data points.

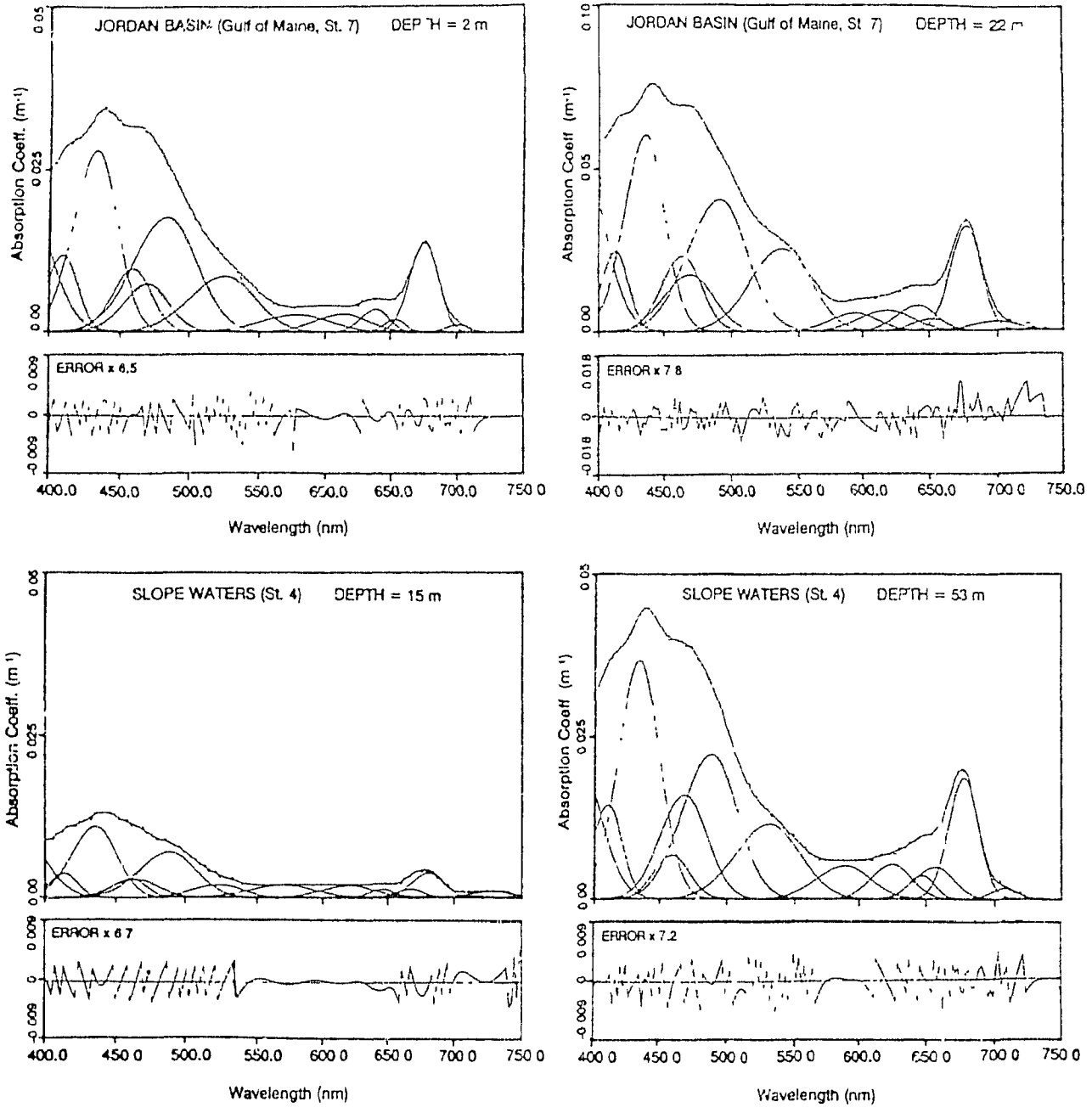

FIGURE 3.5. Decomposition of absorption spectra of natural phytoplankton communities, using the method decribed in Chapter Two. Each absorption spectrum can be represented by the sum of 13 Gaussian bands, reflecting the optical properties of various pigments. Variations in the error are shown in the lower panel for each spectrum.

lower than 1% of the band heights at all wavelengths. The relationship between the height of each Gaussian band and the concentration of the pigment assumed responsible in each case is shown in Figure 3.6.

In all cases, the regressions are significant ($P < 0.01$, $n = 54$), with linear fits that explained more than 75% of the variances. The best fit is observed with chl-*a* and its absorption at 675 nm (Fig. 3.6a) as expected, since contributions due to other pigments are small at this wavelength and this band is the easiest to retrieve. The correlations between chl-*c* and its Gaussian absorption at 460 and 643 (Fig. 3.6c) are more significant than with algal cultures (see Chapter Two Fig. 2.3), probably as a result of a higher efficiency in measuring the concentration of this pigment with HPLC than with conventional spectrophotometric methods.

Note that the regression analyses have been performed on all bands, except those at both ends of the spectrum. Although the absorption values of these bands were normalized to chl-*a* concentration, their presence could not be linked with enough confidence to any specific pigment or group of pigments. Also, band 8 has been allocated to chl-*c*, although it is pointed out, in Chapter Two, that chl-*a* could contribute as well to the light absorption in this spectral range of minimum absorption by phytoplankton.

All regression lines have an intercept not different from 0.. Their slopes constitute an estimation of the specific absorption coefficient, $a_i^*(\lambda)$, of the pigments at the respective absorption maxima of the Gaussian bands. The slopes (Fig. 3.6) are significantly higher than those estimated earlier, in Chapter Two, with algal cultures, which is in general agreement with differences in the methodology used in the two studies: HPLC usually gives lower estimates of pigment concentration than spectrophotometric methods. The differences are not equal for all the pigments.

The specific absorption coefficients of chl-*c* at three wavelengths of maximum absorption (Fig. 3.6c) are higher by a factor of 4 when compared with culture values, whereas this factor is only 1.9 for chl-*b*.

Table 3.2 shows the estimated Gaussian parameters for the 13 bands, averaged over all analysed samples. There are hardly any differences between these values and the initial guesses derived from algal cultures (Chapter Two). This result demonstrates the robustness of the analysis in which each band was allocated to a specific group of pigments on the basis of their known absorption properties (Chapter Two). Differences between the mean values of the specific heights (Gaussian height divided by the corresponding pigment concentration) thus obtained and those derived from the slope of the linear fit in Figure 3.6 are associated with the regression analysis done for a non-zero intercept. The data in Table 3.2 were used with Equation 3.7 to retrieve the spectral varitions of the *in vivo* specific absorption coefficient of each pigment in the entire visible range. The result of this operation is illustrated in Figure 3.7 where the bands for each pigment have been added together to obtain a continuous spectrum for chl-*a*, -*b*, and -*c*, and carotenoids. Bands 1 and 13 were not used in this reconstruction as their affiliation to any pigment remains uncertain.

Values of $a_i^*(\lambda)$ for chl-*c* are unexpectedly high over the entire spectrum, probably because of a systematic underestimation of its concentration in the water using the HPLC technique which could not differentiate chl-c_3 often abundant in Gulf of Maine waters (Chapter One). To correct for this effect, an estimation of chl-c_3 was made by comparing the surface areas under both chl-c_3 and -(c_1 + c_2) peaks on the chromatograms, assuming identical response factors (weight of pigment injected in HPLC divided by peak area) for both pigments. For all samples used in the decomposition, chl-c_3 concentration averaged approximately half that of chl-(c_1 + c_2). This would suggest that the values in Table 3.2 for chl-*c* should be lowered by a factor of 1.5, to account for chl-c_3.

FIGURE 3.6. Maximum Gaussian absorption *versus* pigment concentrations. Chlorophylls-*a*, -*b*, -*c*, and carotenoids have more than one maximum of light absorption in the entire visible range. The slope of each regression line (see text) is a measure of the "*in vivo*" specific absorption coefficient of the pigment responsible, at its maximum absorption.

$$
\begin{aligned}
y_{chla}(415) &= 0.0002 + 0.018[chl-a], & r^2 &= 0.82 \\
y_{chla}(435) &= 0.0017 + 0.044[chl-a], & r^2 &= 0.83 \\
y_{chla}(675) &= 0.0003 + 0.021[chl-a], & r^2 &= 0.91 \\
y_{chlb}(460) &= 0.0015 + 0.097[chl-b], & r^2 &= 0.81 \\
y_{chlb}(655) &= 0.0006 + 0.019[chl-b], & r^2 &= 0.84 \\
y_{chlc}(460) &= 0.0015 + 0.097[chl-c], & r^2 &= 0.77 \\
y_{chlc}(643) &= 0.0005 + 0.037[chl-c], & r^2 &= 0.83 \\
y_{carot.}(490) &= 0.0026 + 0.031[carot.], & r^2 &= 0.84 \\
y_{carot.}(532) &= 0.0007 + 0.018[carot.], & r^2 &= 0.81
\end{aligned}
$$

Figure 3.6

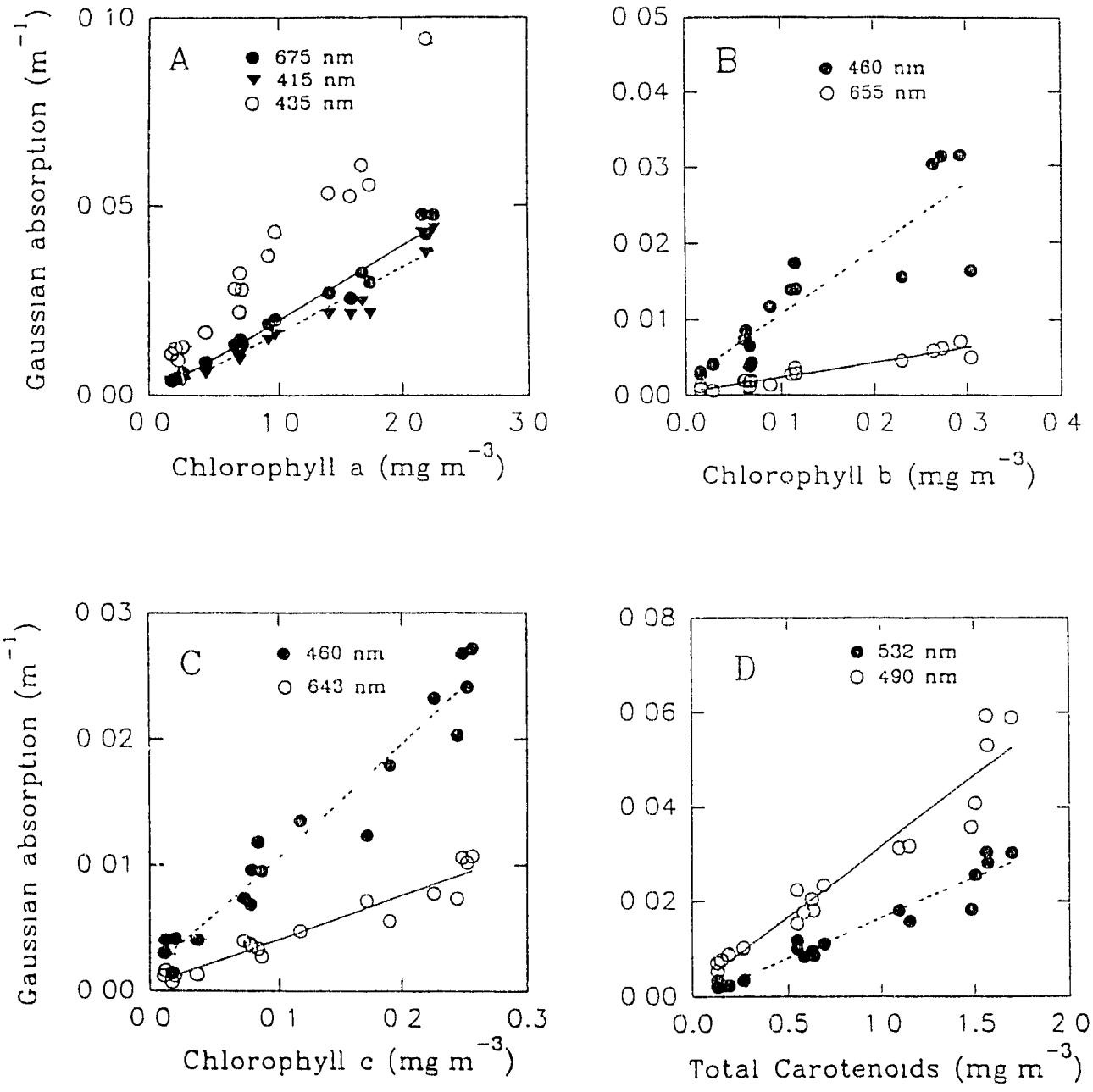
A
675 nm
415 nm
435 nm
Gaussian absorption (m^{-1})
Chlorophyll a (mg m^{-3})
B
460 nm
655 nm
Chlorophyll b (mg m^{-3})
C
460 nm
643 nm
Gaussian absorption (m^{-1})
Chlorophyll c (mg m^{-3})
D
532 nm
490 nm
Total Carotenoids (mg m^{-3})

Characteristic	Gaussian band number and associated pigment species												
	1	2	3	4	5	6	7	8	9	10	11	12	13
	Chl *a*	Chl *a*	Chl-*a*	Chl-*c*	Chl-*b*	Carot	Carot	Chl-*c*	Chl-*a*	Chl-*c*	Chl-*b*	Chl-*a*	Chl-*a*
Input Parameters													
Halfwidth (nm)	53 8	21 3	32 1	27 2	45 0	45 4	45 9	46 3	35 0	28 9	24 4	21 6	33 5
Center (nm)	384	413	435	461	464	490	532	583	623	644	655	676	700
Output parameters													
Halfwidth (nm)	43 2	22 7	34 5	29 3	36 0	46 8	49 6	46 8	38 0	24 9	25 4	24 7	29 0
Center (nm)	381 5	410 8	433 5	459 2	466 6	487 8	532 0	585 6	620 6	640 7	652 9	675 6	699 8
Specific absorption coefficient $[m^2(mg\ Pigment)^{-1}]$	0 042	0 019	0 047	0 110	0 115	0 035	0 019	0 044	0 005	0 044	0 029	0 021	0 002

TABLE 3 2 Input values and mean characteristics of the Gaussian bands reflecting absorption by chlorophylls (chl-) and carotenoids (carot) Specific absorption coefficients of each pigment is the ratio of the Gaussian band absorption and the HPLC concentration of that pigment

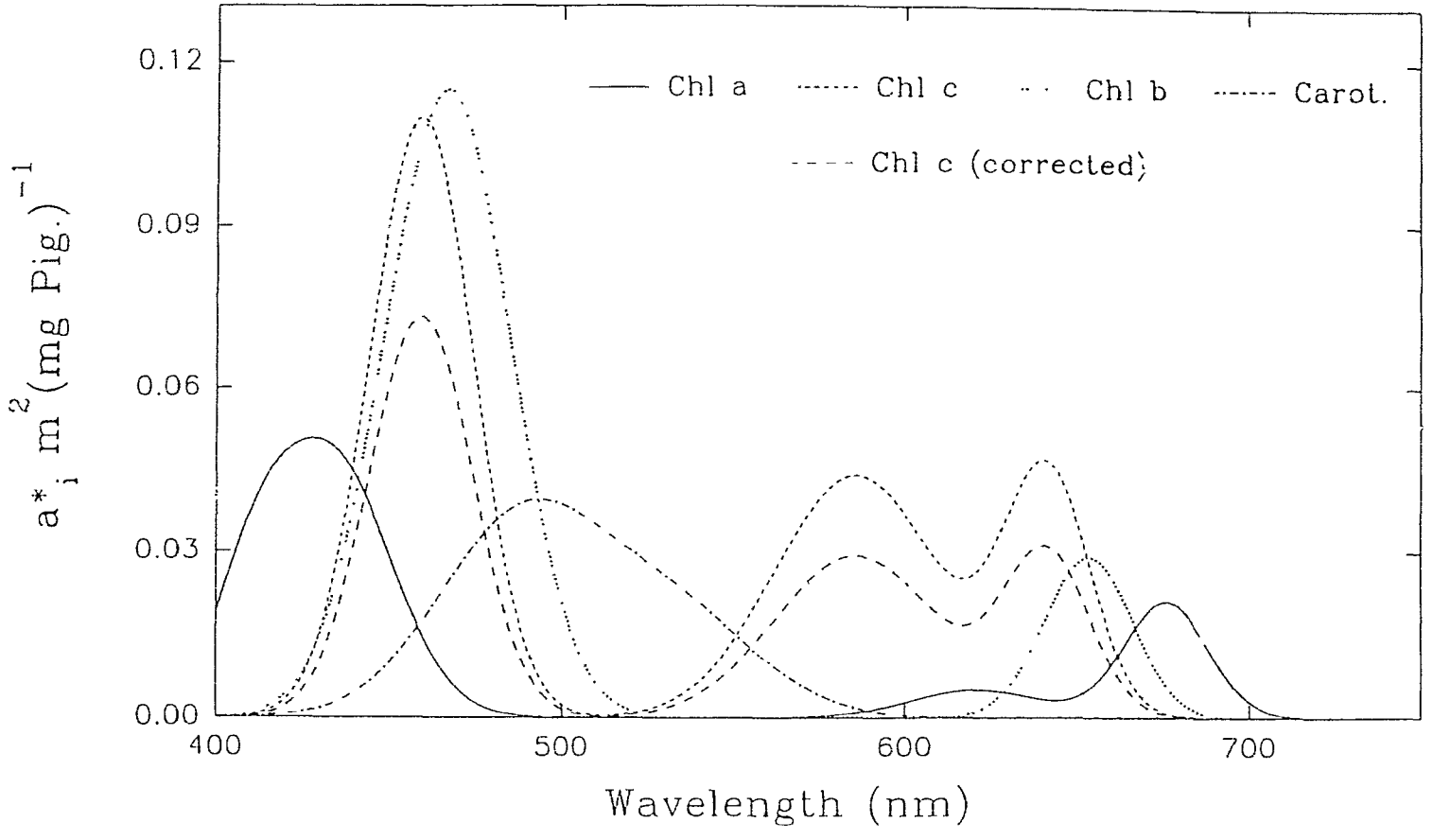

FIGURE 3.7. Computed spectral values of the specific absorption coefficient of chl-*a*, -*b*, -*c*, and carotenoids. Spectrum for chl-*c* are also given after correction for chl-c_3 (see text).

3.3.5. Estimation of pigment concentrations Values of $a_i^*(\lambda)$ from Figure 3.7 and $a_{ph}(\lambda)$ resulting from the non-linear regression analysis are now combined in Equation 3.6 to determine the pigment concentrations. In theory, the computation requires a system of 4 equations at 4 different wavelengths to solve Equation 3.6 for 4 pigments. Ideally, one would choose wavelengths corresponding to the maximum absorption by each pigment and negligible activity from each of the others. Absorption of chl-*a* at 675 nm is close to that ideal case, although chl-*b* may significantly overlap the chl-*a* absorption band as a result of photoadaptative processes under low-light environment (Chapter One). Nevertheless, the following calculation has been conducted using wavelengths selected between 400 and 530 nm, i.e., in a spectral region marked by a strong overlapping of the absorption bands. This choice was motivated by potential applications of this model to remote-sensing of ocean colour. In fact, the efficiency of the model was tested using wavelengths at 412, 443, 490, and 520 nm, corresponding approximately to channels of the satellite ocean colour sensor SeaWIFS, expected to be launched in 1994.

The concentrations of the four pigments obtained by solving the system of four equations are compared in Figure 3.8 with the concentrations measured by HPLC. The resulting regression lines are:

$$[Chl-a]_{calc.} = 0.028 + 0.77\ [Chl-a]_{obs.}, \qquad r^2 = 0.97$$

$$[Chl-b]_{calc.} = 0.042 + 0.65\ [Chl-b]_{obs.}, \qquad r^2 = 0.77$$

$$[Chl-c]_{calc.} = 0.003 + 1.09\ [Chl-c]_{obs.}, \qquad r^2 = 0.92$$

$$[Carotenoid]_{calc.} = 0.026 + 0.83\ [Carotenoid]_{obs.}, \qquad r^2 = 0.96$$

Note that the model is very efficient in retrieving concentrations of chl-*c* and carotenoids as shown by a nearly one-to-one correspondence between both variables. High coefficient of determination is also observed with chl-*a*. The slope of the regression line, however, is significantly different from 1. This result can be

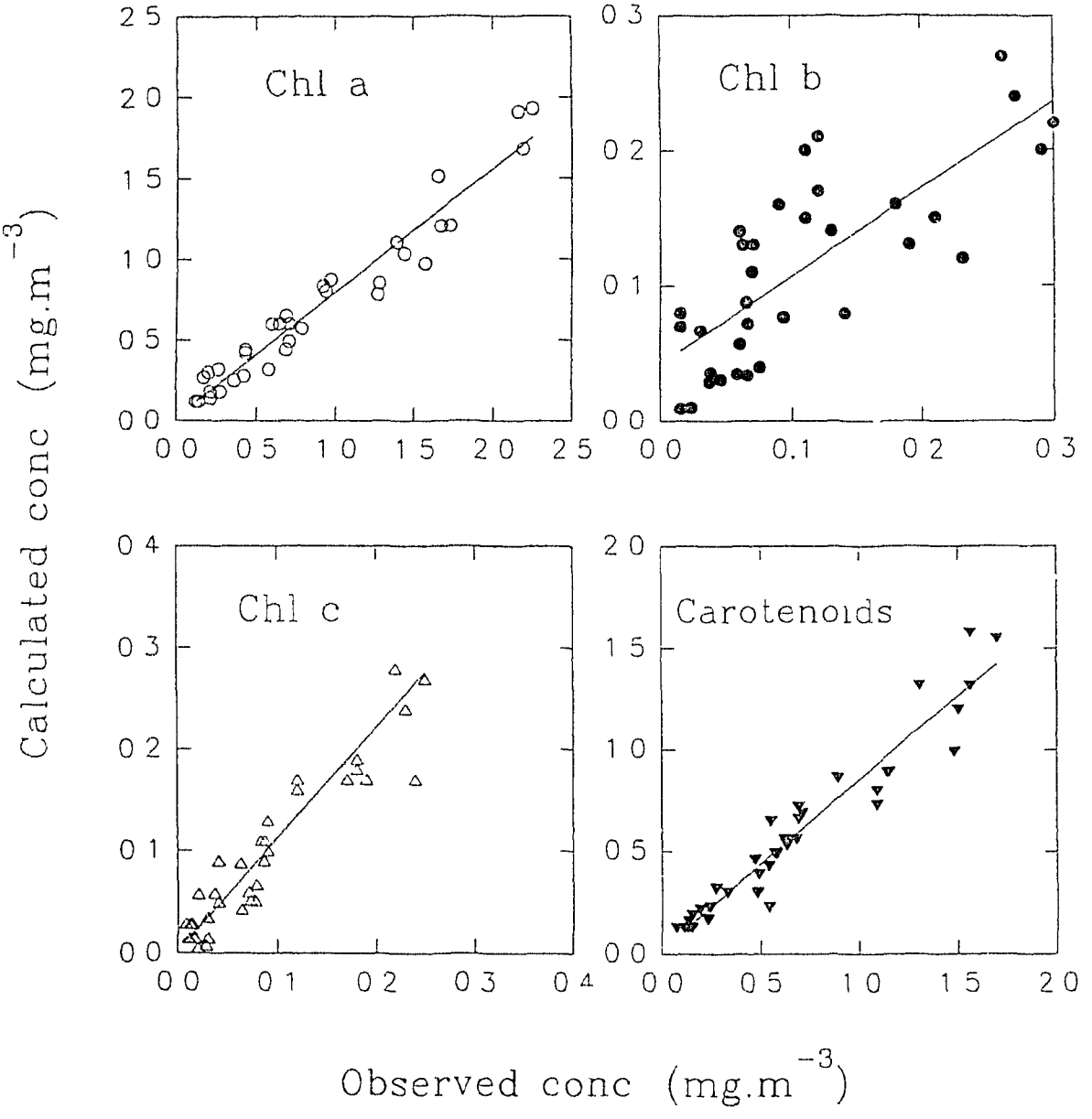

FIGURE 3.8. Computed concentrations of photosynthetic pigments *versus* HPLC field data. Knowledge of the spectral specific absorption coefficient of various pigments allows the determination the pigment concentrations from the *in vivo* absorption spectra of total particle in seawater. Regression lines and coefficient of determination are listed in the text.

explained by the fact that the spectral variation of the specific absorption coefficient of phaeophytin, responsible for band 2 in the decomposition of phytoplankton absorption spectra, is associated in Figure 3.7 to that of chl-*a*. Thus, the specific absorption coefficient of chlorophyll-*a* at 412 nm is overestimated, resulting in a slight underestimation of the concentration of chl-*a* from Equation 3.6. The lowest correlation between observed and calculated values is computed for chl-*b*, although the coefficient of determination is still significant at the 0.05 probability level.

3.4 Discussion

3.4.1. Specific absorption coefficient of pigments In the blue part of the spectrum, absorption per unit of pigment is dominated by accessory chlorophylls (Fig. 3.7), with chl-*b* being more efficient than chl-*c* (after correction for chl-c_3) and -*a*, respectively. This arrangement can also be observed on absorption spectra of chlorophylls extracted in acetone (Prézelin 1981). Further comparisons with the latter study become, however, difficult because of the changes that can occur in the optical properties of individual pigments when freed from their molecular environment (Larkum and Barrett 1983). More recently, two attempts have been made to obtain *in vivo* specific absorption coefficients of individual pigments. Among them, Bidigare *et al.* (1987) observed higher specific absorption by chl-*c* in the blue region. Their results, however, are based on many assumptions which were necessary to combine results from different laboratory studies on unialgal cultures. Sathyendranath *et al.* (1987) used a multiple regression analysis to decompose the absorption spectra of phytoplankton into 5 different groups of pigments, but did not obtain satisfactory results due to correlation between the pigments. Apart from these works, literature data refer only to an "apparent" *in vivo* specific absorption coefficient of phytoplankton, usually estimated from the normalization of the absorption coefficient to chl-*a* concentration. In the blue maximum at 440 nm, these

values vary by a factor of 3, ranging from 0.03 to 0.09 m^2(mg Chl- a)$^{-1}$, with unialgal cultures and natural assemblages (Mitchell and Kiefer 1988, see also Fig. 1.1). This range includes the "true" specific absorption coefficient of chl-a, 0.044 m^2(mg Chl-a)$^{-1}$, obtained in this study (Table 3.2). In the red, a value of 0.021 m^2(mg Chl-a)$^{-1}$ was found at the maximum absorption of chl-a, practically not influenced by the absorbing properties of other pigments. This value corresponds well with other data on cultures reported by Maske and Haardt (1987) and on natural samples from the Sargasso Sea and the upwelling area off Peru (Bricaud and Stramski 1990).

At longer wavelengths, chl-b and -c present slightly higher specific absorption coefficients than chl-a (Fig. 3.7). This is rather surprising since earlier results on spectra of light-harvesting complexes show low absorption properties of accessory chlorophylls compared to that of chl-a in this wavelength region. It is likely that at these wavelengths of lower absorption the data are affected significantly by other pigments not accounted for in the present analysis. According to Chapter Two, an increase in absorption around 590 nm can be partitioned into contributions by chl-c and -a. This would then reduce the absorption by chl-c in the region between 550 and 650 nm. Another important factor to consider is the effect of phycobiliproteins, specific water-soluble pigments usually indicating the presence of cyanobacteria (e.g. *Synechococcus*) in the water column. Although no evidence of a large amount of these pigments are noticeable from the absorption spectra, their presence cannot be ruled out. Phycobiliproteins are mainly composed of phycocyanin with absorption maxima at 620 and 650 nm, and phycoerythrin with maximum around 550 nm (Wood 1985). Accounting for these pigments in the decomposition would reduce even more the absorption by chl-c at these wavelengths, and also that attributed to chl-b at 650 nm. Carotenoids have the lowest specific absorption coefficient (Fig. 3.7), but extend their activity from 400 to nearly 600 nm, partially filling the window left by chlorophylls in the green region of the spectrum.

Station ID	*Intercept*	*Slope*	r^2	*data points*
Georges Bank				
G	−0.0051	1.40	0.98	528
H	−0.0035	1.42	0.97	528
Gulf of Maine				
I	−0.0015	1.06	0.99	880
F	−0.0004	1.00	0.99	1056
E	−0.001	1.03	0.97	1056
Slope waters				
C	0.0003	0.96	0.95	880
Sargasso Sea				
D	0.0003	1.03	0.99	704

TABLE 3.3. Results from regression analyses between observed absorption spectra of phytoplankton and spectra reconstructed from the knowledge of the specific absorption coefficients of various pigments and the concentrations of these pigments.

3.4.2. Particle size effect To validate the technique of spectral decomposition, values of $a_i^*(\lambda)$ were combined with measured pigment concentrations to reconstruct spectral variations of absorption by phytoplankton, $a_{ph}(\lambda)$, using Equation 3.6. This operation was executed on 33 samples distributed among seven stations in the western North Atlantic.

Regression analyses relating observed and reconstructed spectra are shown in Table 3.3 where data have been regrouped for each station. The identification of the stations refers to the cruise sampling schedule described in Chapter One. In all cases, a linear fit to the data explained more than 95% of the variance, with an intercept of the regression lines not different from 0. Differences, however, occurred among the slope values of the regression lines from different regions. At 5 stations within stratified waters of the Gulf of Maine and Sargasso Sea, the slopes were not different from unity, illustrating a one-to-one correspondence between observed and calculated spectra. At stations G and H on Georges Bank, slopes were greater than one, denoting an overestimation of the absorption coefficient of phytoplankton using the technique of spectral decomposition. The reconstructed spectra are compared with measured spectra in Figure 3.9, which shows a close relationship between both observed and calculated spectra in the Gulf of maine and Sargasso Sea. Over Georges Bank, discrepancies between spectra increase at wavelengths of maximum absorption. This pattern is typically of a particle size effect as described by Duysens (1958).

In this study, absorption spectra were not corrected for changes in the particle size distribution within different water masses, to facilitate applications of this bio-optical model in remote sensing. As a result, Gaussian parameters and specific absorption coefficients of pigments in Table 3.2 are representative of an oceanic environment in which organisms with a size range between, say, Prochlorophytes and Coccolithophoridae dominate in the water column, as in stratified waters of the Gulf of Maine and in the open ocean (Chapter One). In Georges Bank waters,

FIGURE 3.9. Comparison of reconstructed absorption spectra of phytoplankton from Equation 3.6 and observed spectra taken from different locations and depths in the western North Atlantic (Chapter One). The significant differences between both spectra in the region of Georges Bank are explained in terms of particle effect.

Figure 3.9

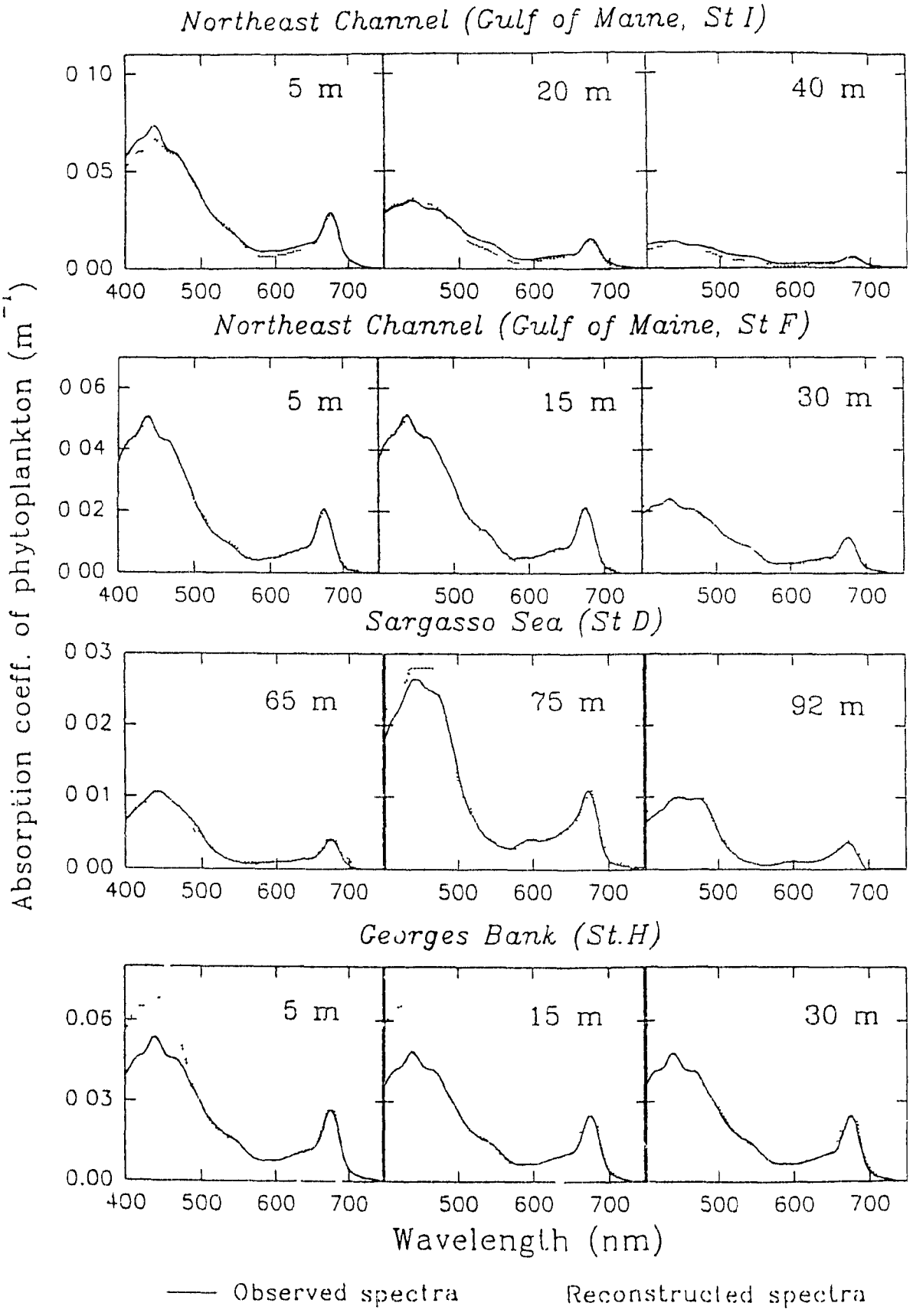
Northeast Channel (Gulf of Maine, St I)
5 m
20 m
40 m
Northeast Channel (Gulf of Maine, St F)
5 m
15 m
30 m
Sargasso Sea (St D)
65 m
75 m
92 m
Georges Bank (St.H)
5 m
15 m
30 m
Absorption coeff. of phytoplankton (m⁻¹)
Wavelength (nm)
Observed spectra
Reconstructed spectra

larger diatoms are abundant (Cura 1987), and are responsible for a particle size distribution significantly different from that in surrounding waters (Kepkay *et al.* 1990). Consequently, a different set of parameters and coefficients are required to apply the model in areas with an abundant community of large phytoplankton cells. The coefficients for Georges Bank are listed in Table 3.4. These are derived from decomposition of 9 absorption spectra of phytoplankton collected in Georges Bank waters. As expected, centres and halfwidths of the Gaussian bands are not different from those in Table 3.2, but the specific Gaussian heights are lower in spectral regions of high absorption. Ratios of specific band heights between both Tables 3.2 and 3.4 average 0.69 for bands 1 to 5, 0.96 for bands 6 to 10, and 0.76 for bands 11 and 12. These values can be considered as measures of flattening effect on communities of large cells, compared to those of nanoplankton.

3.4.3. Absorption by detrital particles The absorption of light by detritus is spectrally featureless (Iturriaga and Siegel 1989), apart from a monotonous increase toward short wavelengths. Morrow *et al.* (1989), using the filter technique (but no solvent extraction), presented a typical absorption spectra of material collected at depth in the water column where particulate matter was essentially made up of phytoplankton breakdown products, including phaeopigments. Similar spectral shapes of absorption by detritus was observed by Iturriaga and Siegel (1989), using a different technique. The method of Kishino *et al.* (1985) implies, however, the extraction of all photosynthetic pigments (except phycobiliproteins) as well as phaeopigments that are contained in the material collected on filters. Thus, the term "detritus" refers, in this case, to material without phaeopigment, whose maximum absorption is typically around 410 nm. A minimum absorption observed sometimes at this wavelength in $a_d(\lambda)$ spectra, as mentionned earlier, represents then an indication of the presence of phaeopigment in the water sample. When the amount of phaeopigment is significantly high compared to chlorophyll-*a*, a correction factor becomes necessary to retrieve spectrum of total detrital particles from the method

Gaussian parameters	Gaussian band number and associated pigment species												
	1	2	3	4	5	6	7	8	9	10	11	12	13
	Chl-*a*	Chl-*a*	Chl-*a*	Chl-*c*	Chl-*b*	Carot.	Carot.	Chl-*c*	Chl-*a*	Chl-*c*	Chl-*b*	Chl-*a*	Chl-*a*
Halfwidth (nm)	43.7	21.8	32.8	28.2	37.9	46.6	50.3	46.4	40.1	28.5	23.4	25.6	34.0
Center (nm)	382.3	411.8	435.2	462.8	466.2	489.3	535.6	586.1	621.6	640.7	653.0	675.7	700.2
Specific absorption coefficient $[m^2(mg\ Pigment)^{-1}]$	0.029	0.013	0.031	0.081	0.074	0.029	0.018	0.044	0.005	0.039	0.020	0.017	0.002

TABLE 3.4. Mean characteristics of the gaussian bands and specific absorption coefficients of chl-*a*, -*b*, -*c*, and carotenoids for Georges Bank waters, where the phytoplankton community is dominated by large Diatoms.

of Kishino *et al.* (1985). In addition, absorption spectra due to solvent-extracted material may contain phycobiliprotein pigments affecting the absorption by detritus at wavelengths ranging from 550 to 630 nm. Bio-optical models such as the one presented in this work become then particularly important to avoid these problems using an exponential parametrization of absorption by detritus which adequately fit observed data.

3.5 Conclusions

The present analysis demonstrates clearly that the concentrations of various phytoplankton pigments can be determined from a knowledge of the absorption spectra of total particles. The spectral shape of light absorption by detritus has been well defined such that its differentiation from total particle absorption only requires an averaged and normalized absorption spectrum of phytoplankton, typically representative of a wide variety of water masses. The non-linear model used to distinguish contributions due to detritus and phytoplankton can explain more than 96% of the variance in observed data from all provinces and depths encountered in the western North Atlantic.

The model presented here has another important application, that of retrieving accessory pigments such as chlorophyll-*c*, -*b*, and carotenoids, in addition of chlorophyll-*a*. The decomposition of phytoplankton absorption spectra into Gaussian bands has been applied successfully with natural communities of phytoplankton and HPLC data to obtain specific coefficients of absorption for each pigment, independently of the structure of the phytoplankton community present in the water column. The model is robust as shown by the effective reconstruction of absorption spectra by phytoplankton, using these coefficients. However, disregarding the size distribution of the cells in the water column limits the utilization of the specific absorption coefficients for the pigments, although it is possible to correct the values

between one phytoplankton community to another, by accounting for the flattening factor.

With the increasing interest in measuring the *in vivo* light absorption by total particulate matter in marine waters, this work opens the possibility to retrieve spectral variations of light absorption by phytoplankton, detritus and the concentration of major phytoplankton pigments from these data. Also, this model can stand as a tool to interpret data on total photon absorption by seawater which is estimated from downwelling and upwelling irradiance measurements (Prieur and Sathyendranath 1981), or from remotely-sensed reflectance of seawater (Gordon and Morel 1983), if there is additional information on backscattering.

Summary and Conclusions

Although the amount of light scattered out of the oceans represents an important variable in the domain of satellite oceanography, its proportion relative to the light entering the sea is very low, usually less than 5% (Morel and Prieur 1977). Therefore, the majority of photons eventually vanish in the water column through the process of absorption by water, dissolved organic substances, and pigmented particulate matter. In this thesis, I have addressed the importance of phytoplankton in the absorption of light in marine waters, and further emphasized the role of accessory pigments in controlling variability in the specific absorption coefficient of phytoplankton.

In Chapter One, significant fluctuations of some optical properties attributed to particulate matter were presented for the western North Atlantic. Phytoplankton and co-varying material appear to be the major factor affecting the beam attenuation coefficient, through changes in species composition and pigment concentration, and through photoadaptation. On the other hand, a combination of detailed pigment analyses and measurements of spectral absorption by phytoplankton suggested a regional distribution in these optical properties, closely related to the structure of the phytoplankton community.

Besides the flattening effect reported by Yentsch and Phinney (1989) as the major contributor to changes in the specific absorption coefficient of phytoplankton at 440 nm, the results obtained in Chapter One indicate the influence of other pigments co-existing with chl-*a* in each cell. For instance, the presence of chl-*b* in Prochlorophytes, abundant in open-ocean waters, likely enhanced the light absorption by phytoplankton in the blue range, when compared with absorption in coastal waters dominated by Prymnesiophytes and Diatoms.

Changes in the shape of spectral absorption by phytoplankton adhered to a similar regional division. Indeed, fucoxanthin-to-chl-*a* ratio increased from open-ocean Sargasso Sea waters to the highly productive area over Georges Bank. This accounts for the drastic changes in the ratio of light absorption at 550 nm and at 440 nm by phytoplankton. Such a result opens the possibility of differentiating between taxonomic groups of phytoplankton, using changes in the shape of their absorption spectra.

In Chapter Two, the parametrization of the *in vivo* specific absorption coefficient of phytoplankton was investigated through the development of a simple model, which accounted for the absorbing properties of individual pigments. A similar idea was developed by Bidigare *et al.* (1987) to retrieve primary production in marine waters, using a bio-optical model. In this latter study, however, some of the specific absorption coefficients of individual pigments were obtained from spectra of extracted pigments (Mann and Myers 1968), which were supposedly corrected for different effects due to solvent extraction. Some other values of specific absorption by individual pigments were taken directly from the absorbing properties of isolated light-harvesting complexes (Bidigare *et al.* 1987). According to Larkum and Barrett (1983), the effects of these operations (extraction and isolation of pigment-protein complexes) on the "*in vivo*" optical properties of pigments are difficult to assess and vary with species. This observation limits then the general applicability of methods such as the one described by Bidigare *et al.* (1987). The model presented here has the advantage of preserving the "*in vivo*" optical properties of the pigments, whose absorption bands are approximated by a Gaussian spectral distribution.

In vivo absorption spectra of several phytoplankton species were successfully decomposed into eleven Gaussian bands, after correction for the particle effect. These bands reflected adequately the specific absorption of 4 pigments: chl-*a*, -*b*, -*c*, and the group of carotenoids. The results showed that chl-*b* can contribute significantly to the absorption by phytoplankton at 440 nm, confirming observations

in Chapter One. Also, the relationship between Gaussian band absorption and pigment concentrations were not affected by phytoplankton species, such that a unique set of specific absorption coefficients were computed for the 4 pigments. These coefficients allowed retrieval of the *in vivo* absorption spectrum of a multi-species sample, from the knowledge of pigment concentrations alone. This represents an improvement in the computation of the specific absorption coefficient of phytoplankton, which is often computed with respect to chl-*a*, and, hence, does not include the effect of the other pigments explicitly. In addition, the method proposed in this chapter offers the possibility to estimate the absorption of light by phytoplankton without direct measurements of the detrital component.

In Chapter Three, the contributions due to detrital particles and phytoplankton to the total light absorption was retrieved efficiently by non-linear regression on the absorption spectra of total particulate matter. The model, described in Chapter Two, was then used with the resulting absorption spectra of phytoplankton to demonstrate that the concentrations of various phytoplankton pigments can be determined from the absorption spectra of total particles alone. More than 76% of the variance in the pigment concentrations over the western North Atlantic were explained through this analysis. However, the results showed that ignoring the size distribution of particles in the water limits the use of the specific absorption coefficients estimated for each pigments to restricted oceanic areas, unless some kind of flattening factor can be determined for regions with phytoplankton of different sizes. Nevertheless, with increasing development of new techniques to measure the absorption coefficient of seawater (Zaneveld *et al.* 1988), the model presented here will be of direct application in estimating the major photosynthetic pigments present in the water, from *in situ* optical measurements.

Following a similar development, the model presented in this thesis could find an important application in remote sensing of ocean colour. The radiance signal

from seawater detected by the remote sensor depends on the reflectance of seawater, which, in turn, can be expressed in terms of some inherent optical properties (Gordon and Morel 1983). At this point, it is common practice to assume that 1) only water and phytoplankton can affect the reflectance of seawater, and 2) only chl-*a* (or chl-*a* and phaeophytin-*a*), and substances that covary with it, can affect the optical properties of phytoplankton at the wavelengths detected by the sensor. With additional knowledge about the backscattering coefficient of seawater, one can use a bio-optical model, such as the one presented in this thesis, to partition the reflectance signal into optical properties of the main constituents in seawater, including detrital particles and phytoplankton. In addition, the model can be used to improve retrieval of chlorophyll-*a* from ocean colour data, and to estimate other phytoplankton pigments that are representative of the major taxonomic groups of phytoplankton. However, further improvements of the method presented here to include the effects of yellow substances and other auxiliary pigments such as phycobilins, remain to be investigated.

APPENDIX

Decomposition of absorption spectra: sensitivity to changes in the initial values of the Gaussian parameters.

The decomposition of absorption spectra is achieved by a non-linear curve fitting procedure in which the sum of a number of Gaussian distributions is made to match the spectral distribution of the absorption coefficient of phytoplankton. Initial estimates of the parameters of the Gaussian bands are based on visual inspection of the total absorption spectrum. The computation proceeds then by iterations, during which the gaussian parameters of each band are modified to minimize the error between the calculated and observed spectrum.

The changes in each parameter are limited according to some specific conditions implemented in the model (described in Chapter Two). These specifications should allow some flexibility regarding the choice of the initial values of the parameters. In the following analyses, the effect of variations in the initial parameters on the final Gaussian parameters and the residual fitting error is monitored.

Sensitivity to changes in one parameter of one band.

Changing band centers and halfwidths by $\pm$ 5nm, or heights by $\pm$ 1 m^{-1}, for one band has little effect on the final result, i.e., no changes are observed in the residual errors after a maximum number of 20 iterations, and the variations in the output parameters for each band are less than $\pm$ 10% in the case of heights and halfwidths, and $\pm$ 0.05% for band centers. An exception, however, is observed with band 2, which shows a $\pm$ 15% change in height when the initial value of its halfwidth is increased by 5 nm (Table A.1) Similarly, changing initial values of centers and halfwidths by $\pm$ 10 nm, or heights by $\pm$ 2 m^{-1} only slightly increases the changes in the output values, and again the maximum change occurs in the height of band 2 ($>$ 30%) as its initial halfwidth is increased by 10 nm (Table A.1). Such a variation in band 2 height takes place without subsequent increase in the residual error, and therefore can be significant in the sense that an error of 30% is higher than the standard error ($\pm$ 17.4%) obtained for the estimate of the specific absorption coefficient of Chl-*a* at the wavelength of maximum absorption for band 2. In all the other cases (this analysis was made on 4 bands), a significant change

in one parameter always induces an increase in the residual error, when compared with the initial run. The effect of such variations in the initial values is reduced when the number of iterations in the main calculation is increased.

Sensitivity to simultaneous and similar changes in all bands. Figure A.1 shows the variations in the output values of each parameter after shifting the center of all bands by 1 to 10 nm towards higher wavelengths. Higher wavelength bands remain rather stable and insensitive to changes in the initial values of band centers. In the short-wave part of the spectrum, differences in sensitivity occur between bands, with bands 1, 3, and 6 presenting no significant variations in the output values after changing all band centers by ca. 5 nm, whereas bands 2, 4, and 5 react more rapidly to a shift in band centers. Note, however, that significant changes occurring in just a few of the output band parameters lead to an increase in the residual error. Increasing the number of iterations in the curve fitting process reduces the differences in the output.

When all the input band centers are changed by more than 8 nm (Fig. A.1), variations in the output heights and halfwidths, as well as the residual error, drop considerably. In parallel, however, a significant change occurs in the band positions 1, 2, and 4 (e.g., band 2, initially centered at ca. 412 nm, is shifted to 438 nm). In this case, although the variation in the curve fitting error when compared with the initial run is minimum, the initial configuration of the bands relative to the position of peaks and shoulders in the total spectrum is altered, with some bands becoming confused with the next one.

Figure A.2 shows the results of a similar analysis after changing the initial values of halfwidths for all bands by 1 to 10 nm. The output is similar for all bands, and show a significant departure from the initial results after a change in halfwidths of 3 or 4 nm. This is also true for the residual error. In most cases,

Variations in the initial values of Band 2 parameters	Variations in the output values of all bands parameters		
	Height	*Center*	*Halfwidth*
Center ±5nm	0.3%	0.0%	0.4%
	(0.0-1.9%)	(0.0-0.2%)	(0.0-2.2%)
Halfwidth ±5nm	1.3%	0.03%	0.78%
	(0.0-15.2%)	(0.0-0.3%)	(0.0-4.5%)
Center ±10nm	2.1%	0.07%	1.74%
	(0.0-10.9%)	(0.0-0.5%)	(0.0-10.2%)
Halfwidth ±10nm	2.41%	0.04%	1.45%
	(0.0-31.1%)	(0.0-0.3%)	(0.0-11.6%)
Height ± 1.0m^{-1}	0.75%	0.0%	0.3%
	(0.0-7.3%)	(0.0-0.2%)	(0.0-1.5%)
Height ± 2.0m^{-1}	1.48%	0.05%	0.73%
	(0.0-15.8%)	(0.0-0.4%)	(0.0-6.2%)

TABLE A.1. Average and range of % variation compared with the original output values of Gaussian parameters, when the initial values of Band 2 parameters are changed. All computations were run for a maximum of 20 iterations.

differences in the residual error, as well as in the output values of the parameters, can be reduced by increasing the number of iterations.

FIGURE A.1 Percentage variations in the output values of Gaussian band parameters and residual errors in the curve fitting, when the initial input values of all band centers were varied by 1 to 10 nm. The percentage variations are all computed with respect to the results obtained with the initial values described in Chapter Two. All computations were run for a maximum of 20 iterations.

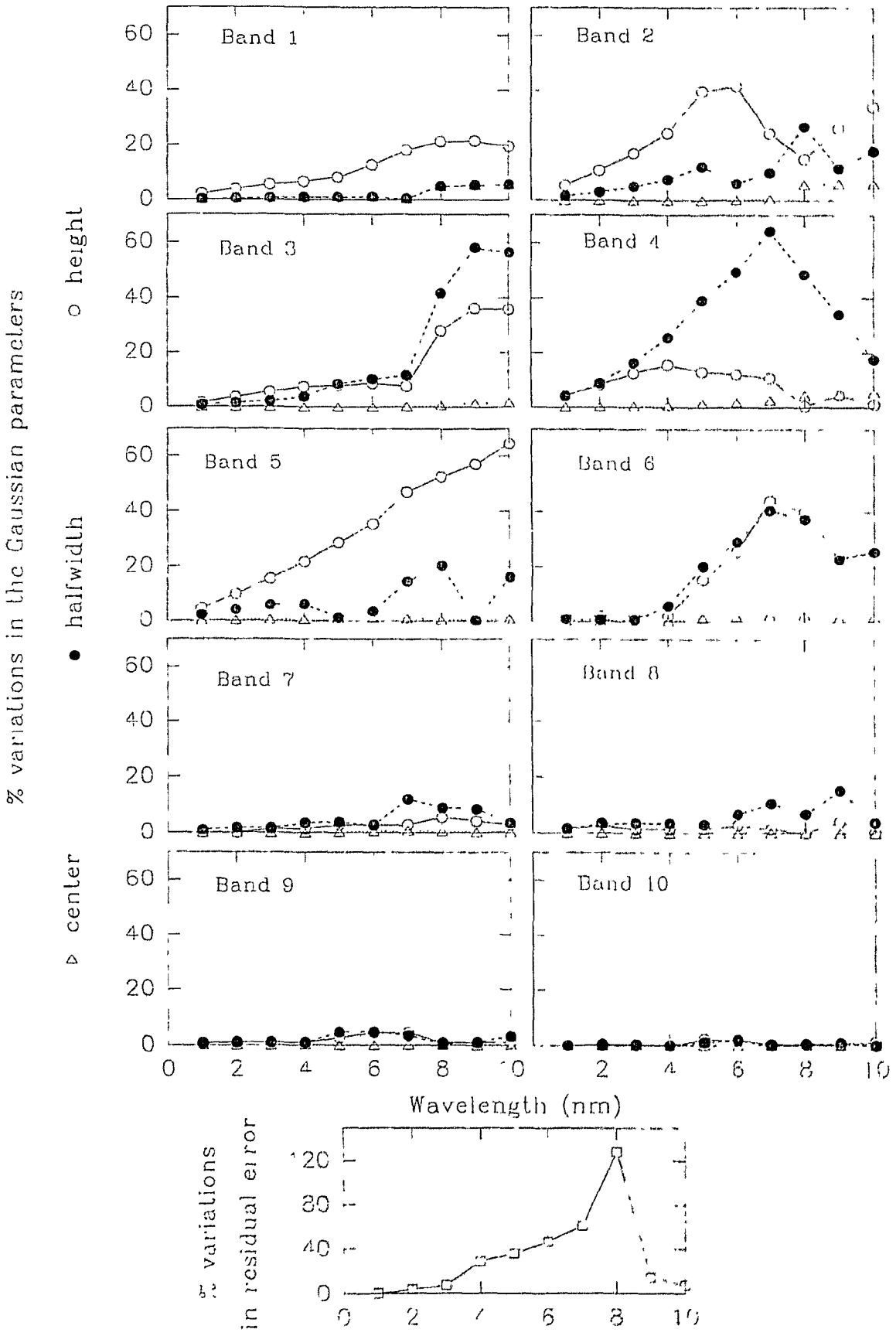
% variations in the Gaussian parameters
o height
• halfwidth
▵ center
Band 1
Band 2
Band 3
Band 4
Band 5
Band 6
Band 7
Band 8
Band 9
Band 10
0
20
40
60
0
2
4
6
8
10
Wavelength (nm)
% variations in residual error
0
40
80
120

FIGURE A.2. Percentage variations in the output values of Gaussian band parameters and residual errors in curve fitting, when the initial input values of all band halfwidths were varied by 1 to 10 nm. All computations were run for a maximum of 20 iterations.

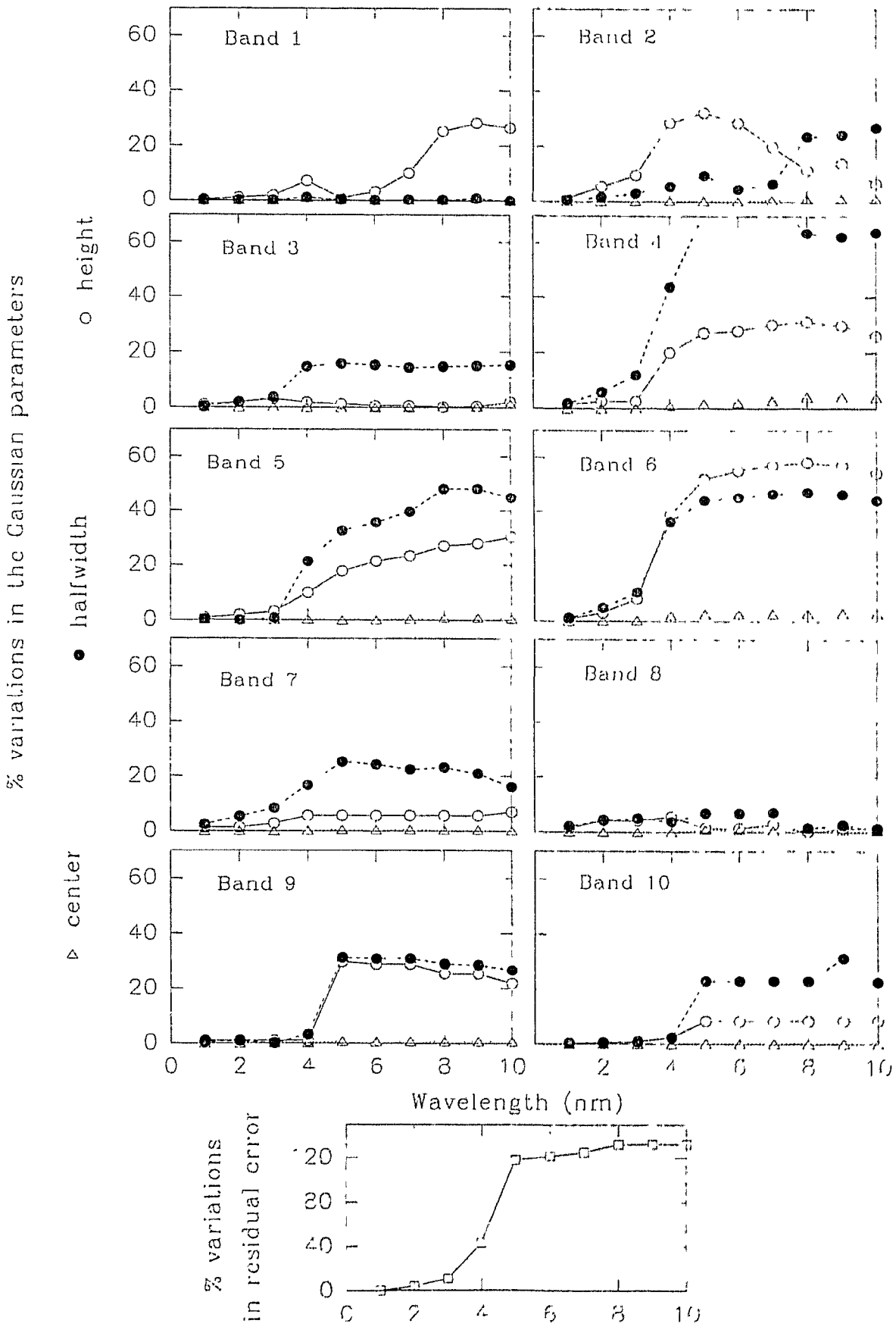
% variations in the Gaussian parameters
o height
● halfwidth
△ center
Band 1
Band 2
Band 3
Band 4
Band 5
Band 6
Band 7
Band 8
Band 9
Band 10
0
20
40
60
0
2
4
6
8
10
Wavelength (nm)
% variations in residual error
0
20
40
60

REFERENCES

Ackleson, S.G., W.M. Balch, and P.M. Holligan. 1988. White waters of the Gulf of Maine. Oceanography 1:18-22.

Balch, W.M., P.M. Holligan, S.G. Ackleson, and K.J. Voss. 1991. Biological and optical properties of mesoscale coccolithophore blooms in the Gulf of Maine. Limnol. Oceanogr., 36:629-644.

Berger, R., S. Liaaen-Jensen, V. McAlister, and R.R.L. Guillard. 1977. Carotenoids of Prymnesiophyceae (Haptophyceae). Biochem. Syst. Ecol. 5:71-75.

Bidigare, R.R., J.H. Morrow, and D.A. Kiefer. 1989. Derivative analysis of spectral absorption by photosynthetic pigments in the western Sargasso Sea. J. Mar. Res. 47:323- 341.

Bidigare, R.R., R.C. Smith, K.S. Baker, and J. Marra. 1987. Oceanic primary production estimates from measurements of spectral irradiance and pigment concentrations. Global Biogeochemical Cycles 1: 171-186.

Boczar, B.A., and B.B. Prézelin. 1989. Organization and comparison of chlorophyll-protein complexes from two fucoxanthin-containing algae: *Nitzschia closterium* (Bacillariophyceae) and *Isochrysis galbana* (Prymnesiophyceae). Plant Cell Physiol. 30: 1047-1056.

Bohren, C.F., and D.R. Huffman. 1983. Absorption and Scattering of light by small particles. John Wiley & Sons Inc., New York.

Bricaud, A., A.-L. Bédhomme, and A. Morel. 1988. Optical properties of diverse phytoplanktonic species: experimental results and theoretical interpretation. J. Plankt. Res. 10: 851-873.

Bricaud, A., and A. Morel. 1986. Light attenuation and scattering by phytoplanktonic cells: a theoretical modeling. Appl. Opt. 25: 571-580.

Bricaud, A., A. Morel, and L. Prieur. 1981. Absorption by dissolved organic matter of the sea (yellow substance) in the UV and visible domains. Limnol.

Oceanogr., 26, 43-53.

Bricaud, A., A. Morel, and L. Prieur. 1983. Optical efficiency factors of some phytoplankters. Limnol. Oceanogr. 28: 816-832.

Bricaud, A., and D. Stramski. 1990. Spectral absorption coefficients of living phytoplankton and nonalgal biogenous matter: a comparison between the Peru upwelling area and the Sargasso Sea. Limnol. Oceanogr. 35:562-583.

Britton, G. 1983. The biochemistry of natural pigments. Cambridge Univ. Press. Cambridge.

Butman, B., and R.C. Beardsley. 1987. Physical Oceanography. p. 88-98. *In* R.W. Backus [ed.]. Georges Bank. MIT press.

Carder, K.L., R.G. Steward, G.R. Harvey, and P.B. Ortner. 1989. Marine humic and fulvic acids: their effects on remote sensing of ocean chlorophyll. Limnol Oceanogr., 34: 68-81.

Chisholm, S.W., R.J. Olson, E.R. Zettler, R. Goericke, J.B. Waterbury, and N.A. Welschmeyer. 1988. A novel free-living prochlorophyte abundant in the oceanic euphotic zone. Nature 334:340-343.

Cotton, T.M., A.D. Trifunac, K. Ballschmiter, and J.J. Katz. 1974 State of chlorophyll *a in vitro* and *in vivo* from electronic transition spectra, and the nature of antenna chlorophyll. Biochim. Biophys. Acta. 368: 181-198.

Cullen, J.J. 1990. On models of growth and photosynthesis in phytoplankton Deep-Sea Res., 37:667-683.

Cura, J.J. 1987. Phytoplankton. p. 213-220. *In* R.W. Backus [ed.]. Georges Bank. MIT press.

Denman, K.L., and A.E Gargett. 1988. Multiple thermoclines are barriers to vertical exchange in the subarctic Pacific during SUPER. May 1984. J. Mar. Res., 46:77-103.

Duysens, L.M.N. 1956. The flattening effect of the absorption spectra of suspensions as compared to that of solutions. Biochim. Biophys. Acta., 19: 1-12.

Everitt, D.A., S.W. Wright, J.K. Volkman, D.P. Thomas, and E.J. Lindstrom. 1990. Phytoplankton community compositions in the western equatorial Pacific determined from chlorophyll and carotenoid pigment distributions. Deep-Sea Res., 37:975-997.

Falkowski, P.G., T.G. Owens, H.C. Ley, and D.C. Mauzerall. 1981. Effects of growth irradiance levels on the ratio of reaction centers in two species of marine phytoplankton. Plant Physiol., 68: 969-973.

Fawley, M.W. 1989. Detection of chlorophylls c_1, c_2 and c_3 in pigment extracts of *Prymnesium parvum* (prymnesiophyceae). J. Phycol., 25: 601-604.

Fawley, M.W., C.A. Douglas, K.D. Stewart, and K.R. Mattox. 1990. Light-harvesting pigment-protein complexes of the ulvophyceae (Chlorophyta): characterization and phylogenetic significance. J. Phycol., 26: 186-195.

Förster, T. 1965. Delocalized excitation and excitation transfer. In: Sinanoğlu, O. (ed.) Modern Quantum Chemistry 3. Academic Press, New York, p. 93-137.

Foss, P., R.R.L. Guillard, and S. Liaaen-Jensen. 1984. Prasinoxanthin: a chemosystematic marker for algae. Phytochemistry, 23:1629-1633.

Fournier, R.O., M. van Det, N.B. Hargreaves, J.S. Wilson, T.A. Clair, and R. Ernst. 1984. Physical factors controlling summer distribution of chlorophyll *a* off southwestern Nova Scotia. Limnol. Oceanogr., 29:517-526.

French, C.S., J.S. Brown, and M.C. Lawrence. 1972. Four universal forms of chlorophyll *a*. Plant Physiol., 49: 421-429.

French, C.S., J.S. Brown, L. Prager, and M.C. Lawrence. 1967. Analysis of spectra of natural chlorophyll complexes. Carnegie Inst. Yearbook, 67: 536-546.

Friedman, A.L., and R.S. Alberte. 1984. A diatom light- harvesting pigment-protein complex. Purification and characterization. Plant Physiol., 76: 483-489.

Friedman, A.L., and R.S. Alberte. 1986. Biogenesis and light regulation of the major light harvesting chlorophyll-protein of diatoms. Plant Physiol., 80: 43-51.

Garrett, C.J.R., J.R. Keeley, and D.A. Greenberg. 1978. Tidal mixing versus thermal stratification in the Bay of Fundy and the Gulf of Maine. Atmosphere-Ocean, 16:403-423.

Gieskes, W.W.C., and G.W. Kraay. 1983a. Unknown chlorophyll *a* derivatives in the North Sea and the tropical Atlantic Ocean revealed by HPLC analysis. Limnol. Oceanogr., 28:757-766.

Gieskes, W.W.C., and G.W. Kraay. 1983b. Dominance of Cryptophyceae during the phytoplankton spring bloom in the central North Sea detected by HPLC analysis of pigments. Mar. Biol., 75:179-185.

Gieskes, W.W., and G.W Kraay. 1986. Floristic and physiological differences between the shallow and the deep nanophytoplankton community in the euphotic zone of the open tropical Atlantic revealed by HPLC analysis of pigments. Mar. Biol., 91: 567-576.

Gieskes, W.W., G.W. Kraay, A. Nontji, D. Setiapermana, and Sutomo. 1988. Monsoonal alternation of a mixed and a layered structure in the phytoplankton of the euphotic zone of the Banda Sea (Indonesia): a mathematical analysis of algal pigment fingerprints. Netherlands J. Sea Res., 22:123-137.

Goedheer, J.C. 1970. On the pigment system of brown algae. Photosynthetica, 4: 97-106.

Gordon, H.R., and A. Morel. 1983. Remote assessment of ocean colour for interpretation of satellite visible imagery. A review. Lecture notes on Coastal and Estuarine Studies, 4. Springer-Verlag, New-York.

Guillard, R.R.L., L.S. Murphy, P. Foss, and S. Liaaen- Jensen. 1985. *Synechococcus* spp. as likely zeaxanthin-dominant ultraphytoplankton in the North Atlantic. Limnol. Oceanogr., 30:412-414.

Hoepffner, N., and L.W. Haas. 1990. Electron microscopy of nanoplankton from the North Pacific Central Gyre. J. Phycol., 26:421-439.

Højerslev, N.K. 1975. A spectral light absorption meter for measurements in the sea. Limnol. Oceanogr., 23:1024-1034.

Højerslev, N.K. 1988. Natural occurences and optical effects of Gelbstoff. 30pp., Univ. Copenhagen Geophys. Inst. Rep., 50.

Højerslev, N.K., and J. Trabjerg. 1990. A new perspective for remote measurements of plankton pigments and water quality. 10pp., Univ. Copenhagen Geophys. Inst. Rep., 51.

Hooks, C.E., R.R. Bidigare, M.D. Keller, and R.R.L. Guillard. 1988. Coccoid eukaryotic marine ultraplankters with four different HPLC pigment signatures. J. Phycol., 24: 571- 580.

Hopkins, T.S., and N. Garfield III. 1979. Gulf of Maine intermediate water. J. Mar. Res., 37:103-139.

Horne, E.P.W., J.W. Loder, W.G. Harrison, R. Mohn, M.R. Lewis, B. Irwin, and T. Platt. 1989. Nitrate supply and demand at the Georges Bank tidal front. Scient Mar., 53:145-158.

Iturriaga, R., and D.A. Siegel. 1989. Microphotometric characterization of phytoplankton and detrital absorption properties in the Sargasso Sea. Limnol. Oceanogr., 34: 1706-1727.

Jeffrey, S.W., M. Sielicki, and F T. Haxo. 1975. Chloroplast pigment patterns in Dinoflagellates. J. Phycol., 11:374-384.

Jeffrey, S.W., and S.W. Wright. 1987. A new spectrally distinct component in preparations of chlorophyll *c* from the microalga *Emiliana huxleyi* (Prymnesiophyceae). Biochim. Biophys. Acta. 894:180-188.

Johansen, J.E., W.A. Svec, and S. Liaaen-Jensen. 1974. Carotenoids of the Dinophyceae. Phytochemistry, 13:2261- 2271.

Katz, J.J., J.R. Norris, and L.L. Shipman. 1977. Models for reaction-center and antenna chlorophyll. Brookhaven Symp. Biol., 28: 16-55.

Kepkay P.E., D.K. Muschenheim, and B.D. Johnson. 1990. Surface coagulation and microbial respiration at a tidal front on Georges Bank. Cont. Shelf Res., 10:573-588.

Kiefer, D.A., and J.B. Soohoo. 1982. Spectral absorption by marine particles of coastal waters of Baja California. Limnol. Oceanogr., 27: 492-499.

Kirk, J.T.O. 1975. A theoretical analysis of the contribution of algal cells to the attenuation of light within natural waters. I. General treatments of suspensions of living cells. New Phytol., 75: 1-20.

Kirk, J.T.O. 1983. Light and photosynthesis in aquatic ecosystems. Cambridge Univ. Press, Cambridge.

Kishino, M., C R. Booth, and N. Okami. 1984. Underwater radiant energy absorbed by phytoplankton, detritus, dissolved matter, and pure water Limnol. Oceanogr., 29: 340-349.

Kishino, M., M. Takahashi, N. Okami, and S. Ichimura. 1985. Estimation of the spectral absorption coefficients of phytoplankton in the sea. Bull. Mar. Sci., 37:634-643.

Kitchen, J.C., and J.R.V. Zaneveld. 1990. On the noncorrelation of the vertical structure of light scattering and chlorophyll a in case 1 waters. J. Geophys. Res., 95(C11):20,237-20,246.

Knox, R.S. 1963. Theory of excitons In. Seitz, F., Turnbull, D. (eds.) Solid state physics. Academic Press, London.

Larkum, A.W.D., and J. Barrett. 1983. Light-harvesting processes in algae. In. Woolhouse, H.W. (ed.) Advances in botanical research. Academic Press, New York, p. 1-219.

Lewis, M.R., J.J. Cullen, and T. Platt. 1984. Relationships between vertical mixing and photoadaptation of phytoplankton: similarity criteria. Mar. Ecol. Prog. Ser., 15:141-149.

Lewis, M.R., J.J. Cullen, and T. Platt. 1983. Phytoplankton and thermal structure in the upper ocean: consequences of nonuniformity in chlorophyll profile. J. Geophys. Res., 88(C4): 2565-2570.

Lewis, M.R., R.E. Warnock, and T. Platt. 1986. Photosynthetic response of marine picoplankton at low photon flux. Can. Bull. Fish. Aquat. Sci., 214:235-250.

Liaaen-Jensen, S. 1985. Carotenoids of lower plants: recent progress. Pure & Appl. Chem., 57:649-658.

Liaaen-Jensen, S., and A.G. Andrewes. 1985. Analysis of carotenoids and related polyene pigments. In, Gottschalk, G. (ed.) Methods in microbiology. Academic Press, New York. p. 235-283.

Lorenzen, C.J. 1967. Determination of chlorophyll and pheopigments: Spectrophotometric equations. Limnol. Oceanogr., 12:343-346.

Mann, J.E., and J. Myers. 1968. On pigments, growth, and photosynthesis of *Phaeodactylum tricornutum*. J. Phycol., 4: 349-355.

Mantoura, R.F.C., and C.A. Llewellyn. 1983. The rapid determination of algal chlorophyll and carotenoid pigments and their breakdown products in natural waters by reverse- phase high-performance liquid chromatography. Anal. Chim. Acta. 151:297-314.

Maske, H., and H. Haardt. 1987. Quantitative *in vivo* absorption spectra of phytoplankton: detrital absorption and comparison with with fluorescence excitation spectra. Limnol. Oceanogr., 32: 620-634.

Melis, A., and J.S. Brown. 1980. Stoichiometry of system I and system II reaction centers and of plastoquinone in different photosynthetic membranes. Proc. Natl. Acad. Sci. USA, 77: 4712-4716.

Mitchell, B.G., and D.A. Kiefer. 1984. Determination of absorption and fluorescence excitation spectra for phytoplankton. In, Holm-Hansen, O., Bolis, L., Giles, R. (eds.) Marine phytoplankton and Productivity. Springer- Verlag, Berlin. p. 157-169.

Mitchell, B.G., and D.A. Kiefer. 1988. Chlorophyll *a* specific absorption and fluorescence excitation spectra for light-limited phytoplankton. Deep-Sea Res. 35: 639-663.

Morel, A. 1974. Optical properties of pure water and sea water, in *Optical aspects of oceanography*, edited by N.G. Jerlov and E. Steemann Nielsen, pp. 1-24. Academic Press, New York.

Morel. A. 1978. Available. usable.and stored radiant energy in relation to marine photosynthesis. Deep-Sea Res.. 25:673-688.

Morel. A. 1988. Optical modeling of the upper ocean in relation to its biogenous matter content (case I waters). J. Geophys. Res.. 93(C9). 10.749 10.768.

Morel, A.. and A. Bricaud. 1981. Theoretical results concerning light absorption in a discrete medium. and application to specific absorption of phytoplankton. Deep- Sea Res.. 28: 1375-1393.

Morel, A.. and L. Prieur. 1977. Analysis of variations in ocean color. Limnol. Oceanogr.. 22: 709-722.

Morrow, J.H.. W.S. Chamberlin. and D.A. Kiefer. 1989. A two- component description of spectral absorption by marine particles. Limnol. Oceanogr.. 34: 1500-1510.

Neori. A.. O. Holm-Hansen. B.G. Mitchell. and D.A. Kiefer. 1984. Photoadaptation in Marine Phytoplankton. Plat Physiol.. 76:518-524.

Olson. R.J.. S.W. Chisholm. E.R. Zettler. M.A. Altabet. and J.A. Dusenberry. 1990. Spatial and temporal distributions of prochlorophyte picoplankton in the North Atlantic Ocean. Deep-Sea Res.. 37:1033-1051.

Owens, T.G. 1986. Light-harvesting function in the diatom *Phaedactylum tricornutum*. II. distribution of excitation energy between the photosystems. Plant Physiol.. 80: 739-746.

Owens, T.G., and E.R. Wold. 1986. Light-harvesting function in the diatom *Phaeodactylum tricornutum*. I. Isolation and characterization of pigment-protein complexes. Plant Physiol.. 80: 732-738.

Owens. T.G., J.C. Gallagher. J.C.. and R.S. Alberte. 1987. Photosynthetic light harvesting function of violaxanthin in *Nannochloropsis* spp. (Eustigmatophyceae). J. Phycol.. 23: 79-85.

Parsons. T.R., Y. Maita, C.M. Lalli. 1984. A manual of chemical and biological methods for seawater analysis. Pergamon Press. Toronto.

Petzold, T.J. 1972. Volume scattering functions for selected natural waters. Scripps Inst. Oceanogr. Visibility Lab. SIO Ref. 72-78.

Platt, T. 1986. Primary production of the ocean water column as a function of surface light intensity: algorithms for remote sensing. Deep-Sea Res., 33: 149-163.

Platt, T., and S. Sathyendranath. 1988. Oceanic primary production: estimation by remote sensing at local and regional scales. Science, 241:1613-1620.

Preisendorfer, R.W. 1961. Application of radiative transfer theory to light measurements in the sea. Int. Geophys. Geod. Monogr., 10: 11-29.

Preisendorfer, R.W 1976. Hydrologic Optics. Pub. of the U.S. Department of Commerce National Oceanic and Atmospheric Administration. Environmental Research Laboratory, Honolulu. 218 pp.

Prézelin, B B. 1981 Light reactions in photosynthesis. Can. Bull. Fish. Aquat. Sci., 210: 1-43.

Prézelin, B.B., and B.A. Boczar. 1986. Molecular bases of cell absorption and fluorescence in phytoplankton: potential applications to studies in optical oceanography. In. Round, F.E., Chapman, D.J. (eds.) Progress in Phycological Research vol.4. Biopress Ltd. Bristol. p. 349-464.

Prieur, L., and S. Sathyendranath. 1981. An optical classification of coastal and oceanic waters based on the specific spectral absorption of phytoplankton pigments, dissolved organic matter, and other particulate materials. Limnol. Oceanogr., 26: 671-689.

Rhiel, E., E. Mörschel, W. Wehrmeyer. 1987. Characterization and structural analysis of chlorophyll *a/c* light harvesting complex and of photosystem I particles isolated from thylakoid membranes of *Cryptomonas maculata* (Cryptophyceae). European J. Cell Biol., 43: 82-92.

Richards, F.A., and T.G. Thompson. 1952. The estimation and charaterisation of plankton populations by pigment analysis.II: a spectrophotometric method for the estimation of plankton pigments. J. Mar. Res., 11:156-172.

Ricker, W.E. 1984. Computation and uses of central trend lines. Can. J. Zool., 62: 1897-1905.

Roesler, C.S., M.J. Perry, and K.L. Carder. 1989. Modeling *in situ* phytoplankton absorption from total absorption spectra in productive inland marine waters. Limnol. Oceanogr., 34:1510-1524.

Rowan, K.S. 1989. Photosynthetic pigments of algae. Cambridge Univ. Press, Cambridge.

Sakshaug, E., D.A. Kiefer, and K. Andresen 1989 A steady state description of growth and light absorption in the marine planktonic diatom *Skeletonema costatum*. Limnol. Oceanogr., 34: 198-20.

Sathyendranath, S. 1986. Remote sensing of phytoplankton: a review, with special reference to picoplankton. Can. Bul. Fish. Aquat. Sci., 214: 561-583.

Sathyendranath, S., A.D. Gouveia, S.R. Shetye, P. Ravindran, and T. Platt. 1991. Biological control of surface temperature in the Arabian Sea. Nature, 349 54-56.

Sathyendranath, S., L. Lazzara, L. Prieur. 1987. Variations in the spectral values of specific absorption of phytoplankton. Limnol. Oceanogr., 32: 403-415.

Sathyendranath, S., and A. Morel. 1983. Light emerging from the sea interpretation and uses in remote sensing, p. 323- 357. *In* A P. Cracknell [ed.], Remote sensing applications in marine science and technology. D Reibel Pub.

Sathyendranath, S., and T. Platt. 1988. The spectral irradiance at the surface and in the interior of the ocean: a model for application in oceanography and remote sensing. J. Geophys. Res., 93(C8): 9270-9280.

Sathyendranath, S., and T. Platt. 1989. Computation of aquatic primary production: extended formalism to include effect of angular and spectral distribution of light. Limnol. Oceanogr. 34: 188-198.

SCOR/UNESCO. 1966. Determination of photosynthetic pigments in sea water. Monogr. Oceanogr. Methodol., 1: 69p.

Seber, G.A.F., and C.J. Wild. 1989. Nonlinear regression. Wiley, New York. 768 pp.

Shipman, L.L., T.M. Cotton, J.R. Norris, and J.J. Katz. 1976. An analysis of the visible absorption spectrum of chlrophyll *a* monomer, dimer, and oligomers in solution. J. Am. Chem. Soc., 98: 8222-8230.

Smith, R.C., and K.S. Baker. 1978. Optical classification of natural waters. Limnol. Oceanogr., 23:260-267.

Smith, R.C., and K.S. Baker. 1981. Optical properties of the clearest natural waters (200-800 nm). Appl. Optics. 20:177-184.

Smith, R.C., J. Marra, M.J. Perry, K.S. Baker, E. Swift, E. Buskey, and D.A. Kiefer. 1989. Estimation of a photon budget for the upper ocean in the Sargasso Sea. Limnol. Oceanogr., 34: 1673-1694.

Sokal, R.R., and F.J. Rohlf. 1969. Biometry. The principles and practice of statistics in biological research. Freeman & Co., San Francisco.

Spinrad, R.W. 1986. An optical study of the water masses of the Gulf of Maine. J. Geophys. Res., 91(C1):1007-1018.

Spitzer, D., and M.R. Wernand. 1981. *In situ* measurements of absorption spectra in the sea. Deep-Sea Res., 28:165-175.

Stauber, J.L., and S.W. Jeffrey. 1988. Photosynthetic pigments in fifty-one species of marine diatoms. J. Phycol., 24:158-172.

Stramski, D 1990. Artifacts in measuring absorption spectra of phytoplankton collected on a filter. Limnol. Oceanogr., 35:1804-1810.

Thornber, J.P., and R.S. Alberte. 1977. The organization of chlorophyll *in vivo*. In. Trebst, A., Avron, M. (eds.) Photosynthesis I: photosythetic electron transport and photophosphorylation. Springer-Verlag, Berlin, p. 574-582.

Townsend, D.W., T.L. Cucci, and T. Berman. 1984. Subsurface chlorophyll maxima and vertical distribution of zooplankton in the Gulf of Maine. J. Plankt. Res., 6:793-802.

Toyozawa, Y. 1958. Theory of line-shapes of the exciton absorption bands. Progr. Theoret. Phys. Kyoto. 20: 53-81.

Tyler, J.E. 1963. Design theory for a submersible scattering meter. Appl. Opt., 2:245-248.

Vernet, M., and C.J. Lorenzen. 1987. The presence of chlorophyll *b* and the estimation of phaeopigments in marine phytoplankton. J. Plankt. Res., 9:255-265.

Welschmeyer, N.A., and N. Hoepffner. Xanthophyll cycling I: dynamics of rapid, light-induced pigment changes in phytoplankton. Limnol. Oceanogr., in press.

Wood, A.M. 1985. Photosynthetic apparatus of marine ultraphytoplankton adapted to natural light fields. Nature, 316: 253-254.

Yentsch, C.S. 1957. A non-extractive method for the quantitative estimation of chlorophyll in algal cultures. Nature, 179:1302-1304.

Yentsch, C.S. 1962. Measurement of visible light absorption by particulate matter in the ocean. Limnol. Oceanogr., 7: 207-217.

Yentsch, C.S., and N. Garfield. 1981. Principal areas of vertical mixing in water of the Gulf of Maine with reference to the total productivity of the area, p. 303-312. *In* J.F.R.C. Gowan [ed.], Oceanography from space. Plenum.

Yentsch, C.S., and D.W. Menzel. 1963. A method for determination of phytoplankton chlorophyll and phaeophytin by fluorescence. Deep-Sea Res., 10:221-231.

Yentsch, C.S., and D.A. Phinney. 1982. The use of the attenuation of light by particulate matter for the estimate of phytoplankton chlorophyll with reference to the Coastal Zone Color Scanner. J. Plankt. Res., 4:93-102.

Yentsch, C.S., and D.A. Phinney. 1989. A bridge between ocean optics and microbial ecology. Limnol. Oceanogr., 34: 1694- 1705.

Zaneveld, J.R V., R. Bartz, J.C. Kitchen, and R.W. Spinrad. 1988. A reflective-tube diffuse attenuation meter and absorption meter. Eos. 69 1125.